Universität Hamburg

Neural recognition molecule CHL1: regulation of the activity of the trimeric protein complex Csp/Hsc70/Sgt and synaptic vesicle recycling in *Mus musculus* (Linnaeus, 1758).

Dissertation

zur Erlangung des Doktorgrades des Departments Biologie der Fakultät für Mathematik, Informatik und Naturwissenschaften an der Universität Hamburg

vorgelegt von Aksana Andreyeva

Hamburg, 2008

Genehmigt vom Department Biologie
der Fakultät für Mathematik, Informatik und Naturwissenschaften
an der Universität Hamburg
auf Antrag von Frau Professor Dr. M. SCHACHNER
Weiterer Gutachter der Dissertation:
Herr Professor Dr. L. RENWRANTZ
Tag der Disputation: 28. März 2008

Hamburg, den 11. März 2008

Jörg Ganzhorn

Professor Dr. Jörg Ganzhorn
Leiter des Departments Biologie

HPI
Heinrich-Pette-Institut für Experimentelle Virologie
und Immunologie an der Universität Hamburg

Carol Stocking, Ph.D.
AG Molecular Pathology
HPI · Martinistraße 52 · 20251 Hamburg

Tel.: (+49)40-480-51-273
Fax.: (+49)40-480-51-187
e-mail: stocking@hpi.uni-hamburg.de

Fachbereich Biologie
Universität Hamburg
Martin Luther King-Platz 2
D-20146 Hamburg

24. Januar 2007

Sehr geehrte Damen und Herrn,

hiermit bestätige ich, dass die von Frau Aksana Andreyeva mit dem Titel ""Neural recognition molecule CHL1: regulation of the activity of the trimeric protein complex Csp/Hsc70/Sgt and synaptic vesicle recycling in Mus musculus (Linnaeus, 1758)" vorgelegte Doktorarbeit in korrektem Englisch geschrieben ist.

Mit freundlichen Grüssen,

Carol Stocking

Dr. Carol Stocking
Leiterin, AG Mol Path
(Amerikanerin)

Abstract

In this study the regulation of chaperone activity by the cell recognition molecule CHL1 (close homologue of L1) is analyzed. Previously it was shown that CHL1 is able to interact via its intracellular domain with the chaperone Hsc70 (70 kDa heat shock cognate protein), which is constitutively expressed in the cell. Here we demonstrate that CHL1 via its intracellular domain modulates the chaperone function in synapses. CHL1 regulates the refolding activity of synaptic chaperons Hsc70, Csp (cysteine string protein) and αSgt (small glutamine-rich tetratricopeptide repeat-containing protein) via the direct interactions with these proteins. *In vitro* protein binding assay and the analysis of the complexes that are present on synaptic vesicles and synaptic plasma membranes show the predominant formation of CHL1/Hsc70/αSgt and CHL1/Csp complexes. We found that the substrate for CHL1/Hsc70/αSgt chaperone complex is Snap25 (synaptosomal associated protein of 25 kDa), whereas CHL1/Csp complex refolds Vamp2 (vesicle-associated membrane protein). Snap25, Vamp2 together with Syntaxin1 assemble the SNARE (soluble N-ethylmaleimide-sensitive factor attachment protein receptor) complex that participates in the fusion of synaptic vesicles with the presynaptic plasma membrane during exocytosis. In CHL1 deficient synaptosomes we observed reduced ability of the components of the SNARE machinery to re-associate. On the other hand, stressful conditions, such as exposure to heat or prolonged synaptic activity, result in a pronounced degradation of SNARE complex components in the brain of CHL1 deficient mice. The defect of SNARE machinery formation following the prolonged stimulation of synaptic activity leads to the inhibition of the synaptic vesicle recycling in CHL1 deficient neurons. In other words, CHL1 deficient neurons are not able to sustain prolonged synaptic activity. We also show that CHL1 is involved in synaptic vesicle recycling by the modulation of clathrin-uncoating function of Hsc70. The obtained data suggest that cell recognition molecule CHL1 participates in two steps of synaptic vesicle recycling: in exocytosis as a modulator of chaperons that refold SNARE proteins and in endocytosis by the regulation of uncoating of clathrin-coated synaptic vesicles.

Key words: CHL1, Hsc70, Csp, αSgt, chaperone, SNARE complex, synaptic vesicle exocytosis, clathrin, synaptic vesicle endocytosis.

Contents

Abstract 3
Contents 4
Notation and abbreviations 6
I. Introduction 10
1. The close homologue of L1 (CHL1). 10
1.1. Cell adhesion molecules. 10
1.2. Structural features and binding partners of CHL1. 10
1.3. CHL1 functions and related diseases. 11
2. Heat shock cognate protein Hsc70 is a binding partner of CHL1. 12
2.1. Heat shock cognate proteins. 12
2.2. Structure and functions of Hsc70. 13
3. The Hsc70/Csp/Sgt trimeric complex. 16
3.1. The cysteine string protein (Csp) is a co-chaperone of Hsc70. 16
3.2. Sgt is the third component of the trimeric chaperone complex. 18
4. Possible substrates of Hsc70/Csp/Sgt chaperone protein complex. 19
5. The role of chaperones in the degradation of unfolded proteins. 20
5.1. Ubiquitin-proteasome system. 21
5.2. Lysosomal proteolysis. 21
6. Impaired chaperone activity leads to neurodegenerative diseases. 22
II. Aim of the study 24
III. Materials 25
1. Chemicals. 25
2. Antibodies. 25
3. Solutions and buffers. 28
4. Bacterial media. 35
5. Bacterial strains and cell lines. 35
6. Cell culture medium and reagents for transfection. 35
7. Kits. 36
8. Molecular weight standards. 37
9. Restriction endonucleases, buffers and other enzymes used for molecular cloning. 37
10. Proteins. 38
11. Plasmids. 38
12. Primers. 40
IV. Methods 41
1. Animals. 41
2. Molecular biological methods. 41
2.1. Molecular cloning. 41
2.2. DNA restriction. 43
2.3. Horizontal agarose gel electrophoresis of DNA. 43
2.4. Determination of DNA concentration. 43
2.5. Competent bacteria production. 43
2.6. Transformation of bacteria. 44
2.7. Purification of plasmid DNA. 44
2.7.1. Small scale plasmid DNA production. 44
2.7.2. Large scale plasmid DNA production. 44
3. Protein biochemical methods. 45
3.1. Production of recombinant proteins. 45
3.1.1. Expression of recombinant proteins in E. coli. 45

3.1.2. Purification of recombinant proteins. 45
3.1.3. Elution of recombinant proteins by thrombin cleavage. 45
3.1.4. Expression and purification of CHL1-Fc recombinant protein. 45
3.2. Determination of protein concentration. 46
3.3. Gel electrophoresis and Western blot analysis. 46
3.3.1. SDS-PAGE. 46
3.3.2. Nondenaturing (native) PAGE. 47
3.3.3. Coomassie staining of polyacrylamide gels. 47
3.4. Subcellular fractionation. 47
3.4.1. Preparation of homogenates and synaptosomes. 47
3.4.2. Stimulation of synaptosomes with 47 mM or 90 mM K^+. 48
3.4.3. Isolation and purification of synaptic vesicles. 48
3.4.4. Isolation of lysosomes. 49
3.5. Enzymatic assays. 49
3.5.1. Acid phosphatase assay. 49
3.5.2. Luciferase refolding assay. 49
3.5.3. ATPase assay 50
3.6. Binding protein assays. 50
3.6.1. Co-immunoprecipitation. 50
3.6.2. Pull down assay. 51
3.6.3. ELISA (enzyme-linked immunosorbent assay) – protein ligand binding assay. 51
4. Immunocytochemistry. 51
4.1. Cultures of hippocampal neurons. 51
4.2. Loading of FM1-43FX in synaptic boutons. 52
4.3. Immunofluorescence labeling. 52
4.4. Immunofluorescence and FM uptake quantification. 52
4.5. Synapto-pHluorin fluorescence quantification. 53
V. Results 54
1. CHL1 deficiency results in abnormally reduced protein refolding activity in the brain. 54
2. CHL1 directly interacts with Hsc70, Csp and αSgt and regulates their activity. 58
3. CHL1 deficiency results in reduced levels of αSgt at synapses and synaptic vesicles. 60
4. CHL1 inhibits formation of the Hsc70/Csp/αSgt complex by promoting formation of the CHL1/Csp and CHL1/Hsc70/αSgt complexes. 62
5. CHL1 associates with the SNARE complex proteins and regulates their refolding. 66
6. CHL1 deficiency results in increased degradation of the SNARE complex proteins in response to stress. 73
7. CHL1 deficiency is associated with reduced recovery of the SNARE complex and inhibition of synaptic vesicle exocytosis following prolonged and stressful synapse activity. 77
8. CHL1 is important for the clathrin-dependent endocytosis. 80
VI. Discussion 82
VII. Summary 87
VIII. References 88
Publications 105
Acknowledgments 106

Notation and abbreviations

aa	amino acid
ABGP	ankyrin-binding glycoprotein
ABTS	2,2'-azino-bis(3-ethylbenzthiazoline-6-sulphonic acid)
ADP	adenosine 5′-diphosphate
Amp	Ampicillin
AMPA	α-amino-3-hydroxy-5-methylisoxazole-4- propionic acid
APP	amyloid precursor protein
APs	adaptor proteins
AP-2	adaptor protein 2
AP-5	2-amino-5-phosphonovaleric acid
ATP	adenosine 5′-triphosphate
A280	absorbance at 280 nm
Bag-1	Bcl-2-associated athanogene-1
BCA	bicinchoninic acid
BSA	bovine serum albumin
CALL	cell adhesion L1-like, human ortholog of CHL1
CAM	cell adhesion molecule
Chip	carboxyl terminus of Hsc70-interacting protein
CHL1	close homologue of L1
CHL1-ICD	intracellular domain of CHL1
CHL1+/+ (+/+)	CHL1 wild-type
CHL1-/- (-/-)	CHL1-deficient
CHO	Chinese Hamster Ovary
CNQX	6-cyano-7-nitroquinoxaline-2,3-dione
Cpr3	cyclosporin-sensitive proline rotamase-3
Csp	cysteine string protein
DCC	deleted in colorectal cancer
DGEA	aspartic acid-glycine-glutamic acid-alanine
Dj2	DnaJ protein homolog 2
DNA	deoxyribonucleic acid
DTT	dithiothreitol or threo-1,4-Dimercapto-2,3-butanediol
DF	dilution factor

e	molar coefficient
E. coli	Escherichia coli
ECL	enhanced chemiluminescence
EDTA	ethylenediamine tetraacetic acid
FGF	fibroblast growth factor
FIGAY	phenylalanine-isoleucine-glycine-alanine-tyrosine
ELISA	enzyme-linked immunosorbent assay
Fc	fragment crystallizable
FM	fluorescence microscopy
g (RCF)	standard gravity is used as a unit of acceleration (relative centrifugal force)
FN	fibronectin
G-MEM	Glasgow Minimum Essential Medium
GPI	glycosylphosphatidylinisotol
GPTIEEVD	glycine-proline-threonine-isoleucine-glutamic acid-glutamic acid-valine-aspartic acid
GST	glutathione-s-transferase
HBSS	Hanks' Balanced Salt Solution
HEPES	4-(2-Hydroxyethyl)piperazine-1-ethanesulfonic acid
Hip	Hsc70-interacting protein
His	histidine
HOMO buffer	buffer for homogenization
Hop	Hsc70/Hsp90-organizing protein
HPD	histidine-proline-aspartic acid
Hsj1	heat-shock protein DnaJ-like-1
Hsc70	heat shock cognate protein of 70 kDa
Hsp	heat shock protein
HspBP1	Hsp70 cochaperone heat shock protein-binding protein 1
Ig	immunoglobulin
IgG	immunoglobulin G
IgM	immunoglobulin M
IPTG	isopropyl β-D-1-thiogalactopyranoside
J-domain	DnaJ domain
Kana	kanamycin
KFERQ	lysine-phenylalanine-glutamic acid-arginine-glutamine

KLH	key-hole limpet hemocyanin
KO	knockout
Lamp2	lysosome-associated membrane protein type 2
LB	Luria-Bertani
LSM	laser scanning microscope
M	concentration of solution in mol/L
MOPS	3-(N-Morpholino)-propanesulfonic acid
MW	molecular weight
MWCO	Molecular Weight Cut-Off
Ng-CAM	neuron-glia cell adhesion molecule
NMDA	N-methyl-D-aspartic acid
Nr-CAM	neuron-glia-related cell-adhesion molecule
NSF	N-ethylmaleimide-sensitive fusion protein
NTA	nitrilotriacetic acid
PAGE	polyacrylamide gel electrophoresis
PBS	phosphate buffered saline
PBD	peptide-binding domain
PCR	polymerase chain reaction
PES	polyethersulfone
Pi	inorganic phosphate
PMSF	phenylmethanesulfonylfluoride
PTIEEVD	proline-threonine-isoleucine-glutamic acid-glutamic acid-valine-aspartic acid
PTX	picrotoxin
Q-rich	glutamine-rich
RGD	arginine-glycine-aspartic acid
RIPA	RadioImmunoPrecipitation Assay
RSLE	arginine-serine-leucine-glutamate
SDS	sodium dodecylsulfate
Sgt	small glutamine-rich tetratricopeptide repeat-containing protein
Snap25	synaptosomal associated protein of 25 kDa
SNARE	soluble N-ethylmaleimide-sensitive factor attachment protein receptor
SV	synaptic vesicle
SV2	synaptic vesicle protein 2

TAE	tris-acetate-EDTA
TBS	tris buffered saline
TE	tris-EDTA
TEMED	N,N,N',N'-Tetramethylethylenediamine
TFB	transformation buffer
TPR	tetratricopeptide repeat
Tris	trishydroxymethylaminomethane or 2-amino-2-hydroxymethyl-1,3-propanediol
Triton X-100	polyethylene glycol p-(1,1,3,3-tetramethylbutyl)-phenyl ether
Tween 20	polyoxyethylene (20) sorbitan monolaurate
ubiquitin	ubiquitous immunopoietic polypeptide
Vamp	vesicle-associated membrane protein or Synaptobrevin
W	tryptophan
Y	tyrosine

I. Introduction

1. The close homologue of L1 (CHL1).

1.1. Cell adhesion molecules.

The close homologue of L1 (CHL1) was discovered almost ten years ago as an adhesion molecule (Holm et al., 1996). Cell adhesion molecules (CAMs) constitute a group of proteins which are responsible for homo- and heterophilic adhesive interactions. The adhesive, as well as signalling properties of CAMs (Panicker et al., 2003), ensure the involvement of these molecules in the processes of cell migration, proliferation and differentiation (Walsh et al., 1997; Kiryushko et al., 2004). The group comprises the immunoglobulin (Ig) superfamily, the selectins, the integrins and the cadherins. Since Ig-like domains were found in the structure of CHL1, this molecule was included in the immunoglobulin superfamily. The Ig superfamily consists of several subfamilies, such as NCAM family, L1 family, DCC family, GPI-linked cell adhesion molecules and molecules with enzymatic cytoplasmic domains (Crossin et al., 2000). Because of the structural homology with L1, CHL1 is a member of L1 family. Other vertebrate members of this family are L1, Nr-CAM, Ng-CAM, neurofascin, neuroglian and ABGP (Crossin et al., 2000). All of them are characterized by the presence of six Ig-like domains and four to five FNIII domains in the extracellular portion, followed by a transmembrane region and a short cytoplasmic domain (Brummendorf et al., 1998). They are involved in a variety of developmental processes including neuronal migration, axon growth and guidance, axon fasciculation, myelination and synaptic plasticity (Hoffman, 1998; Hortsch, 2000; Panicker et al., 2003).

1.2. Structural features and binding partners of CHL1.

CHL1 is a transmembrane protein of 185 kDa molecular weight. It can be proteolytically cleaved to 165 kDa and 125 kDa fragments. The molecule of transmembrane CHL1 consists of an extracellular domain (1081 aa), a transmembrane portion (23 aa) and an intracellular domain (105 aa) (Fig. 1). The extracellular portion of CHL1 contains six Ig-like domains, followed by four full-length and one rudimentary half-length FN-like repeats. The second Ig-like domain contains the RGD tripeptide, which is also present in extracellular domains of other L1 family members, such as L1 (Thelen et al., 2002), Ng-CAM (Burgoon et al., 1991), neurofascin (Koticha et al., 2005). RGD motif has originally been found within fibronectin as

a sequence that mediates cell attachment via the interaction with subset of integrins (D'Souza et al., 1991). The sixth Ig-like domain of CHL1 possesses also DGEA sequence which is unique for CHL1 in contrast to other members of L1 family. Through this site CHL1 interacts with β1 integrin (Buhusi et al., 2003). The reduced fifth FN-like repeat also distinguishes CHL1 from other members of L1 family. The intracellular domain of CHL1 contains two highly conserved regions that are typical for L1 family. One is close to and partially within the plasma membrane (amino acid residues 1105-1119), and another is located at the C-terminal end (amino acid residues 1175-1187) (Holm et al., 1996). The RSLE motif, which is present in the intracellular domains of other L1 family members, was not found in CHL1 structure (Holm et al., 1996). In the cytoplasmic domain of L1 family members, RSLE peptide generates a tyrosine-based signal. This signal triggers the sorting of L1-CAM protein to the growth cones and the AP-2 mediated endocytosis of this adhesion molecule via clathrin-coated pits (Kamiguchi et al., 1998). The FIGAY sequence within the cytoplasmic domain of CHL1 recruits membrane-cytoskeleton linker protein ankyrin to the plasma membrane (Buhusi et al., 2003). Recently, it was found that the HPD tripeptide within the intracellular domain of CHL1 is the binding site for the heat shock cognate protein Hsc70 (Leshchyns'ka et al., 2006).

CHL1 is a glycoprotein: N-glycosidally linked carbohydrates make up 20% of its molecular weight.

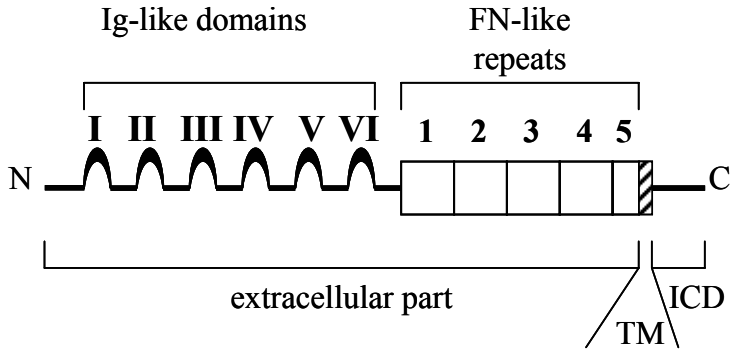

Figure 1: Domain structure of CHL1. Cell recognition molecule CHL1 consists of three portions – (i) an extracellular portion containing six Ig-like domains (I-VI) (they are represented by horseshoes) and four and a half FN-like repeats (1-5) (they are symbolized by boxes), (ii) the transmembrane peptide (TM) (denoted by hatched box) and (iii) intracellular domain (ICD).

1.3. CHL1 functions and related diseases.

CHL1 is highly expressed at the early stages of the brain development and as an adhesion molecule is likely to be involved in regulation of the brain development, synapse formation

and function, and regeneration (Mason et al., 2003; Hillenbrand et al., 1999; Holm et al., 1996; Hillenbrand et al., 1999). In fact, it was shown that during the brain development CHL1 regulates migration of neurons (Liu et al., 2000; Buhusi et al., 2003), neuronal positioning (Demyanenko et al., 2004) and neurite outgrowth (Hillenbrand et al., 1999; Dong et al., 2002). In the adult central and peripheral nervous system, CHL1 is involved in axonal regeneration (Chaisuksunt et al., 2000a, 2000b, 2003; Zhang et al., 2000) and promotes the survival of the motoneurons (Nishimune et al., 2005), and cerebellar and hippocampal neurons (Chen et al., 1999). CHL1 also participates in axon guidance and regulates synapse formation, elaboration of neuronal networks and dendrite orientation (Montag-Sallaz et al., 2002; Demyanenko et al., 2004). However, the molecular mechanisms by which CHL1 exerts its functions remain unclear up to now.

The importance of CHL1 was underscored by the studies on CHL1-deficient mice: These mice showed altered exploratory behaviour (Montag-Sallaz et al., 2002), reduced anxiety, cognitive and attention deficits (Pratte et al., 2003). CHL1-deficient mice are less aggressive, more sociable and fail to notice the novelty of the environment (Frints et al., 2003; Pratte et al., 2003). Montag-Sallaz and colleagues (2003) showed that the brain of CHL1-deficient mice processed the familiar and novel stimuli less distinctly than the wild type mice. Since the incorrect marking of the information as new or known is a basic disturbance underlying the symptoms of schizophrenia (Arnold, 1999), it was hypothesized that the information processing in the brain of CHL1-deficient mice may be impaired in a similar way as in schizophrenic patients (Montag-Sallaz et al., 2003). The involvement of the chromosome 3p26 locus, which encodes CALL (the human ortholog of CHL1), in the etiology of schizophrenia (Sakurai et al., 2002; Chen et al., 2005) strongly supports this hypothesis. It was also found that CALL is related with another neurodegenerative disorder, 3p-syndrome (Wei et al., 1998; Angeloni et al., 1999; Frints et al., 2003).

2. Heat shock cognate protein Hsc70 is a binding partner of CHL1.

2.1. Heat shock cognate proteins.

Recently, our laboratory discovered that CHL1 interacts with the heat shock cognate 70 (Hsc70), the member of the 70 kDa heat shock protein family (Hsp70s) (Leshchyns'ka et al., 2006). This finding suggests that CHL1 could be involved in some processes that require chaperone Hsc70.

Hsc70 belongs to the heat shock 'cognate' (Hsc) protein group that is a part of the heat shock protein family. In contrast to others members of the family, heat shock cognate proteins are

expressed under the normal physiological conditions (De Maio, 1999; Gething et al., 1992). They assist the folding of newly translated proteins (Hartl, 1996), guide translocation of proteins across the membrane (Pilon et al., 1999), rearrange oligomeric protein structures (Rothman et al., 1986; DeLuca-Flaherty et al., 1990), prevent irreversible aggregation of unfolded proteins, dissolute protein aggregates (Hartl et al., 2002; Ben-Zvi et al., 2001, 2004) and, finally, they are involved in the degradation of rapidly turned-over proteins (Hohfeld et al., 2001; Morishima, 2005).

2.2. Structure and functions of Hsc70.

Hsc70 (also known as Hsp73 or Hsp70-8) was discovered twice: first, as an 'uncoating protein' involved in the clathrin uncoating during synaptic vesicle recycling (Braell et al., 1984; Schlossman et al., 1984; Schmid et al., 1984) and, second, as a protein encoded by the gene related to Hsp70 in Drosophila (Ingolia et al., 1982; Ungewickell, 1985; Chappell et al., 1986). Hsc70 is a soluble cytoplasmic protein highly expressed in developing and adult nervous system (Loones et al., 1997; D'Souza et al., 1998).

Hsc70 is composed of a 44 kDa N-terminal nucleotide-binding domain (ATPase domain) and a 30 kDa C-terminal peptide-binding domain (PBD). The latter can be subdivided into an 18 kDa peptide-binding subdomain and a 10 kDa C-terminal subdomain (Chappell et al., 1987; Wang et al., 1993) (Fig. 2). The N-terminal domain of Hsc70 possesses an intrinsic ATPase activity (Flaherty et al., 1990; Huang et al., 1993; Ha et al., 1994) which can be stimulated by the binding of peptides, unfolded proteins and co-chaperons (Sadis et al., 1992; Chamberlain et al., 1997a). The 18 kDa C-terminal subdomain is responsible for the binding of unfolded proteins (Morshauser et al., 1999; Wu et al., 1999) and for the self-oligomerization (Fouchaq et al., 1999). The 10 kDa subdomain is necessary but not sufficient for Hsc70-peptide complex formation (Hu et al., 1996; Wu et al., 1999). ATPase domain and peptide-binding domain are interdependent: ATPase activity is strongly stimulated by the binding to substrate, and the release of the substrates is dependent upon the nature of the bound nucleotide (Bukau et al., 1998; Ha et al., 1995).

Functioning of Hsc70 is modulated by its binding partners. Most of the partners can be attributed to three groups. The first group includes J-domain containing proteins which belong to the J-protein family. The prototypical member of the J-protein family is DnaJ protein, which is located in the cytoplasm of Escherichia coli (E. coli). It has a J-domain, which consists of about 80 amino acids. In all members of this family J-domains possess four structural features: four helical regions (I - IV), precisely placed interhelical contact residues,

a lysine-rich surface on helix II and the diagnostic sequence HPD between the helices II and III. The second helix has a charged structure, which is essential for the interaction with ATPase domain of Hsc70 and Hsp70. The J-domain is able to stimulate the ATPase activity of Hsc70 and Hsp70 (Kelley et al., 1998; Walsh et al., 2004). Hsc70 binds to the J-domain via its ATPase- and substrate-binding domains (Stahl et al., 1999). Among J-domain containing proteins interacting with Hsc70 are auxilin (Morgan et al., 2001), Csp (cysteine string protein) (Chamberlain et al., 1997a), Hsp40 (also known as Hdj-1 or Dj1) (Minami et al., 1996; Gebauer et al., 1997), Dj2 (also known as Hdj-2, Rdj1 or Hsdj), Cpr3 (also known as Dnj3, Hirip4, Rdj2 or Dj3) (Terada et al., 2000), and Hsj1 (Cheetham et al., 1994).

The second group consists of the TPR-containing proteins. These functionally unrelated proteins contain tetratricopeptide repeat (TPR) motif, which mediates protein-protein interactions. TPR motif is composed of 34 amino acids and folds into a helix-turn-helix structure. Eight amino acid residues (-W-L-G-Y-A-F-A-P-), which show a higher frequency of conservation, define the motif (Lamb et al., 1995; Blatch et al., 1999; D'Andrea et al., 2003). It was shown that different TPR-containing proteins interact via its TPR domains with a distinct combination of functional groups in the PTIEEVD motif at the C-terminal end of Hsc70 (Wu et al., 2001). Among TPR-domain containing proteins interacting with Hsc70 are Hip (also known as p48) (Hohfeld et al., 1995; Gebauer et al., 1997; Liu et al., 1999), Chip (Ballinger et al., 1999), Tpr1 (Liu et al., 1999), Tpr2 (Liu et al., 1999), Sgt (Liu et al., 1999) and Hop (also known as p60 or Stil1) (Gebauer et al., 1997; Liu et al., 1999).

Finally, the third group includes the nucleotide exchange factors Bag-1 (also known as Rap-46 or Hap) (Hohfeld et al., 1997; Gebauer et al., 1997) and HspBP1 (Kabani et al., 2002).

Different binding partners of Hsc70 (its co-chaperons) can play a role of the adaptors that involve chaperone Hsc70 in the appropriate reactions (Ohtsuka et al., 2000). With the help of the co-chaperons, the abilities of Hsc70 to facilitate the correct protein folding, oligomeric assembly (Flynn et al., 1989; Joglekar et al., 2005), degradation (Bercovich et al., 1997; Terlecky et al., 1992) and protein translocation through the intracellular membranes (Chirico et al., 1988; Deshaies et al., 1988; Imamoto et al., 1992) are employed for endocytosis (Chang et al., 2002), exocytosis (Bronk et al., 2001) and cell dividing (Brown et al., 1996).

Hsc70 is required in the clathrin-dependent endocytosis in order to release clathrin from clathrin coated vesicles (DeLuca-Flaherty et al., 1990; Newmyer et al., 2001) and to chaperone clathrin to prevent its polymerization in cytosol and to prime it to reform clathrin-coated pits (Jiang et al., 2000). Two co-chaperones are involved in this function of Hsc70: auxilin (Ungewickell et al., 1995; Morgan et al., 2001) and dynamin (Newmyer et al., 2003).

The clathrin-dependent endocytosis starts from the association of adaptor proteins (APs) with the plasma membrane. APs bind the cargo proteins and recruit clathrin. Oligomerized clathrin recruits auxilin, which in turn recruits Hsc70. Hsc70/auxilin chaperone activity induces the conformational changes within clathrin coat and drives the formation of invaginated pit. Then the dynamin is recruited by a yet unknown mechanism and redistributes the Hsc70/auxilin complex to the neck of the forming pit. The pit is constricted with the help of dynamin-Hsc70-auxilin complex and pinches off to the cytoplasm (Newmyer et al., 2003). The clathrin coat of released vesicle is dissociated by Hsc70 (Schlossman et al., 1984) and auxilin (Ungewickell et al., 1995).

Hsc70 is also involved in neurotransmitter exocytosis through its interaction with cysteine-string protein (Csp) (Bronk et al., 2001).

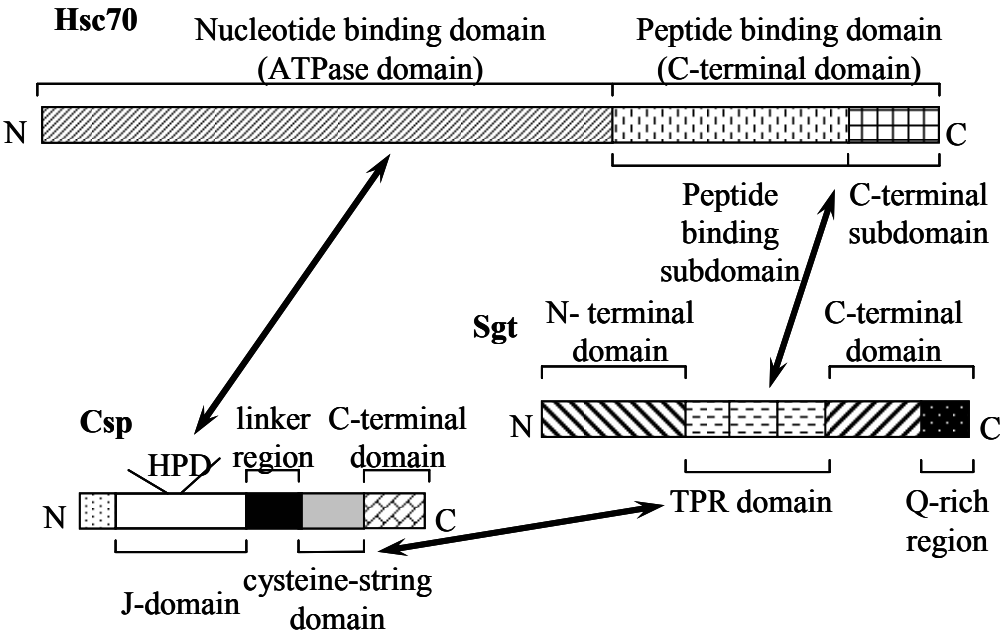

Figure 2: Schematic domain structure of Hsc70, Csp, Sgt and the model of the trimeric protein complex. Heat shock cognate protein Hsc70 consists of two domains – a nucleotide binding domain that possesses ATPase activity and C-terminal domain that binds to peptides and unfolded proteins. Via the nucleotide binding domain Hsc70 could directly interact with the J-domain of cysteine string protein (Csp) that up-regulates chaperone activity of Hsc70. Csp has four domains – J-domain, linker region, cysteine-string domain and C-terminal domain. Hsc70 interacts with TPR domain of small glutamine-rich tetratricopeptide repeat-containing protein (Sgt) via the peptide binding domain. On the other hand, Csp and Sgt directly interact with each other. Three proteins – Hsc70, Csp and Sgt can create *in vitro* tripartite complex that possesses several times higher chaperone activity than Hsc70 alone.

3. The Hsc70/Csp/Sgt trimeric complex.

3.1. The cysteine string protein (Csp) is a co-chaperone of Hsc70.

Csp is a synaptic vesicle associated protein (Mastrogiacomo et al., 1994) which binds to Hsc70 through the conserved HPD tripeptide within the J-domain (Kelley, 1998; Chamberlain et al., 1997b) and stimulates its ATPase activity (Braun et al., 1996; Zhang et al., 1999) (Fig. 2). A highly palmitoylated hydrophobic cysteine-string domain in Csp structure permits Csp to associate with membrane lipids (Gundersen et al., 1994). Additionally, it confers initial membrane targeting of Csp (Chamberlain et al., 1998), palmitoylation-dependent sorting (Greaves et al., 2006) and participation of this protein in exocytotic membrane fusion (Gundersen et al., 1994). It was also shown that the other two domains of Csp, a glycine/phenylalanine rich linker region and a variable C-terminus, are important for exocytosis (Zhang et al., 1999).

Csp is required for regulated exocytosis at different stages. It is involved in the synaptic vesicle filling with the neurotransmitter (Hsu et al., 2000; Jin et al., 2003), the synaptic vesicle docking (Sakisaka et al., 2002; Evans et al., 2003), the regulation of Ca^{2+} influx into nerve terminals and the presynaptic Ca^{2+} homeostasis (Gundersen et al., 1992; Ranjan et al., 1998; Bronk et al., 2005). It also modulates G protein-mediated signal transduction (Natochin et al., 2005). Vesicle-associated Csp may function to increase activity of Ca^{2+}-channels at the sites of vesicle docking on the presynaptic membrane, thus ensuring that Ca^{2+} entry is the greatest through the channels that are physically linked to vesicles. Recently identified interactions of Csp with Ca^{2+} sensor for exocytosis Synaptotagmin (Evans et al., 2002) and P/Q type calcium channels (Leveque et al., 1998) support this hypothesis. Csp is also involved in the last step of exocytosis by regulating the synaptic vesicle fusion through the interaction with members of the exocytotic machinery, the soluble N-ethylmaleimide-sensitive fusion protein receptor (SNARE). SNARE is a stable SDS-resistant complex, also called the core complex (Evans et al., 2003). This complex is composed of Syntaxin and Snap25 located on the plasma membrane and Vamp on the vesicle membrane (Chen et al., 2001) (Fig. 3). Structural studies revealed that the core complex has a form of the four-helix bundle (Sutton et al., 1998), which acts as a mechanism to bring synaptic vesicle membrane and plasma membrane close together, thus mediating the membrane fusion (Lin et al., 1997). Csp interacts directly with Syntaxin (Chamberlain et al., 2001; Nie et al., 1999; Wu et al., 1999; Evans et al., 2001; Fergestad et al., 2001 ; Swayne et al., 2006) and makes a complex with Vamp (Leveque et al., 1998). Csp also binds to Synaptotagmin (Evans et al., 2002), which modulates exocytosis through the interaction with SNARE complex (Wang et al., 2001; Fergestad et al., 2001).

Hence, Csp can regulate synaptic vesicle exocytosis. The mechanism of regulation can be explained by the capability of Csp to be a synaptic chaperone (Chamberlain et al., 1997b; Chamberlain et al., 2000). The chaperone function of Csp is strongly supported by the analysis of Csp mutants in flies and mice (Zinsmaier et al., 1994; Fernandez-Chacon et al., 2004).

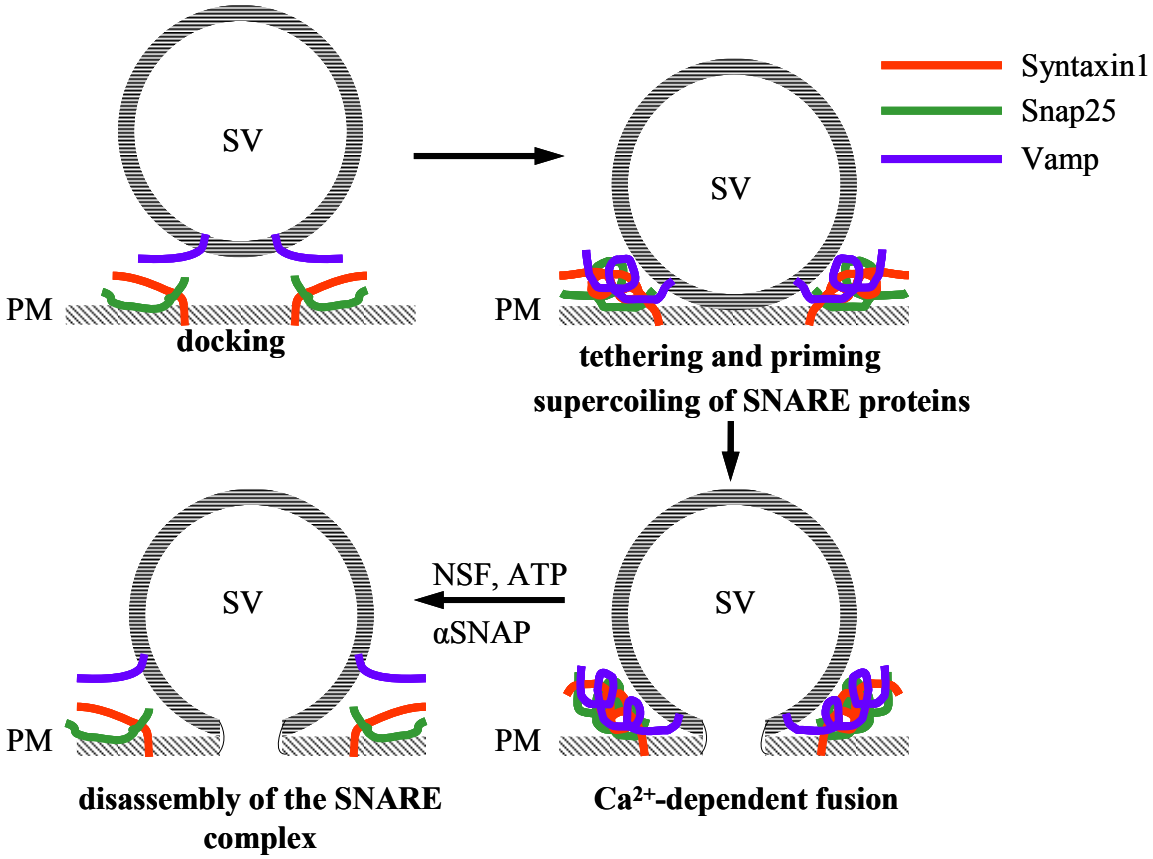

Figure 3: The schematic model of SNARE complex formation and dissociation during synaptic vesicle recycling. Following stimulation, Syntaxin1 and Snap25 at the presynaptic plasma membrane (PM) and Vamp associated with docked synaptic vesicle (SV) form a SNARE complex. Then the SNARE complex undergoes the coiling and supercoiling and draws vesicle to the plasma membrane. The process is resulting in membrane fusion, after which the SNARE complex disassembles.

As a co-chaperone of Hsc70 and chaperone itself, Csp can renature SNARE complex components and other nerve terminal proteins that are misfolded during the continuous operation of synaptic vesicle cycle. A possible role of Csp in presynaptic neurotransmission would be to perform a chaperone function in the synapse with Vamp and Syntaxin as substrates. The abnormality of SNARE complex assembly in the brain of Csp knockout (KO) mice strongly supports this hypothesis (Chandra et al., 2005). Csp can also promote assembly or disassembly of synaptic protein complexes to facilitate Ca^{2+}-channel activation (Leveque et

al., 1998). Csp is essential for keeping nerve terminals alive in an activity-dependent manner (Schmitz et al., 2006). Csp KO flies have a temperature-sensitive phenotype with impaired synaptic transmission and electron-dense 'debris' in synaptic terminals, possibly caused by neuronal degeneration (Zinsmaier et al., 1994). Csp deficient mice have a defect in presynaptic functions (Fernandez-Chacon et al., 2004) and develop a lethal neurodegeneration 2-3 weeks after birth (Chandra et al., 2005), which appears most probably because of use-dependent loss of nerve terminal integrity (Fernandez-Chacon et al., 2004). Csp is also implicated in the mechanism of such neurodegenerative disorder as Huntington's disease (Miller et al., 2003).

In vitro, Hsc70/Csp dimeric complex possesses 12 times higher ATPase activity than Hsc70 alone (Chamberlain et al., 1997b). Most probably, Csp is involved in the folding of synaptic proteins as a part of Hsc70/Csp complex also *in vivo* by adapting Hsc70 to renature the synaptic proteins that are misfolded during the exocytosis. This hypothesis is strongly supported by the observation that Hsc70-4 KO flies have the phenotype similar to Csp KO flies (Bronk et al., 2001). It was also shown that Hsc70 directly interacts with Syntaxin (Swayne et al., 2006). Most probably, Hsc70/Csp complex is involved in the last step of exocytosis: Together with Csp, Hsc70 could regulate the interactions between SNARE complex-associated proteins that are involved in the synaptic vesicle fusion (Zinsmaier et al., 2001). On the other hand, vesicle-associated Csp may recruit Hsc70 to synaptic vesicles (Hsu et al., 2000).

3.2. Sgt is the third component of the trimeric chaperone complex.

Hsc70 and Csp form *in vitro* a tripartite complex with the third component – a small glutamine-rich tetratricopeptide repeat-containing protein (Sgt), the member of TPR protein family (Tobaben et al., 2001). The broad distribution within the cell and known interactions suggest that the function of Sgt depends on its subcellular localization and binding partners (Cziepluch et al., 2000; Winnefeld et al., 2004; Tobaben et al., 2001). Sgt plays a role in the regulation of gene expression (Cziepluch et al., 2000), in cell division (Winnefeld et al., 2004) and modulates the chaperone activity of Hsc70 (Wu et al., 2001).

Two isoforms of Sgt were identified - the ubiquitously expressed αSgt and βSgt, which is almost exclusively expressed in the brain (Tobaben et al., 2003). Sgt consists of the N-terminal domain, the C-terminal region containing glutamine-rich (Q-rich) fragment (ca. 55 amino acids) and the protein interaction domain, which is composed of three copies of a 34-amino acid residue motif named tetratricopeptide repeat (TPR) (Liou et al., 2005) (Fig. 2).

The C-terminal Q-rich region has the capacity to interact with hydrophobic amino acid segments within polypeptides (Liou et al., 2005). Sgt recognizes the hydrophobic segments with broad sequence specificity (Liou et al., 2005). The central TPR domain mediates the interaction with both Hsc70 (Liu et al., 1999) and Csp in two different modes (Tobaben et al., 2003) (Fig. 2). In contrast to the electrostatic interaction between Sgt and Hsc70, Sgt binding to Csp has a hydrophobic character (Tobaben et al., 2003). Sgt binds to GPTIEEVD peptide of 30 kDa C-terminal end of Hsc70 and inhibits the refolding activity of this chaperone (Wu et al., 2001). The binding site for Sgt within Csp is created by C-terminal domain and cysteine string region (Tobaben et al., 2001) (Fig. 2).

In connection with the observation that Hsc70 binds to the J-domain of Csp through ATPase domain and the substrate-binding domain (Stahl et al., 1999), the existence of the interactions between Sgt and Hsc70, Sgt and Csp allows to conclude that three proteins could create a trimeric complex (Tobaben et al., 2001). The situation could be even more complex because of the capacity of the components to self-associate. Sgt is able to oligomerize through its N-terminal domain (Liou et al., 2005), Hsc70 – by its 17 kDa peptide-binding subdomain (Fouchaq et al., 1999) and Csp – through residues 83-136, encoding the linker region and cysteine string region (Swayne et al., 2003). The hypothesis is supported by the study with recombinant Hsc70, Csp and Sgt, which suggests that stoichiometry of the trimeric complex is 2:2:2 rather than 1:1:1 (Tobaben et al., 2001). In *in vitro* assay it was shown that the association of the complex was ADP-dependent, whereas ATP abolished the interaction between the components of the trimeric complex (Tobaben et al., 2001). However it was not yet shown *in vivo* that Hsc70/Csp/Sgt complex is formed in the brain.

4. Possible substrates of Hsc70/Csp/Sgt chaperone protein complex.

Hsc70/Csp/Sgt complex possesses *in vitro* refolding activity for artificial substrates, such as denatured firefly luciferase. It is 19 times higher than the activity of Hsc70 and almost three times higher than that of Hsc70/Csp complex (Tobaben et al., 2001). The stimulation effect of Sgt on the activity of Hsc70/Csp dimeric complex, in comparison with its direct negative effect on Hsc70 activity, can be explained by the stabilization of Hsc70/Csp complex by Sgt (Tobaben et al., 2003). The physiological function of Hsc70/Csp/Sgt complex and the substrates of its refolding activity in the brain are unknown. But the localization of Hsc70, Csp and Sgt in synaptic vesicles could suggest the important role of Hsc70/Csp/Sgt complex in synapses (Tobaben et al., 2001). As it was previously mentioned, Csp and Hsc70 regulate

the protein interactions associated with SNARE complex (Zinsmaier et al., 2001; Joglekar et al., 2005). The overexpression of Sgt leads to the reduction in the size of the ready releasable pool of synaptic vesicles, reduction in vesicular release probability and, as a result, to impaired synaptic transmission (Tobaben et al., 2001).

Among possible substrates for the chaperone activity of the trimeric complex are synaptic proteins involved in the synaptic vesicle fusion. This hypothesis is supported by studies showing direct interactions between Csp and SNARE proteins (Chamberlain et al., 2001; Nie et al., 1999; Leveque et al., 1998) and Syntaxin and components of Hsc70/Csp/Sgt complex (Swayne et al., 2006). Mutations or absence of one of SNARE complex members (Vamp, Syntaxin or Snap25) lead to the impaired synaptic transmission (Fergestad et al., 2001; Washbourne et al., 2002; Ando et al., 2005). Thus, the damages which come after repetitive folding/unfolding of these proteins during the repetitive cycles of membrane fusion have to be immediately eliminated – a function which might be performed by Hsc70/Csp/Sgt chaperone complex.

The phosphoprotein Synapsin1, which is involved in the neurotransmitter release, could also be the substrate of the trimeric chaperon complex activity. The absence of Synapsin1, one of the four neuron-specific members of Synapsin family, leads to altered synaptic vesicle organization at presynaptic terminals, decreased glutamate release from nerve endings and increased response to electrical stimulation (Li et al., 1995).

5. The role of chaperones in the degradation of unfolded proteins.

During the refolding of denatured proteins molecular chaperones could cooperate with degradation machinery. In case of heavy damages, that do not allow the protein to attain its correct tertiary structure, it could be directed by chaperones to degradation. Hsc70 has several binding partners that play a role of adaptors for chaperoning (Sgt, Csp) (Angeletti et al., 2002; Stahl et al., 1999) or degradation (Chip) (McDonough et al., 2003; Murata et al., 2003). Difficulty with folding and, therefore, a large amount of time spent by proteins in a partially folded conformation increases the probability that a degradation pathway will be chosen. The age, disease and stress can affect the balance between protein ‘rescue’ and protein degradation.

There are two groups of selective intracellular proteolytic systems – soluble systems (the proteases from Ice family, calcium-activated calpains and ubiquitin-proteasome system) and particulate systems (lysosomal proteolysis and proof-reading proteolysis in endoplasmic reticulum). Hsc70 is involved in lysosomal and ubiquitin-proteasome pathways.

5.1. Ubiquitin-proteasome system.

Ubiquitin-proteasome pathway plays a crucial role in the degradation of cytosolic proteins. 26S proteasome consists of two subcomplexes: a 20S core particle and a 19S regulatory particle (cap). The cylinder of the core particle is composed of four heptameric rings. Two inner rings (proteolytic chamber) consist of the β subunits and possess a catalytic activity. The α subunits compose two outer rings that control the substrate passage in and out of the proteolytic chamber. The attachment of ATPase-containing 19S cap to the core is necessary to degrade the ubiquitinated substrate and to enhance the peptidase activity (Glickman et al., 2005). 26S proteasome substrates are covalently modified (ubiquitinated) by a cascade of E1 ubiquitin-activating, E2 ubiquitin-conjugating and E3 ubiquitin ligase activities. The substrate selection for the degradation depends on the proteins that possess the E3 ubiquitin ligase activity. Each of them recognizes and ubiquitinates the specific protein that needs to be degraded. Chip (carboxyl-terminus of Hsc70 interacting protein), the binding partner of Hsc70 (Ballinger et al., 1999), possesses the E3 ubiquitin ligase activity and acts to tilt the folding-refolding machinery toward the degradation pathway (Jiang et al., 2001; Murata et al., 2003; McDonough et al., 2003). CHL1, as a binding partner of Hsc70 (Leshchyns'ka et al., 2006), also could be involved in regulation of protein degradation.

The components of the ubiquitin-proteasome system were found in synapses (Speese et al., 2003; Bingol et al., 2005). Synaptic activity promotes the recruitment of proteasomes, which locally remodel the protein composition in synapses (Bingol et al., 2006). On the other hand, proteasomes are involved in neurotransmitter release (Willeumier et al., 2006). It has been shown that Syntaxin1 (Chin et al., 2002), Snap25 (Ma et al., 2005), Synaptophysin (Wheeler et al., 2002) and synaptic vesicle priming protein Dunk-13 (Speese et al., 2003) are regulated by ubiquitin-proteasome system. In the case of impaired chaperoning Syntaxin and Snap25 would be directed for degradation, probably, via ubiquitin-proteasome pathway.

5.2. Lysosomal proteolysis.

Hsc70 is also involved in the lysosomal pathway of protein degradation (Dice et al., 1990). Lysosomes are organelles that contain acid hydrolases (proteases, carbohydrases, lipases, nucleases, phosphatases) and participate in the degradation of cytosolic and membrane proteins. Of all the variety of lysosome pathways, the cytosolic proteins are degraded by chaperone-mediated autophagy. In this type of lysosomal degradation the damaged proteins

are delivered inside the organelle without employing vesicular traffic (Majeski et al., 2004). Instead, KFERQ-related peptide within the cytosolic protein is captured by a molecular chaperone complex which contains Hsc70 and its co-chaperones (Hip, Hop, Bag-1, Hsp40, Hsp90) (Agarraberes et al., 2001). Then, this complex is recognized by Lamp2a at the surface of the lysosomal membrane (Cuervo et al., 1996). The cytosolic protein containing KFERQ-related peptide is unfolded with the help of cytosolic Hsc70 (Salvador et al., 2000) and pulled into the lysosomal lumen by lysosomal Hsc70 (Cuervo et al., 1997).

The presence of direct interactions of Hsc70 with the components of SNARE machinery makes it possible that lysosomes could be also involved in the degradation of these proteins. During the repetitive cycles of synaptic vesicle fusion Snap25, Syntaxin and Vamp rapidly change the conformation with the help of chaperones. Under certain conditions, when chaperones cannot repair misfolded proteins, chaperone-mediated targeting to the ubiquitin-proteasome system or to lysosome results in selective degradation. CHL1, as a binding partner of Hsc70, could be involved in the chaperone function of the complexes containing Hsc70 and participate in the balancing of SNARE protein folding and degradation.

6. Impaired chaperone activity leads to neurodegenerative diseases.

Alterations in the functional capacity of molecular chaperones lead to neurodegenerative diseases, termed ‘protein-misfolding disorders’ (Muchowski et al., 2005). This group of diseases includes Alzheimer’s disease, Parkinson’s disease, familial amyotrophic lateral sclerosis, Huntington’s disease and polyglutamine expansion disease. All of them are characterized by the accumulation of aggregated protein (Spillantini et al., 1998; Shao et al., 2007). The neurons are particularly vulnerable to intracellular aggregation of misfolded proteins because they cannot dilute potentially toxic protein accumulations through cell division. There is some evidence that molecular chaperone malfunction can cause these diseases. First, it was shown that mutations in chaperones could lead to familial amyotrophic lateral sclerosis (Watanabe et al., 2001), Alzheimer’s (Hamos et al., 1991) and Parkinson’s (Auluck et al., 2002) disorders. On the other hand, overexpression of cytosolic chaperons in cell lines and transgenic mice markedly decreases the formation and toxicity of inclusion body (Cummings et al., 2001; Auluck et al., 2002; Takeuchi et al., 2002).

Parkinson’s and Huntington’s diseases are associated with decreased proteasome activity (McNaught et al., 2003; Seo et al., 2004; Rubinsztein, 2006). This data are complemented with observation that genetic deficiencies of the ubiquitin-proteasome system are sufficient

for the neurodegeneration (Shimura et al., 2000). It suggests that proteasomal dysfunction is an important factor in protein-misfolding disorders. Since all three proteins found to be mutated in neurodegeneration – APP (Alzheimer's disease), Synuclein (Parkinson's disease) and Huntingtin (Huntington's disease) – contain KFERQ-like motifs, chaperone-mediated autophagy could be also involved in the neurodegenerative process (Massey et al., 2004).

Recently it was shown that molecular chaperones are involved in the etiology of schizophrenia (Arion et al., 2007). The increased expression of genes involved in chaperone function (Arion et al., 2007), decreased levels of SNARE proteins in the brain of schizophrenia patients (Fatemi et al., 2001; Mukaetova-Ladinska et al., 2002; Honer et al., 2002) and impaired neurotransmission in animal models (Sarter et al., 2007) suggest that refolding of synaptic fusion machinery is defective in the brain of people with schizophrenia. It is interesting that CHL1 is also involved in the etiology of schizophrenia (Chen et al., 2005; Irintchev et al., 2004). All these data suggest that CHL1 could modulate SNARE proteins refolding. Impairment of this regulatory mechanism would lead to neurological disease, known as schizophrenia.

II. Aim of the study

The ability of synaptic contacts to pass signals from one neuron to another is required for continuous processing of information in the brain. To remain functional for prolonged periods of activity synaptic connections should be continuously provided with important for neurotransmission proteins in their functional state. The proteins involved in the synaptic vesicle recycling undergo substantial conformational changes during the synaptic vesicle fusion and must refold. The refolding of these proteins is facilitated by synaptic chaperones. Therefore chaperones play an important role in the neurotransmission providing the processes of endo- and exocytosis with sufficient amount of correctly folded proteins. Previously we showed that cell adhesion molecule CHL1 directly interacts with chaperone Hsc70 and recruits this protein to synapses (Leshchyns'ka et al., 2006). The aims of this study were: (i) to analyse whether CHL1 regulates the chaperone activity in synapses; (ii) to identify a new binding partners of CHL1 among synaptic chaperones; (iii) to investigate possible regulation of the activity of synaptic chaperones (in particular, Hsc70 and its co-chaperones) and their complexes by CHL1; (iv) to determine the proteins that are refolded by CHL1 containing chaperone complexes that probably exist in synapses; (v) to investigate the role of CHL1 in neurotransmission.

III. Materials

1. Chemicals.

All chemicals were purchased from the following companies: Amersham Pharmacia Biotech (Freiburg, Germany), Bio-Rad (Hercules, CA, USA), Invitrogen (Karlsruhe, Germany), Carl Roth (Karlsruhe, Germany), Macherey-Nagel (Duren, Germany), Merck (Darmstadt, Germany), Serva (Heidelberg, Germany) and Sigma-Aldrich (St. Louis, MO, USA). Glutathione-agarose was obtained from Sigma-Aldrich. Ni-NTA agarose was purchased from Qiagen (Hilden, Germany). Bio-Beads SM2 were obtained from Bio-Rad.

2. Antibodies.

anti-actin	The rabbit polyclonal antibody against actin was from Sigma. It was used for immunoblotting (1:1000).
anti- γ-adaptin	The monoclonal antibody against γ-adaptin from BD Biosciences (San Jose, CA, USA) was used for immunoblotting (1:1000).
2C2	The monoclonal antibody reacting with the cytoplasmic domain of L1 and CHL1 (Montag-Sallaz et al., 2002) was a kind gift of Marty Grumet (Rutgers University, Piscataway, NJ, USA). It was used for ELISA assay (1:20000) and immunoblotting 1:2000.
Anti-caspase 3	The polyclonal antibodies were produced by immunizing rabbits with a synthetic peptide coupled to KLH (key-hole limpet hemocyanin) corresponding to residues surrounding the cleavage site and the amino-terminus of the large fragment of human caspase 3. The antibody recognizes full-length non-active and cleaved active enzyme. The antibodies were purchased from Cell Signaling (Beverly, MA, USA) and used for immunoblotting (1:1000).
anti-CHL1	The polyclonal antibody was raised against the extracellular domain of mouse CHL1 (Rolf et al., 2003). It was used for immunoblotting (1:1000) and immunoprecipitation. It was produced in the lab of Prof. Schachner.
anti-clathrin	The monoclonal antibody against the clathrin heavy chain was

	purchased from BD Biosciences and used for immunoblotting (1:1000).
anti-Csp	The rabbit polyclonal antibody against Csp was a kind gift from Guido Meyer (Max-Planck-Institute for Experimental Medicine, Göttingen, Germany). It was used for immunoblotting (1:5000).
anti-Csp	The mouse monoclonal antibody against Csp was purchased from BD Biosciences. For the production of this antibody a recombinant protein from rat Csp (amino acids 81-198) was used as the immunogen. The antibody was used for immunoblotting (1:1000).
anti-EEA1	The monoclonal antibody against EEA1 was purchased from BD Biosciences. It was used for immunoblotting (1:1000).
α6F	The monoclonal antibody against the α1 subunit of Na,K-ATPase was purchased from the Developmental Studies Hybridoma Bank, (Iowa City, IA, USA). It was used for immunoblotting (1:20).
anti-GST	The mouse monoclonal antibody against GST was from Novagen (Darmstadt, Germany). It was used for immunoblotting (1:2000).
Hsc70 (K-19): sc-1059	The affinity-purified goat polyclonal antibody against a peptide mapping at the carboxy terminus of Hsc70 of human origin (identical to corresponding mouse sequence) was purchased from Santa Cruz Biotechnology and used for immunoblotting (1:500).
Hsc70 (SPA-815B)	Biotin conjugated rat monoclonal antibody against Hsc70 from Stressgen (Victoria, BC, Canada) was used for immunoblotting (1:500).
anti-Hsc70 (1B5)	The rat monoclonal (1B5) antibody was produced against full length native Hsc70 (Hamster), which was purified from sodium arsenite treated heat-resistant variants of Chinese hamster cells. It was purchased from Abcam (Cambridge, UK). It was used for immunoblotting (1:1000).
Hsp70 (W27): sc-24	This is the mouse monoclonal antibody raised against Hsp70 from HeLa cells. It was purchased from Santa Cruz Biotechnology and used for immunoblotting (1:500).
anti-His6	The rabbit polyclonal antibody against His6 tag was purchased from Cell Signaling. It was used for immunoblotting (1:1000).
anti-L1	The rabbit polyclonal antibody against the extracellular domain of

	L1 (Rolf et al., 2003) was produced in the lab of Prof. Schachner. It was used for immunoblotting (1:1000).
anti Lamp2b	The rabbit polyclonal antibody was produced against a synthetic peptide conjugated to KLH derived from within residues 350 of the C-terminus of human Lamp2b. It was purchased from Abcam. It was used for immunoblotting (1:1000).
anti-neuronal class III β-tubulin	The rabbit polyclonal antibody was purchased from Covance (Berkeley, CA, USA). The antibody is highly reactive to neuron specific class III β-tubulin, but does not identify β-tubulin found in glial cells. It was used for immunoblotting (1:2000).
anti-20S proteasome core subunits	The rabbit polyclonal antibody, which recognizes the ~ 27-30 kDa 20S proteasome core subunits (α5, α7, β1, β5i, β7). It was purchased from Calbiochem (San Diego, USA) and used for immunoblotting (1:1000).
anti-αSgt	The rabbit polyclonal antibody against αSgt was a kind gift from Guido Meyer (Max-Planck-Institute for Experimental Medicine, Göttingen, Germany). It was used for immunoblotting (1:5000).
anti-αSgt	The chicken polyclonal antibody, produced to synthetic peptide, corresponding to amino acids 61-313 of SgtA, near C-terminus. It was purchased from Abcam. It was used for immunoblotting (1:1000).
anti-βSgt	The rabbit polyclonal antibody against βSgt was a kind gift from Guido Meyer (Max-Planck-Institute for Experimental Medicine, Göttingen, Germany). It was used for immunoblotting (1:1000).
anti-Snap25	The mouse monoclonal antibody against Snap25 from BD Biosciences was used for immunoblotting (1:1000).
anti-SV2	The mouse monoclonal antibody against SV2 was purchased from the Developmental Studies Hybridoma Bank. It was used for immunofluorescence labeling.
anti-Synapsin1	The mouse monoclonal antibody was raised against purified Synapsin1, epitope not yet determined. The antibody was purchased from Synaptic Systems (Göttingen, Germany). It was used for immunoblotting (1:1000).
anti-Synaptobrevin	The mouse monoclonal antibody raised against N-terminal peptide

(anti-Vamp2)	of rat Synaptobrevin 2 (also known as Vamp2) was purchased from Synaptic Systems. It was used for immunoblotting (1:10000).
anti-Syntaxin1B	The rabbit polyclonal antibody against Syntaxin1B was from Synaptic Systems. The antigen is synthetic peptide (GKLAIFTDDIKMDSQMT) corresponding to residues 171-187 (in mouse) coupled to KLH via an added N-terminal cysteine residue. The antibody was used for immunoblotting (1:1000).
anti-Synaptophysin	The rabbit polyclonal antibody against Synaptophysin (a kind gift of Reinhard Jahn, Max-Planck-Institute for Biophysics, Göttingen, Germany) was used for immunoblotting (1:5000).
anti-Synaptophysin (C-20): sc-7568	The affinity-purified goat polyclonal antibody was raised against a peptide mapping at the carboxy terminus of Synaptophysin of human origin. The antibody was purchased from Santa Cruz Biotechnology and used for immunolabeling of cultured hippocampal neurons.
Peroxidase-conjugated mouse anti-rabbit IgG (H + L)	Peroxidase-conjugated AffiniPure mouse anti-rabbit IgG was purchased from Dianova (Hamburg, Germany). It has minimal cross-reactivity to human, goat, mouse and sheep serum proteins. The antibody was used for immunoblotting (1:10000).
Peroxidase-conjugated rabbit anti-goat IgG	Peroxidase-conjugated AffiniPure rabbit anti-goat IgG was purchased from Dianova. It has minimal cross-reactivity to human serum proteins. The antibody was used for immunoblotting (1:10000).
Peroxidase-conjugated goat anti-mouse IgG + IgM (H + L)	Peroxidase-conjugated AffiniPure goat anti-mouse IgG + IgM (H + L) was purchased from Dianova. It has minimal cross-reaction to human, bovine and horse serum proteins. The antibody was used for immunoblotting (1:10000).

3. Solutions and buffers.

Ampicillin stock solution (1000x)	100 mg/ml in H_2O, store in aliquots in - 20°C
ABTS solution (ELISA assay)	100 mM acetate buffer, pH 5.0 0.1% ABTS
Basis solution	2 mM $MgCl_2$

(Stimulation of synaptosomes)	10 mM glucose 10 mM HEPES 2 mM $CaCl_2$
Blocking buffer (Western blot)	0.1 % Tween 20 in TBS, pH 7.4 5 % skimmed milk powder
Buffer for homogenization of brain (Synaptic vesicles isolation)	4 mM HEPES, pH 7.4 320 mM sucrose
Buffer I for continuous sucrose gradient (Synaptic vesicles isolation)	4 mM HEPES, pH 7.4 50 mM sucrose
Buffer II for continuous sucrose gradient (Synaptic vesicles isolation)	4 mM HEPES, pH 7.4 800 mM sucrose
Buffer for resuspention of synaptic vesicles (Synaptic vesicles isolation)	4 mM HEPES, pH 7.4 30 mM sucrose
Buffer for denaturation of luciferase (Luciferase refolding assay)	30 mM Tris-HCl, pH 7.2 2 mM DTT 8 M guanidine hydrochloride
Buffer for refolding of luciferase (Luciferase refolding assay)	30 mM HEPES, pH 7.4 2 mM DTT 50 mM KCl 3 mM $MgCl_2$ 1mM ATP
Buffer for lysis of bacterial cell culture (Purification of GST-tagged recombinant proteins)	PBS, pH 7.5 1% Triton X-100
Buffer for lysis of bacterial cell culture (Purification of His-tagged recombinant proteins)	50 mM NaH_2PO_4, pH 8.0 300 mM NaCl 10 mM imidazole
Buffer I for step sucrose gradient (Synaptosomes isolation)	5 mM Tris-HCl, pH 7.4 1 mM $MgCl_2$ 1 mM $CaCl_2$ 1 mM $NaHCO_3$ 0.65 M sucrose
Buffer II for step sucrose gradient (Synaptosomes isolation)	5 mM Tris-HCl, pH 7.4 1 mM $MgCl_2$

	1 mM $CaCl_2$ 1 mM $NaHCO_3$ 0.85 M sucrose
Buffer III for step sucrose gradient (Synaptosomes isolation)	5 mM Tris-HCl, pH 7.4 1 mM $MgCl_2$ 1 mM $CaCl_2$ 1 mM $NaHCO_3$ 1 M sucrose
Buffer IV for step sucrose gradient (Synaptosomes isolation)	5 mM Tris-HCl, pH 7.4 1 mM $MgCl_2$ 1 mM $CaCl_2$ 1 mM $NaHCO_3$ 1.2 M sucrose
De-staining solution (Coomassie staining of polyacrylamide gel)	45 % methanol 10 % acetic acid
De-staining solution (90 mM K^+) (Loading of FM dyes in synaptic boutons and stimulation of synaptosomes)	64 mM NaCl 90 mM KCl 2 mM $MgCl_2$ 10 mM glucose 10 mM HEPES 2 mM $CaCl_2$
DNA-sample buffer (5x) (Horizontal gel electrophoresis of DNA)	20 % (w/v) glycerol in TAE buffer 0.025 % (w/v) orange G
Elution buffer for GST-tagged recombinant proteins (Purification of recombinant proteins)	50 mM Tris-HCl, pH 8.0 10 mM glutathione, reduced form
Elution buffer for His-tagged recombinant proteins (Purification of recombinant proteins)	50 mM NaH_2PO_4, pH 8.0 300 mM NaCl 200 mM imidazole
Ethidium bromide staining solution (Horizontal gel electrophoresis of DNA)	10 µg/ml ethidium bromide in TAE
HOMO buffer (Homogenate preparation, synaptosomes isolation)	50 mM Tris-HCl, pH 7.4 1 mM $MgCl_2$ 1 mM $CaCl_2$

	1 mM $NaHCO_3$
HOMO-A buffer (Synaptosome isolation)	50 mM Tris-HCl, pH 7.4 1 mM $MgCl_2$ 1 mM $CaCl_2$ 1 mM $NaHCO_3$ 0.32 M sucrose
Incubation buffer (Pull down assay)	PBS, pH 7.5 3% BSA 0.1% Tween 20 0.1 mM PMSF 1mM ADP (or ATP)
IPTG (1M) stock solution (1000x)	238 mg/ml in H_2O, store in aliquots in - 20°C
Kanamycin stock solution (1000x)	25 mg/ml in H_2O, store in aliquots in - 20°C
Laemmli buffer (5x) (SDS-PAGE)	62.5 mM Tris-HCl, pH 6.8 40 % (w/v) glycerol 2 % SDS 5 % 2-mercaptoethanol 0.04 % bromphenol blue
Laemmli buffer (5x) (Nondenaturing PAGE)	62.5 mM Tris-HCl, pH 6.8 40 % (w/v) glycerol 5 % 2-mercaptoethanol 0.04 % bromphenol blue
Loading solution (47 mM K^+) (Loading of FM dyes in synaptic boutons and stimulation of synaptosomes)	107 mM NaCl 47 mM KCl 2 mM $MgCl_2$ 10 mM glucose 10 mM HEPES 2 mM $CaCl_2$
Luciferase cell culture lysis 5x reagent	Promega
Lysis buffer (RIPA buffer) (Co-immunoprecipitation)	50 mM Tris-HCl, pH 7.5 150 mM NaCl 1% Nonidet P-40 1 mM $Na_2P_2O_7$ 1 mM NaF

	1 mM EDTA 2 mM $NaVO_4$ 0.1 mM PMSF
Lysis buffer (Nondenaturing PAGE)	50 mM Tris-HCl, pH 7.5 1% Triton X-100 1 mM $Na_2P_2O_7$ 1 mM NaF 2 mM $NaVO_4$ 0.1 mM PMSF
Modified Tyrode solution (4 mM K^+) (Loading of FM dyes in synaptic boutons and stimulation of synaptosomes)	150 mM NaCl 4 mM KCl 2 mM $MgCl_2$ 10 mM glucose 10 mM HEPES 2 mM $CaCl_2$
Nondenaturing PAGE running buffer (10x) (Nondenaturing PAGE)	0.25 M Tris-HCl, pH 8.3 1.92 M glycine
Phosphate Buffered Saline (PBS)	8.1 mM Na_2HPO_4 1.739 mM NaH_2PO_4, pH 7.4 150 mM NaCl
PBS-M (Purification of CHL1-Fc recombinant protein)	10 mM Na_2HPO_4 1.8 mM KH_2PO_4, pH 7.4 136 mM NaCl 2.7 mM KCl
PBS-T (ELISA assay)	8.1 mM Na_2HPO_4 1.739 mM NaH_2PO_4, pH 7.4 150 mM NaCl 0.05% Tween 20
12% resolving gel (SDS-PAGE)	1.72 ml H_2O 3 ml 1 M Tris-HCl, pH 8.8 0.08 ml 10% SDS 3.2 ml Acrylamide- Bis, solution (37.5:1), 30 % (w/v) 8 µl TEMED

	16 µl 10 % ammonium persulfate
6% resolving gel (Nondenaturing PAGE)	3.4 ml H_2O 3 ml 1 M Tris-HCl, pH 8.8 1.6 ml Acrylamide- Bis, solution (37.5:1), 30 % (w/v) 8 µl TEMED 16 µl 10 % ammonium persulfate
SDS-PAGE running buffer (10x) (SDS-PAGE)	0.25 M Tris-HCl, pH 8.3 1.92 M glycine 1 % SDS
Stripping buffer (Western blot analysis)	0.5 M acetic acid 0.5 M NaCl
4% stacking gel (SDS-PAGE)	2.10 ml H_2O 0.38 ml 1M Tris-HCl, pH 6.8 0.04 ml 10 % SDS 0.5 ml Acrylamide- Bis, solution (37.5:1), 30 % (w/v) 6 µl TEMED 15 µl 10 % ammonium persulfate
4% stacking gel (Nondenaturing PAGE)	2.14 ml H_2O 0.38 ml 1M Tris-HCl, pH 6.8 0.5 ml Acrylamide- Bis, solution (37.5:1), 30 % (w/v) 6 µl TEMED 15 µl 10 % ammonium persulfate
Staining solution (Coomassie staining of polyacrylamide gel)	1 % (w/v) Coomassie Brilliant Blue R-250 45 % methanol 10 % acetic acid
TAE buffer (50x) (Horizontal gel electrophoresis of DNA)	2 M Tris-acetate, pH 8.0 100 mM EDTA
TE buffer	10 mM Tris-HCl, pH 8 1 mM EDTA
TFB I (Competent bacteria production)	30 mM potassium acetate 50 mM $MnCl_2$

	100 mM RbCl 10 mM $CaCl_2$ 15 % Glycerol adjust to pH 5.8 with 0.2 M acetic acid
TFB II (Competent bacteria production)	10 mM MOPS 75 mM $CaCl_2$ 10 mM RbCl 15 % Glycerol adjust to pH 7.0 with NaOH
Transfer buffer (SDS-PAGE)	10 % methanol 0.025 M Tris-HCl, pH 8.3 0.192 M glycine 0.001 % SDS
Transfer buffer (Nondenaturing PAGE)	5 % methanol 0.012 M Tris-HCl, pH 8.3 0.096 M glycine
Tris Buffered Saline (TBS)	10 mM Tris-HCl, pH 7.4 150 mM NaCl
Wash solution (TBS-T) (Western blot analysis)	10 mM Tris-HCl, pH 7.4 150 mM NaCl 0.1 % Tween 20
Wash buffer I (Purification of His-tagged recombinant proteins)	50 mM NaH_2PO_4, pH 8.0 300 mM NaCl 20 mM imidazole
Wash buffer II (Purification of His-tagged recombinant proteins)	50 mM NaH_2PO_4, pH 8.0 300 mM NaCl 40 mM imidazole
Wash buffer (Pull down assay)	PBS, pH 7.5 3% BSA 0.1% Tween 20 0.1 mM PMSF 1mM ADP (or ATP)

4. Bacterial media.

(Media were autoclaved and antibiotics were added before using)

LB medium	10 g/l peptone from casein pancreatically digested 5 g/l yeast extract 10 g/l NaCl adjust to pH 7.5
LB/Amp medium	100 mg/l ampicillin in LB medium
LB/Amp agar plate	20 g/l agar in LB medium 100 mg/l ampicillin
LB/ Kana medium	25 mg/l kanamycin in LB medium
LB/ Kana agar plates	20 g/l agar in LB medium 25 mg/l kanamycin

5. Bacterial strains and cell lines.

Escherichia coli DH5α	Invitrogen
Escherichia coli M15 [pREP4]	Qiagen
Escherichia coli BL21 (DE3)	Novagen
CHO-K1	*Chinese Hamster Ovary* dehydrofolatreductase deficient hamster cell line

6. Cell culture medium and reagents for transfection.

Hanks´ BSS (1x) (HBSS)	without Ca and Mg with phenol red (PAA Laboratories, Colbe, Germany)
Trypsin EDTA (1:250) 1x concentrate	0.5 g/l Trypsin 0.2 g/l EDTA (4Na) PBS without Ca, without Mg (PAA Laboratories)
CHO cell medium	Glasgow MEM (G-MEM) (BHK-21) (with L-Glutamine)

	(Invitrogen), supplemented with 10% foetal calf serum 20 ml/l penicillin/ streptomycin solution (100x) (PAA Laboratories) 10 ml/l MEM non essential amino acids solution (100X) (Invitrogen) 1 mM sodium pyruvate MEM (Invitrogen) 0.4 mM L-glutamic acid 0.45 mM aspartic acid 0.026 mM adenosine 0.025 mM guanosine 0.029 mM cytidine 0.029 mM uridine 0.029 mM thymidine
Neurobasal A medium	Invitrogen
B-27 Supplement	Invitrogen
Glutamine	Invitrogen
FGF	R&D Systems, Wiesbaden-Nordenstadt, Germany
Lipofectamine 2000	Invitrogen
Pulsin	Biomol, Hamburg, Germany
modified Tyrode solution	150 mM NaCl 4 mM KCl 2 mM $MgCl_2$ 2 mM $CaCl_2$ (~310 mOsm) 10 mM glucose 10 mM HEPES, pH 7.4

7. Kits.

Acid Phosphatase Assay Kit	Sigma-Aldrich
BCAssay Kit	KMF Laborchemie Handels GmbH, St. Augustin, Germany
Complete protease inhibitor cocktail tablets, EDTA-free	Roche Diagnostics, Mannheim, Germany

Detergent-OUT, SDS Removal Kit	Calbiochem
ECL Western Blotting Detection Reagents	Amersham Pharmacia Biotech
Luciferase assay system	Promega, Madison, WI, USA
Lysosome Isolation Kit	Sigma-Aldrich
Malachite Green Phosphate Detection Kit	R&D Systems
mi-Plasmid Mini Prep Kit (mi-PM200)	Metabion, Martinsried, Germany
NucleoSpin Plasmid	Macherey-Nagel
PureLink™ HiPure Plasmid Maxiprep Kit	Invitrogen
PureLink™ Quick Plasmid Miniprep Kit	Invitrogen
PureLink™ Gel Extraction Kit	Invitrogen
PureLink™ PCR Purification Kit	Invitrogen
QIAfilter Plasmid Maxi Kit	Qiagen
SuperSignal West Pico Chemiluminescent Substrate	Pierce Chemical Co., Rockford, IL, USA
Thrombin Cleavage Capture Kit	Novagen

8. Molecular weight standards.

Ready-Load™ 1 kb Plus DNA Ladder	Invitrogen
Precision plus protein all blue standards	Bio-Rad

9. Restriction endonucleases, buffers and other enzymes used for molecular cloning.

BamHI	Invitrogen
EcoRI, recombinant	New England Biolabs, Frankfurt, Germany
NotI	New England Biolabs
SalI	New England Biolabs
NEBuffer 3	New England Biolabs
NEBuffer Pack for EcoR I	New England Biolabs
100x Purified BSA	New England Biolabs
PfuUltra II Fusion HS DNA polymerase	Stratagene, La Jolla, CA, USA
T4 DNA ligase	New England Biolabs

10. Proteins.

protein	source	
QuantiLum recombinant Luciferase	E. coli strain that carries a plasmid for the cloned Luciferase gene from the North American firefly, *Photinus pyralis*	Promega
Snap25 recombinant protein	E. coli transformed with a plasmid for the cloned Snap25 gene from *C. elegans*	ProSpec, Rehovot, Israel
Synaptophysin recombinant protein	E. coli transformed with a plasmid for the cloned Synaptophysin gene from *H. sapiens*	Abnova, Taipei, Taiwan
Fc-fragment	Human IgG, Fc-fragment	Dianova

11. Plasmids.

Received plasmids

plasmid	source	tag	encoded protein	cell type for expression	selection antibiotic	Reference
Csp-pGEX-KG	Rattus norvegicus	GST	Csp	E. coli	ampicillin	Tobaben et al, 2001
Hsc70-pGEX-KG	Rattus norvegicus	GST	Hsc70	E. coli	ampicillin	Tobaben et al, 2001
Hsc70-pQE30	Mus musculus	His6	Hsc70	E. coli	ampicillin	Leshchyns'ka et al., 2006
αSgt-pGEX-KG	Rattus norvegicus	GST	αSgt	E. coli	ampicillin	Tobaben et al, 2003
αSgt-pET-28a	Rattus norvegicus	His6	αSgt	E. coli	kanamycin	Tobaben et al, 2001
βSgt-pGEX-KG	Rattus norvegicus	GST	βSgt	E. coli	ampicillin	Tobaben et al, 2003
Snap25-pET-28b	Rattus norvegicus	His6	Snap25	E. coli	kanamycin	Fasshauer et al., 1997
CHL1-ICD-pQE30	Mus musculus	His6	CHL1-ICD	E. coli	ampicillin	Leshchyns'ka et al., 2006
L1-ICD-pET-28a	Mus musculus	His6	L1-ICD	E. coli	kanamycin	Richter, 2002
pEE14-CHL1-Fc	Mus musculus	Fc	CHL1	CHO cells	L-methionine sulphoximine	Chen et al, 1999
pGEX-4T-2			GST	E. coli	ampicillin	Amersham Pharmacia Biotech

IOM20345-pBAD-DEST49	Mus musculus	His6	Synaptophysin	E. coli	ampicillin	RZPD, Berlin, Germany
Vamp2-pET-28b	Rattus norvegicus	His6	Vamp2	E. coli	kanamycin	Fasshauer et al., 1997
Synapto-pHluorin	Mus musculus	pH-sensitive mutants of GFP	Vamp2	Mammalian cell	kanamycin	Miesenböck et al., 1998

Created plasmids

plasmid	source	tag	encoding protein	host cell	selection in expression host
CHL1-ICD-pGEX-4T-2	Mus musculus	GST	full length CHL1-ICD (1105-1209 aa of CHL1)	E. coli	ampicillin
CHL1-1105-1190-pGEX-4T-2	Mus musculus	GST	CHL1-ICD fragment (1105-1190 aa of CHL1)	E. coli	ampicillin
CHL1-1105-1170-pGEX-4T-2	Mus musculus	GST	CHL1-ICD fragment (1105-1170 aa of CHL1)	E. coli	ampicillin
CHL1-1105-1150-pGEX-4T-2	Mus musculus	GST	CHL1-ICD fragment (1105-1150 aa of CHL1)	E. coli	ampicillin
CHL1-1105-1130-pGEX-4T-2	Mus musculus	GST	CHL1-ICD fragment (1105-1130 aa of CHL1)	E. coli	ampicillin
CHL1-1130-1209-pGEX-4T-2	Mus musculus	GST	CHL1-ICD fragment (1130-1209 aa of CHL1)	E. coli	ampicillin

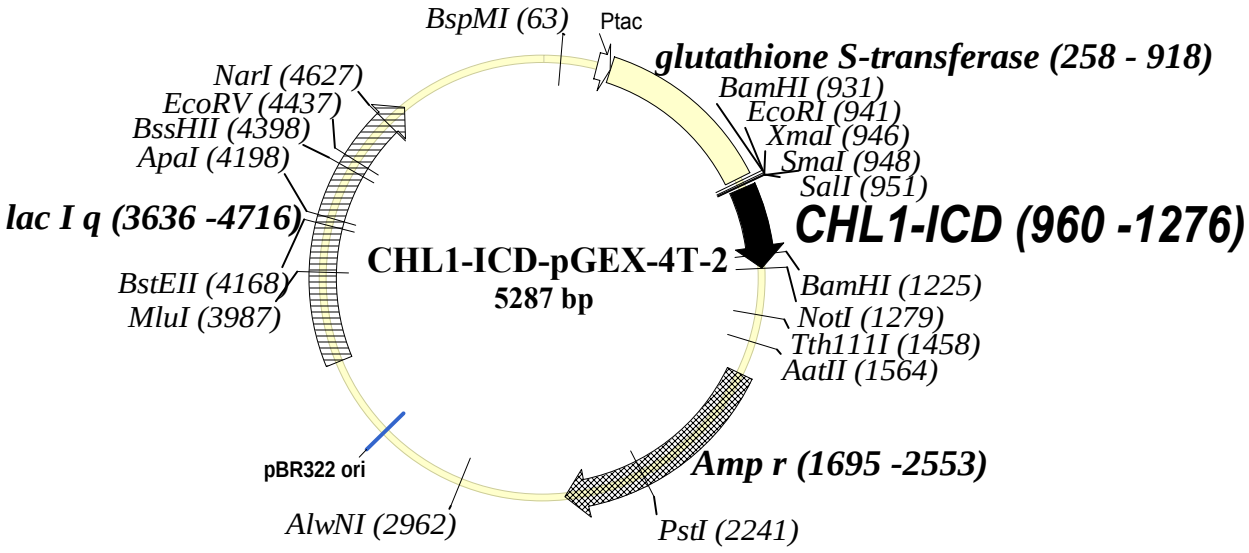

Figure 4: Map of CHL1-ICD-pGEX-4T-2 construct.

Intracellular domain of CHL1 (CHL1-ICD) (1105 aa – 1209 aa of the full length CHL1)

1 bp	AAG	AGG	AAC	AGA	GGT	GGA	AAG	TAT	TCA	GTA	AAA	GAA
1105aa	K	R	N	R	G	G	K	Y	S	V	K	E
13 bp	AAG	GAA	GAT	TTA	CAC	CCA	GAT	CCA	GAA	GTT	CAG	TCA
1117aa	K	E	D	L	H	P	D	P	E	V	Q	S
25 bp	GCA	AAA	GAT	GAA	ACT	TTT	GGT	GAA	TAC	AGC	GAC	AGT
1129aa	A	K	D	E	T	F	G	E	Y	S	D	S
37 bp	GAT	GAA	AAA	CCT	CTC	AAG	GGA	AGC	CTT	CGG	TCC	CTG
1141aa	D	E	K	P	L	K	G	S	L	R	S	L
49 bp	AAT	AGG	AAC	ATG	CAG	CCC	ACA	GAG	AGT	GCT	GAC	AGT
1153aa	N	R	N	M	Q	P	T	E	S	A	D	S
61 bp	TTA	GTG	GAA	TAT	GGA	GAG	GGA	GAC	CAG	TCC	ATA	TTC
1165aa	L	V	E	Y	G	E	G	D	Q	S	I	F
73 bp	AAC	GAA	GAT	GGA	TCG	TTT	ATT	GGC	GCA	TAC	ACT	GGA
1177aa	N	E	D	G	S	F	I	G	A	Y	T	G
85 bp	GCT	AAG	GAG	AAG	GGA	TCC	GTT	GAA	AGC	AAT	GGA	AGT
1189aa	A	K	E	K	G	S	V	E	S	N	G	S
97 bp	TCA	ACT	GCC	ACC	TTC	CCA	CTC	CGG	GCA	TG		
1201aa	S	T	A	T	F	P	L	R	A			

12. Primers.

Oligonucleotides	Sequence
CHL1-ICD/ 5’-SalI	5’-GGGGTCGACTATGAAGAGGAACAGAGGTGGAAAGTATTCA-3’
CHL1-ICD/ 3’-NotI	5’-GGGGCGGCCGCTCATGCCCGGAGTGGGAAGGT-3’
CHL1-1105-1190/ 3’- NotI	5’-GGGGCGGCCGCTCACTTAGCTCCAGTGTATGCGCCAATAAA-3’
CHL1-1105-1170/ 3’- NotI	5’-GGGGCGGCCGCTCACTCTCCATATTCCACTAAACTGTCAGCA-3’
CHL1-1105-1150/ 3’- NotI	5’-GGGGCGGCCGCTCACCGAAGGCTTCCCTTGAGAGG-3’
CHL1-1105-1130/ 3’- NotI	5’-GGGGCGGCCGCTCATTTTGCTGACTGAACTTCTGGATCTGG-3’
CHL1-1130-1209/ 5’-SalI	5’-GGGGGGTCGACTGATGAAACTTTTGGTGAATACAGCGACAGTG-3’

IV. Methods

1. Animals.

In this study three month old wild type (C57BL/6J) and CHL1-deficient mice (Montag-Sallaz et al, 2002) were used. CHL1-deficient mice were back-crossed into a C57BL/6J genetic background. The genotype of mutant and wild type mice was determined using polymerase chain reaction (PCR) with template DNA isolated from tail biopsies. The animals were housed under standard conditions (12:12 light/dark cycle with light on at 06:00; 21 ± 2°C room temperature, free access to food and water).

2. Molecular biological methods.

2.1. Molecular cloning.

For the generation of expression constructs encoding GST-tagged full length or fragments of CHL1-ICD they were amplified by PCR from the plasmid containing the full length murine CHL1 in pcDNA3 vector. PCR was performed using PfuUltra II Fusion HS DNA polymerase (Stratagene).

The reaction mixture for PCR amplification

Component	Amount per reaction
DNA template (full length of murine CHL1 in pcDNA3 vector or plasmid L1-ICD in pET28 vector) (10 ng/µl)	1 µl
plus strand primer (10 µM)	1 µl
minus strand primer (10 µM)	1 µl
dNTP mix (25 mM each dNTP)	1 µl
10x PfuUltra II reaction buffer	5 µl
PfuUltra II fusion HS DNA polymerase	1 µl
50 mM $MgCl_2$ (Invitrogen)	1 µl
Autoclaved, distilled water	39 µl

Cycling parameters

Segment	Cycles	Temperature	Time
1	1	95°C	5 min
2	30	95°C	30 s
		60°C	30 s
		72°C	1 min 30 s
3	1	72°C	10 min
4		4°C	Forever

The PCR product that contained SalI and NotI restriction sites was digested with appropriate restriction enzymes to release the insert that was between SalI and NotI restriction sites. Then the insert was purified by PureLink™ PCR Purification Kit (Invitrogen) and ligated into the SalI–NotI sites of the vector pGEX-4T-2 (Amersham Pharmacia Biotech). Vector was prepared for the ligation by the restriction with SalI and NotI enzymes and subsequent purification using PureLink™ Gel Extraction Kit (Invitrogen). For the ligation, T4 DNA ligase (New England Biolabs) was used. The amount of PCR product, which has been taken for the ligation, was calculated as:
((ng of vector x size of insert in kb) / size of vector in kb) x ratio (insert / vector). The ratios (insert /vector) which have been used are 4/1, 8/1.

The reaction mixture for a ligation

Component	Amount per reaction
Vector	100 ng
Insert	As required
10x buffer for T4 DNA ligase	1 µl
T4 DNA ligase	1 µl
Autoclaved, distilled water	up to 10 µl

The reaction mixture was incubated at room temperature for 1 hour and than at 16°C for 16 hours. Finally, E. coli DH5α were transformed with 5 µl of ligation mixture and selected by an appropriate antibiotic. Positive clones were analysed by the restriction analysis and sequence analysis.

The map of CHL1-ICD-pGEX-4T-2 construct was created using Vector NTI Advance 10 software (Invitrogen).

2.2. DNA restriction.

The reaction mixture, which contained the plasmid DNA (up to 500 ng), endonuclease(s) (1 µl), a buffer appropriate for the restriction enzyme and water to adjust the volume up to 20 µl, was incubated at 37°C for 1 h.

2.3. Horizontal agarose gel electrophoresis of DNA.

To determine the purity of DNA, the horizontal agarose-gel electrophoresis was used (Sambrook et al., 1989). Restricted DNA was separated in 1% agarose gel in Bio-Rad electrophoretic chambers in TAE buffer. The DNA-sample buffer was added to the DNA samples, before they were loaded on the gel. Then agarose gel was incubated with 0.5 µg/ml ethidiumbromide in TAE buffer and visualized by E.A.S.Y. UV-light documentation system at 360 nm wave length (Herolab, Wiesloh, Germany).

2.4. Determination of DNA concentration.

The ratio of the absorbance of DNA solution and the absorbance of the dissolvent was measured at 260 nm wave length by BioSpec-mini spectrometer (Shimadzu, Duisburg, Germany). Then DNA concentration was evaluated using a calibration curve. The ratio of the DNA absorbance at 260 nm and 280 nm was used to estimate the purity of DNA because proteins absorb at wave length 280 nm. The ratio of DNA absorbance at 260 nm and 230 nm also shows the contamination extent, since carbohydrates, phenols, peptides and aromatic compounds can absorb at wave length 230 nm.

2.5. Competent bacteria production.

For competent bacterial cell production the protocol described in Inoue et al., 1990, was used with some modifications. Frozen E. coli cells (M15 [pREP4], DH5α or BL21) were thawed and streaked on an LB agar plate and then incubated overnight at 37°C. Then single colony was picked up from the plate, inoculated in 3 ml of LB medium and incubated overnight at 37°C with vigorous shaking. 1 ml of the overnight culture was transferred to 100 ml of LB medium and incubated at 37°C with vigorous shaking until the optical density of 0.5 at 600 nm wave length was reached. Then the culture was placed on ice for 10 min and subsequently

centrifuged at 5000 g for 10 min at 4°C. The pellet was resuspended in ice-cold 30 ml TFB I and incubated on ice for 10 min. After the centrifugation of cell suspension at 5000 g for 10 min the pellet was gently resuspended in 4 ml of TFB II and incubated on ice for 10 min. Then the cell suspension was aliquoted for 100 µl and frozen at -80°C.

2.6. Transformation of bacteria.

100 µl of competent cells (E. coli strains M15 [pREP4], DH5α or BL21) were mixed with 50-100 ng of plasmid DNA and incubated on ice for 15 min. Then the heat shock (42°C for 90 s) followed by chilling on ice (for 2 min) was performed. After 45 min incubation at 37°C with 450 µl of LB medium in shaking incubator, 50 µl of transformed bacteria were plated on LB agar plates containing the appropriate antibiotic (Sambrook et al., 1989).

2.7. Purification of plasmid DNA.

2.7.1. Small scale plasmid DNA production.

A culture of 3 ml LB medium containing appropriate selective antibiotic (25 µg/ml of kanamycin or 100 µg/ml ampicillin) was inoculated with a single colony and incubated overnight at 37°C with vigorous shaking (220 rpm). Then bacteria were harvested by centrifugation at 12000 g for 1 min at room temperature. The plasmid was isolated according to the manufacturer instructions (Macherey-Nagel) and eluted by 50 µl of TE buffer.

2.7.2. Large scale plasmid DNA production.

This method was used for preparation of up to 500 µg of plasmid DNA. 3 ml of starter bacterial culture was prepared by inoculation of single bacterial colony from freshly streaked selective plate. The inoculation was performed in LB medium with appropriate selective antibiotic. The starter culture was then incubated at 37°C for approximately 8 h with vigorous shaking. Then the starter culture was diluted 1:1000 into selective LB medium and incubated overnight with vigorous shaking at 37°C. The bacteria were harvested by centrifugation at 6000 g for 15 min. For DNA plasmid isolation the QIAfilter Plasmid Maxi Kit (Qiagen) was used. Isolated DNA was dissolved in TE buffer.

3. Protein biochemical methods.

3.1. Production of recombinant proteins.

3.1.1. Expression of recombinant proteins in E. coli.

Recombinant His_6-Hsc70, GST-Hsc70, GST-Csp, GST-αSgt, His_6-αSgt, GST-βSgt, His_6-Vamp2, His_6-Snap25, His_6-Synaptophysin, GST, His_6-L1-ICD, His_6-CHL1-ICD, GST-CHL1-ICD, GST-CHL1-1105-1190, GST-CHL1-1105-1170, GST-CHL1-1105-1150, GST-CHL1-1105-1130, GST-CHL1-1130-1209 were produced in E. coli strain BL21. The protein expression was induced by IPTG. The bacteria were lysed with lysis buffer, pH 7.5, containing PBS, 1 mg/ml lysozyme, 0.1% Triton X-100 and 5 μg/ml DNAse using French-Pressure-20K-chamber (Spectronic Instruments/SLM Aminco).

3.1.2. Purification of recombinant proteins.

Recombinant proteins were bound to Ni-NTA agarose beads (Qiagen) via the His_6 tag or glutathione-agarose beads (Sigma) via the GST tag and used for further experiments or purified according to the manufacturer's instructions. His-tagged proteins were eluted from Ni-NTA beads by 200 mM imidazole. In the case of GST-tagged proteins for the elution 10 mM reduced glutathione was used.

3.1.3. Elution of recombinant proteins by thrombin cleavage.

Site-specific protease thrombin was used to elute Csp and αSgt without GST tag from glutathione-agarose beads. The protocol from Thrombin Cleavage Capture Kit (Novagen) was slightly modified to optimize specificity and efficiency of cleavage. GST-tagged protein coupled to glutathione-agarose beads was incubated with biotinylated thrombin (0.4 U/ml) for 30 min at 4°C. After the cleavage, GST coupled to glutathione agarose was removed by centrifugation at 1000 g for 5 min. The biotinylated thrombin was captured by streptavidin agarose during 30 min incubation at 4°C. The target protein was recovered by spin-filtration at 1000 g for 5 min. The elution buffer was exchanged by appropriate buffer using Microcon YM-3 Centrifugal Filter Unit (Millipore, Billerica, USA) or Vivaspin Polyethersulfone Membrane (Vivascience, Goettingen, Germany).

3.1.4. Expression and purification of CHL1-Fc recombinant protein.

CHL1-Fc recombinant protein contains the extracellular portion of mouse CHL1 which is fused to human Fc tag. The plasmid pEE14-CHL1-Fc for the expression of CHL1-Fc was

provided by Suzhen Chen (Chen et al., 1999). The expression of CHL1-Fc was performed in stable transfected CHO cells, which secreted this protein in the cell culture medium. CHO cells were cultured in CHO cell medium at 37°C in 75 cm^2 flasks. After 3-4 days the medium was removed. The cells were washed once by Hanks´ BSS, detached from the walls by the incubation with trypsin EDTA for 3 min at 37°C and mixed with fresh CHO cell medium. After 4-5 days the medium was removed and centrifuged at 10000 g for 15 min. The resulting supernatant was filtrated through Steritop ™ vacuum-driven bottle top filter (Millipore Corporation, Billerica, MA, USA) and concentrated with an Amicon ultrafiltration unit (Millipore Corporation, Billerica, MA, USA). CHL1-Fc was purified by the affinity chromatography on Protein A-Sepharose column, equilibrated by PBS-M, pH 7.5. The elution was performed by 0.1 M sodium-acetate buffer, pH 4.0. The eluted solution containing CHL1-Fc was neutralized by 1 M Tris-HCl pH 8.0. Then the buffer was exchanged into PBS in Vivaspin 20 concentrator (30000 MWCO PES) (Vivascience AG, Hanover, Germany). The protein concentration was determined by the BCAssay Kit (KMF Laborchemie Handels).

3.2. Determination of protein concentration.

For the determination of the protein concentration in the brain homogenates, synaptosomal fractions, synaptic vesicle fractions, cell lysates and purified proteins the BCAssay (bicinchoninic acid assay) Kit (KMF Laborchemie Handels) was used. 10 µl of the sample were placed on a microplate and incubated for 30 min at 37°C with 200 µl of the solution which was prepared according to the kit manual. Then the absorbance was measured at 562 nm wave length by µQuant™ universal microplate spectrophotometer (Bio-Tek Instruments Inc., Winooski, Vermont, USA). The protein concentration was evaluated from the absorbance using a calibration curve.

3.3. Gel electrophoresis and Western blot analysis.

3.3.1. SDS-PAGE.

Proteins were separated by 8% - 16% SDS-PAGE (sodium dodecyl sulfate-polyacrylamide gel electrophoresis) and electroblotted onto 0.2 µm nitrocellulose transfer membrane PROTRAN (Schleicher & Schuell, Dassel, Germany) overnight at 40 V. Immunoblots were incubated with appropriate primary antibodies followed by incubation with peroxidase-labeled secondary antibodies and visualized using Super Signal West Pico reagents (Pierce Chemical Co.) on BIOMAX film (Sigma). Molecular weight markers were prestained protein

standards (Bio-Rad). Chemiluminescence was quantified using TINA 2.09 software (University of Manchester, UK).

3.3.2. Nondenaturing (native) PAGE.

To analyze protein complexes, samples containing synaptic vesicles and plasma membranes were lysed for 1 h at room temperature in 50 mM Tris-HCl buffer, pH 7.4, containing 1% Triton X-100, 1 mM $Na_2P_2O_7$, 1 mM NaF, 2 mM $NaVO_4$, 0.1 mM PMSF and complete protease inhibitor cocktail (Roche Diagnostics). After removal of Triton X-100 from the samples using Bio-Beads SM-2 (Bio-Rad, Hercules, CA, USA) (Horigome et al., 1983), 2-mercaptoethanol was added to the samples to increase protein solubility and prevent protein aggregation. Proteins were then separated by 6% PAGE and electroblotted onto 0.2 μm nitrocellulose transfer membrane PROTRAN (Schleicher & Schuell) overnight at 40 V. Immunoblots were incubated with appropriate primary antibodies followed by incubation with peroxidase-labeled secondary antibodies and visualized using Super Signal West Pico reagents (Pierce Chemical Co.) on BIOMAX film (Sigma). Molecular weight markers were prestained protein standards (Bio-Rad) and apoferritin (Sigma). Chemiluminescence was quantified using TINA 2.09 software (University of Manchester, UK).

3.3.3. Coomassie staining of polyacrylamide gels.

To detect proteins directly on the polyacrylamide gel, the dye staining with Coomassie Brilliant Blue R-250 was used. After the electrophoresis, the polyacrylamide gel was stained for 1 h at room temperature in staining solution with constant agitation. Then the gel was incubated in the de-staining solution approximately for 1 h at room temperature.

3.4. Subcellular fractionation.

3.4.1. Preparation of homogenates and synaptosomes.

Mouse brain homogenates were prepared in HOMO buffer (1 mM $MgCl_2$, 1 mM $CaCl_2$, 1 mM $NaHCO_3$, 5 mM Tris-HCl, pH 7.4) containing 0.32 M sucrose (HOMO-A) and used for synaptosome isolation, as described (Kleene et al., 2001). All steps were performed at 4°C. Briefly, homogenates were centrifuged at 1400g for 10 min. The supernatant and pellet were resuspended in HOMO-A buffer and centrifuged for 10 min at 700 g. The resulting supernatants were combined and centrifuged at 17500g for 15 min. The pellet was resuspended in HOMO-A buffer and applied on the top of a step gradient with interfaces of

0.65 M, 0.85 M, 1 M, 1.2 M sucrose in HOMO buffer. The 700 g pellets were combined, adjusted to 1 M sucrose in HOMO buffer and layered on 1.2 M sucrose in HOMO buffer. HOMO-A buffer was applied on the top of the gradient. The crude synaptosomal fractions were collected at the 1 M / 1.2 M interface after centrifugation for 2 h at 100000 g and combined. The crude synaptosomal fraction was again adjusted to 1 M sucrose and layered on the top of the 1.2 M sucrose. HOMO-A buffer was applied on the top of the gradient. After centrifugation for 2 h at 100000 g, synaptosomes were collected at the 1 M / 1.2 M interface, resuspended in HOMO-A buffer and pulled down by centrifugation for 30 min at 100000 g.

3.4.2. Stimulation of synaptosomes with 47 mM or 90 mM K^+.

30 µl of synaptosomes were stimulated by 1.5 ml of loading solution (47 mM K^+), de-staining solution (90 mM K^+) or modified Tyrode solution (4 mM K^+) for 90 s at room temperature. The stimulation was stopped by immediate adjustment of the mixture to a final concentration of 4 mM K^+, using the basis solution (2 mM $MgCl_2$, 10 mM glucose, 10 mM HEPES, 2 mM $CaCl_2$) with appropriate concentrations of KCl and NaCl. The synaptosomes were pulled down by the centrifugation for 40 min at 140000 g and 4°C.

3.4.3. Isolation and purification of synaptic vesicles.

Synaptic vesicles were isolated essentially as described (Thoidis et al., 1998; Huttner et al., 1983). Briefly, 4 to 5 adult mouse brains were homogenized in 320 mM sucrose / 4 mM HEPES, pH 7.4, and centrifuged at 1100 g for 10 min. All steps were performed at 4°C. The resulting supernatant and pellet, which was resuspended in cold 320 mM sucrose/ 4 mM HEPES, pH 7.4, were centrifuged for 15 min at 9200 g and 10500 g, respectively. The resulting pellets (crude synaptosomal fraction) were lysed by diluting them in 9 volumes of ice-cold H2O and treated by immediate adjustment by 1 M HEPES, pH 7.4, to a final concentration of 7.5 mM HEPES. After incubation on ice for 30 min, the lysate was centrifuged at 25500 g for 20 min. The supernatant was then centrifuged for 2 h at 130000 g. The resulting pellet representing the crude synaptic vesicle fraction was resuspended in 30 mM sucrose / 4 mM HEPES, pH 7.4, homogenized by passage through a 25-gauge needle, loaded on a continuous gradient of 50-800 mM sucrose / 4 mM HEPES, pH 7.4, and centrifuged at 100000 g for 5h. A broad band in the 200-400 mM sucrose region containing synaptic vesicles was collected and pooled by centrifugation at 250000 g for 2h. The pellet was resuspended in 30 mM sucrose / 4 mM HEPES, pH 7.4 and was found to be highly

enriched in the synaptic vesicle marker synaptophysin and negative for plasma membrane marker Na,K-ATPase and endosomal marker EEA1.

3.4.4. Isolation of lysosomes.

Lysosomes were isolated on a discontinuous OptiPrep gradient using the lysosome isolation kit (Sigma). Fractions were collected at the interfaces of the OptiPrep gradient and assayed for the activity of acid phosphatase, a hydrolase highly accumulated in lysosomes, using the acid phosphatase assay kit (Sigma). The fraction containing the highest acid phosphatase activity (at the interface between 12% and 16% of the OptiPrep) was taken as purified lysosomes. Western blot analysis confirmed that this lysosomal fraction was highly enriched in lysosomal protein lamp2b and negative for trans-Golgi marker protein γ-adaptin.

3.5. Enzymatic assays.

3.5.1. Acid phosphatase assay.

The activity of acid phosphatase was assessed using acid phosphatase assay kit (Sigma-Aldrich). After the incubation at 37°C for 20 min with 4-nitrophenyl phosphate in 0.09 M citrate buffer, pH 4.8 the enzymatic activity was stopped by 0.5 N sodium hydroxide. Then the absorbance was measured at 405 nm wave length by μQuant^{TM} universal microplate spectrophotometer (Bio-Tek Instruments). The acid phosphatase activity was evaluated from the absorbance using an equation as recommended by the manufactured protocol.

3.5.2. Luciferase refolding assay.

For the luciferase refolding assay, brain homogenates, synaptosomes and synaptic vesicles (with a total protein concentration 0.6, 0.23 and 0.64 mg/ml, respectively) or recombinant His_6-Sgt, GST-Csp, His_6-Hsc70 or His_6-CHL1-ICD (50 nM of each protein) were used. Before analysis, brain homogenates were lysed in 1x Luciferase cell culture lysis reagent (Promega) for 15 min on ice and centrifuged at 14000 g for 5 min to collect the supernatants to be used in the assay. Crude synaptosomal fraction was lysed by dilution with 9 volumes of ice-cold H_2O and 1M HEPES, pH 7.4, to a final concentration of 7.5 mM HEPES, and incubation for 30 min on ice. Recombinant luciferase (20 nM, QuantiLum Recombinant Luciferase, Promega) was denatured by incubation for 2 h at 25°C in 8 M guanidine hydrochloride / 2 mM DTT / 30 mM Tris, pH 7.2. Denatured luciferase was then diluted 50-fold in 50 mM KCl / 30 mM HEPES, pH 7.4 / 2 mM DTT/ 3 mM $MgCl_2$ / 1 mM ATP and

mixed (1:1) with the samples. The mixture was incubated for 1h at 30°C and the activity of the refolded luciferase was measured using the Promega luciferase assay system and a TD-20/20 luminometer (Turner Biosystems, Sunnyvale, CA, USA). The activities of equal amounts of denatured and native luciferase in PBS, pH 7.4 were set to 0% and 100%, respectively.

3.5.3. ATPase assay.

ATPase activity was measured by estimating inorganic phosphate (Pi) released during ATP hydrolysis. Recombinant Snap25, synaptophysin and Vamp2 were denatured by incubating them for 10 min at 42°C in 25 mM HEPES buffer, pH 7.5, containing 150 mM KCl, 2 mM DTT, and 5 mM $MgCl_2$. Various combinations of recombinant GST-tagged Csp and His_6-tagged αSgt, Hsc70 and CHL1-ICD (3 μM of each protein) were incubated with denatured or non-denatured Snap25, Synaptophysin or Vamp2 (0.24 μM for each protein) in 20 mM HEPES buffer, pH 7.5, containing 40 mM KCl, 1 mM $(NH_4)_2SO_4$, 2 mM $MgCl_2$, 500 μM DTT, 1.2 mM ATP for 1 h at 30°C. Inorganic phosphate released from ATP was measured using the Malachite green phosphate detection kit (R&D Systems) and μQuantTM universal microplate spectrophotometer (Bio-Tek Instruments) at 660 nm waive length.

3.6. Binding protein assays.

3.6.1. Co-immunoprecipitation.

Homogenates from adult mouse brains were prepared in 50 mM Tris-HCl buffer, pH 7.5, containing 1mM of $CaCl_2$, 1 mM $MgCl_2$, and 1mM $NaHCO_3$. Samples containing 1 mg of total protein were lysed for 40 min at 4°C with lysis buffer, pH 7.5 (RIPA buffer), containing 50 mM Tris-HCl, 150 mM NaCl, 1% Nonidet P-40, 1 mM $Na_2P_2O_7$, 1 mM NaF, 1 mM EDTA, 2 mM Na_3VO_4, 0.1 mM PMSF and complete protease inhibitor cocktail (Roche Diagnostics), and centrifuged for 5 min at 14000g at 4°C. Supernatants were cleared with protein A/G-agarose beads (Santa Cruz Biotechnology) (3 h at 4°C) and incubated with corresponding antibodies or non-specific control Ig (overnight, 4°C), followed by precipitation with protein A/G-agarose beads (1 h, 4°C). The beads were washed 3 times with lysis buffer, 2 times with PBS and boiled in Laemmli buffer. Eluted material was used for Western blot analysis. Co-immunoprecipitation was performed in cooperation with Dr. Leshchyns'ka in the group of Melitta Schachner.

3.6.2. Pull down assay.

In a typical pull down experiment, beads with the bound "prey" protein were incubated with the purified potential binding partners or control proteins overnight at 4°C in 3% BSA, 0.1% Tween 20, 0.1 mM PMSF and 1 mM ADP or ATP in PBS, pH 7.5. After washing with PBS pH 7.5 containing 3% BSA, 0.1% Tween 20, 0.1 mM PMSF, 1 mM ADP (or ATP), protein complexes were eluted from the beads by incubation in Laemmli buffer and analyzed by SDS-PAGE and Western blot using appropriate antibodies.

3.6.3. ELISA (enzyme-linked immunosorbent assay) – protein ligand binding assay.

Csp (0.08 - 1 μM) was immobilized overnight on 96-well polyvinyl chloride plates (Nunc, Roskilde, Denmark) in PBS, pH 7.4. The wells were then blocked for 9 h at 37°C with PBS, pH 7.4, containing 5% BSA. Then they were incubated overnight at 4°C with CHL1-ICD or L1-ICD (33 μM) diluted in PBS, pH 7.4, containing 3% BSA. The plates were washed 5 times with PBS, pH 7.4, containing 0.05% Tween 20 (PBS-T) for 5 min and incubated for 1.5 h at 37°C with monoclonal antibodies 2C2 against CHL1-ICD/ L1-ICD in PBS-T with 3% BSA. After washing with PBS-T, the wells were incubated with peroxidase-coupled secondary antibodies in PBS-T with 3% BSA for 1.5 h at 37°C, then washed 5 times with PBS-T and developed with 0.1% ABTS (Roche Diagnostics) in 100 mM acetate buffer, pH 5.0. The reaction was stopped with 100 mM NaF. The optical density was measured at 405 nm.

4. Immunocytochemistry.

4.1. Cultures of hippocampal neurons.

The experiments with primary cultures of hippocampal neurons were performed in cooperation with Dr. Leshchyns'ka and Dr. Vladimir Sytnyk in the group of Melitta Schachner. Cultures of hippocampal neurons were prepared from 1- to 3-day-old mice. Neurons were grown for 14-21 days in Neurobasal A medium (Invitrogen) supplemented with 2% B-27 (Invitrogen), glutamine (Invitrogen) and basic FGF (2 ng/ml, R&D Systems) on glass coverslips (for live imaging and immunocytochemsitry) or in 6-well plastic plates (for biochemistry) coated with poly-L-lysine (100 μg/ml). For live cell imaging, neurons were transfected 12 days after plating using Lipofectamine 2000 (Invitrogen) according to the manufacturer's instructions. Peptides were introduced to neurons 12 days after plating using Pulsin (Biomol) according to the manufacturer's instructions.

4.2. Loading of FM1-43FX in synaptic boutons.

Loading of FM1-43FX in synaptic boutons was performed in cooperation with Dr. Leshchyns'ka and Dr. Vladimir Sytnyk in the group of Melitta Schachner. Synaptic boutons of hippocampal cultured neurons were loaded with FM1-43FX by incubating neurons for 10 min in the medium containing FM1-43FX (15 μM) (Invitrogen) in the presence of 50 μM PTX (Tocris, Ballwin, MO, USA).

4.3. Immunofluorescence labeling.

Immunofluorescence labeling was performed in cooperation with Dr. Leshchyns'ka and Dr. Vladimir Sytnyk in the group of Melitta Schachner. Immunolabeling was performed as described (Sytnyk et al., 2002). All steps were performed at room temperature. Neurons were fixed for 15 min in 4% formaldehyde in PBS, pH 7.4, permeabilized with 0.25% Triton X-100 in PBS, pH 7.4 for 5 min and blocked with 1% BSA in PBS for 20 min. Primary antibodies were applied in 1% BSA in PBS for 2 hours and detected with corresponding secondary antibodies applied for 45 min. Coverslips were embedded in Aqua-Poly/Mount (Polysciences Inc., Warrington, PA, USA). Images were acquired at room temperature using a confocal laser scanning microscope LSM510 (Zeiss, Jena, Germany).

4.4. Immunofluorescence and FM uptake quantification.

Immunofluorescence and FM uptake quantification were performed in cooperation with Dr. Leshchyns'ka and Dr. Vladimir Sytnyk in the group of Melitta Schachner. In fixed and permeabilized neurons, labeling with SV2 antibodies was used to identify synaptic boutons that were defined as SV2 accumulations with a mean intensity of at least 30% higher than background. The background was defined as the mean intensity of pixels in the square 30x30 pixel area located in the vicinity of the synaptic bouton in the part of the image devoid of synaptic boutons. Synaptic boutons were outlined using a threshold function of the ImageJ software (National Institutes of Health, Bethesda, MD, USA). Within the outlines, mean intensities of the SV2 labeling and FM dye were measured and expressed in arbitrary units defined as 8 bit pixel values of the gray scale image. In each experiment, images were acquired using identical settings and the same threshold was used for all groups.

4.5. Synapto-pHluorin fluorescence quantification.

Synapto-pHluorin fluorescence quantification was performed in cooperation with Dr. Leshchyns'ka and Dr. Vladimir Sytnyk in the group of Melitta Schachner. During recordings, live hippocampal neurons transfected *in vitro* with synapto-pHluorin were maintained at room temperature in modified Tyrode solution (150 mM NaCl, 4 mM KCl, 2 mM $MgCl_2$, 10 mM glucose, 10 mM HEPES and 2 mM $CaCl_2$ (pH 7.4, ~310 mOsm)) or 47mM K^+ buffer (modified Tyrode solution containing equimolar substitution of KCl for NaCl) to induce synaptic vesicle exo- and endocytosis (Virmani et al., 2003). All procedures were performed in the presence of 10 μM CNQX and 50 μM AP-5 to prevent recurrent activation elicited by AMPA and NMDA receptors, respectively. Changes in synapto-pHluorin fluorescence were monitored with time by acquiring images with 1 s intervals interval using a LSM510. With these recorded time series, synaptic boutons were identified as accumulations of synapto-pHluorin fluorescence that appeared following the first application of 47 mM K^+. Fluorescence signals were at least 30% brighte than the background synapto-pHluorin fluorescence before application of 47 mM K^+. Synapto-pHluorin clusters were outlined using ImageJ when synapto-pHluorin fluorescence reached the maximum following the first application of 47 mM K^+. These outlines were then used to measure synapto-pHluorin fluorescence intensity on all images that were recorded before, during and after the first and second application of 47 mM K^+.

V. Results

The results described in this chapter appear in the publications Leshchyns'ka et al. (2006) and Andreyeva et al. (submitted).

1. CHL1 deficiency results in abnormally reduced protein refolding activity in the brain.

Hsc70, identified as a binding partner for the intracellular domain of CHL1 (CHL1-ICD) (Leshchyns'ka et al., 2006), is a constitutively expressed molecular chaperone whose activity is regulated by its binding partners. Thus, we analyzed whether CHL1 regulates chaperone activity in the brain by estimating the efficiency of the refolding of an artificial substrate, denatured firefly luciferase, in brain homogenates from wild type (CHL1+/+) and CHL1 deficient (CHL1-/-) mice. This method has been widely used to study chaperone activities of proteins, among them Hsc70, since enzymatic activity of luciferase reactivated by refolding can be analyzed by measuring its bioluminescence (Tobaben et al., 2001, 2003). Luciferase reactivation was reduced in CHL1-/- versus CHL1+/+ brain homogenates by approximately 50% (Fig. 5A).

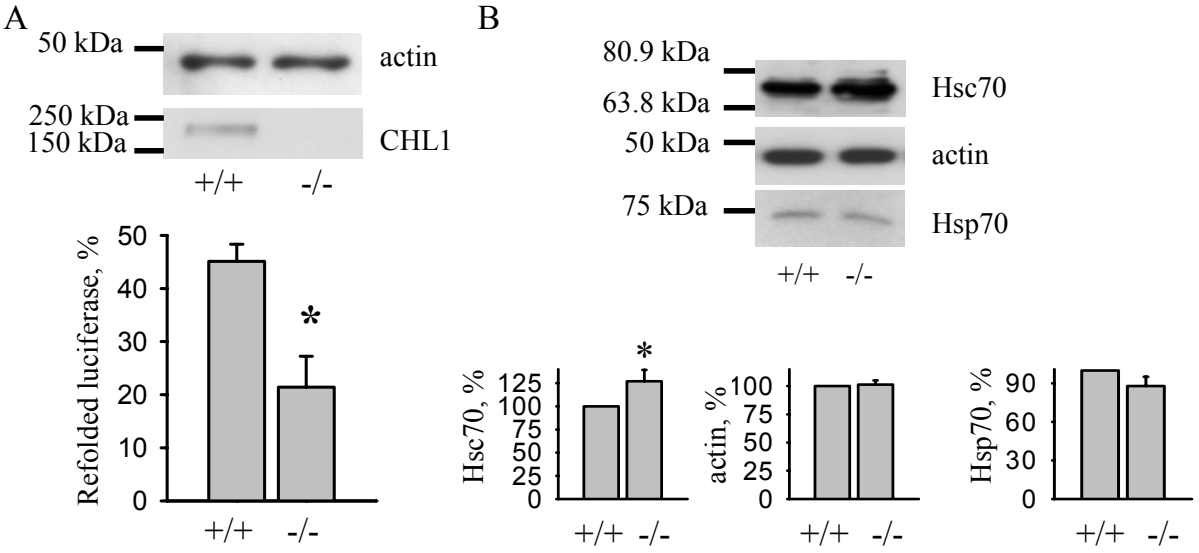

Figure 5: Refolding activity is reduced in CHL1-/- brains. A – Graphs show mean levels of activity ± SEM (n=6) of luciferase reactivated by refolding in CHL1+/+ or CHL1-/- brain homogenates normalized to activity levels of native luciferase set to 100%. The probes used for luciferase reactivation assay were probed by Western blot with antibodies against CHL1 and actin. Similar levels of actin in the probes indicate similar total protein

levels. Reactivation of luciferase is reduced in CHL1-/- probes. *p<0.05, paired t-test. B – Brain homogenates from CHL1+/+ and CHL1-/- mice were probed by Western blot with antibodies against Hsc70, Hsp70 and actin. Diagrams show quantitation of the blots from six experiments. Optical density in wild type was set to 100%. Mean values ± SEM are shown. *p<0.05, paired t-test. Levels of Hsc70 are increased, whereas levels of actin are not changed, in CHL1-/- brain homogenates. Levels of Hsp70 are not changed in CHL1-/- brain homogenates.

Reduced luciferase reactivation in CHL1-/- brains is not due to lower expression of Hsc70, since levels of Hsc70 were upregulated in CHL1-/- brains (Fig. 5B). The latter observation also suggests abnormalities in protein folding in CHL1-/- brains, since synthesis of heat shock proteins is activated in response to intracellular accumulation of denatured proteins (Ananthan et al., 1986; Goff et al., 1985; Parsell et al., 1989).

In differentiated neurons CHL1 accumulates presynaptically, being enriched in the surface membrane of the presynaptic boutons and synaptic vesicles where it interacts with Hsc70 (Fig. 6; Leshchyns'ka et al., 2006).

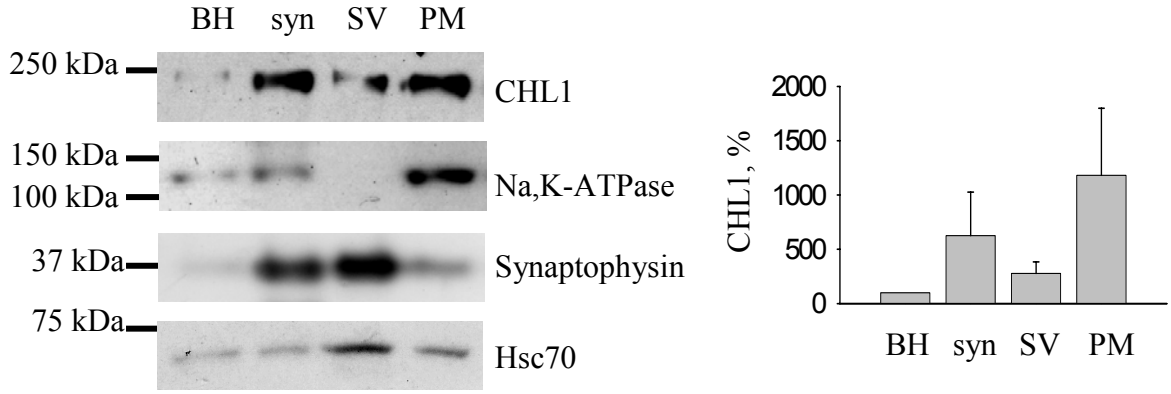

Figure 6: CHL1 accumulates at the synaptic membrane. Brain homogenates (BH), synaptosomes (syn), crude synaptic vesicles (SV), and synaptic plasma membranes (PM) were probed by Western blot with antibodies against CHL1, Na,K-ATPase as a marker of PM, Synaptophysin as a marker of SV, and Hsc70. The diagram shows quantitation of CHL1 labeling from six experiments, with the optical density in Western blot of the homogenate set to 100%. Mean values ± SEM are shown. CHL1 is enriched in the synaptic plasma membrane and is present in SVs.

To analyze whether CHL1 deficiency affects protein refolding activity in synapses, denatured luciferase was incubated with CHL1+/+ or CHL1-/- synaptosomes or synaptic vesicles. Reactivation of the luciferase by chaperone complexes endogenously present in these fractions was reduced in CHL1-/- versus CHL1+/+ probes (Fig. 7), indicating that protein refolding activity is deficient in CHL1-/- presynaptic boutons.

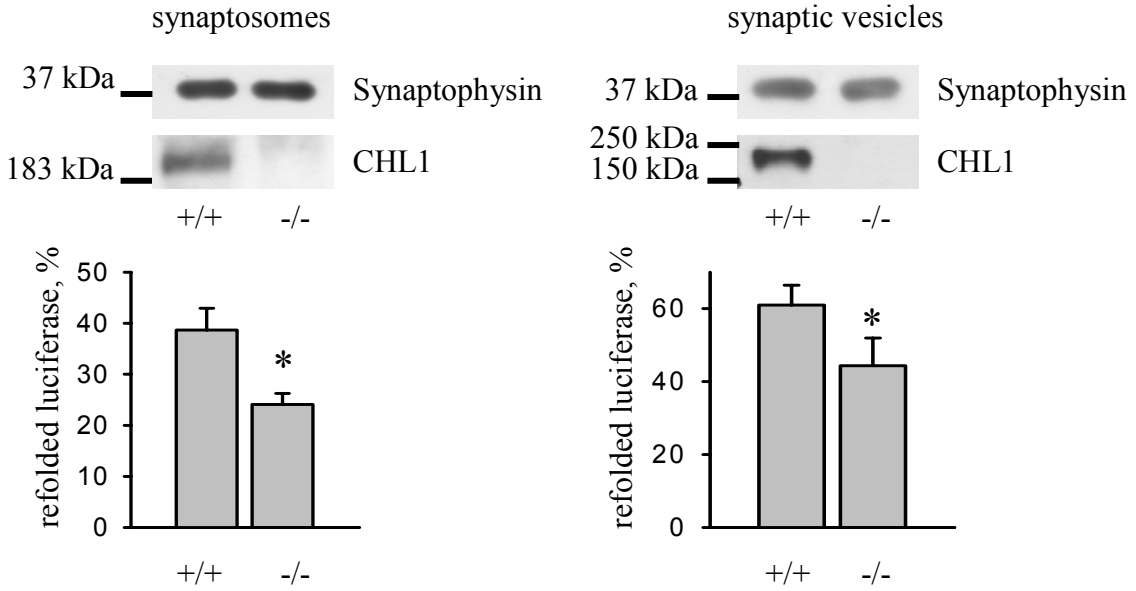

Figure 7: Refolding activity is reduced in synaptosomes and synaptic vesicles from CHL1-/- brains. Graphs show mean levels of activity ± SEM (n=6) of luciferase reactivated by refolding in CHL1+/+ or CHL1-/- synaptosomes or synaptic vesicles normalized to activity levels of native luciferase set to 100%. The probes used for luciferase reactivation assay were probed by Western blot with antibodies against CHL1 and Synaptophysin. Similar levels of Synaptophysin in the probes indicate similar total protein levels. Reactivation of luciferase is reduced in CHL1-/- probes. *p<0.05, paired t-test.

Reactivation of luciferase activity was increased to CHL1+/+ levels when CHL1-/- synaptosomes were preincubated with CHL1-ICD (Fig. 8). In contrast, the intracellular domain of the cell adhesion molecule L1, extracellular domain of CHL1 fused to Fc or Fc alone did not influence luciferase reactivation in CHL1-/- synaptosomes (Fig. 8).

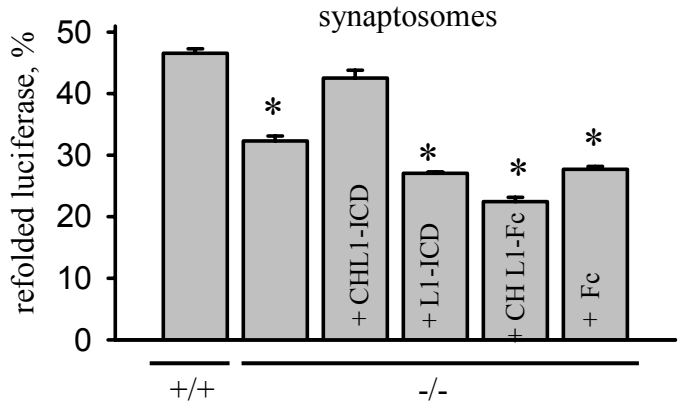

Figure 8: Refolding activity is regulated by CHL1 intracellular domain (CHL1-ICD). Graph shows mean levels of activity ± SEM (n=6) of luciferase reactivated by refolding in CHL1+/+ or CHL1-/- synaptosomes, or in CHL1-/- synaptosomes pre-incubated with recombinant CHL1-ICD, L1 intracellular domain (L1-ICD), CHL1 extracellular domain fused to Fc (CHL1-Fc) or Fc alone. Values were normalized to activity levels of native

luciferase set to 100%. Reactivation of luciferase in CHL1-/- synaptosomes pre-incubated with CHL1-ICD is increased. *p<0.05, paired t-test (compared to CHL1+/+ brain homogenates).

A possible explanation for this phenomenon could be that CHL1-ICD possesses refolding activity. The efficiency of luciferase reactivation in the presence of CHL1-ICD was, however, approximately three times lower than in the presence of recombinant Hsc70 analyzed for comparison (Fig. 9A), suggesting low intrinsic refolding activity for CHL1-ICD. Since the ATPase activity of chaperones presumably provides free energy for refolding of misfolded proteins, we also analyzed whether CHL1-ICD possesses intrinsic ATPase activity by estimating the amount of free phosphate released from ATP in the presence of CHL1-ICD. ATPase activity in the presence of CHL1-ICD was negligible when compared to Hsc70 (Fig. 9B). Since CHL1-ICD has very low intrinsic protein refolding and ATPase activity, intracellular domain of CHL1 could promote protein refolding by activating chaperones, probably including Hsc70.

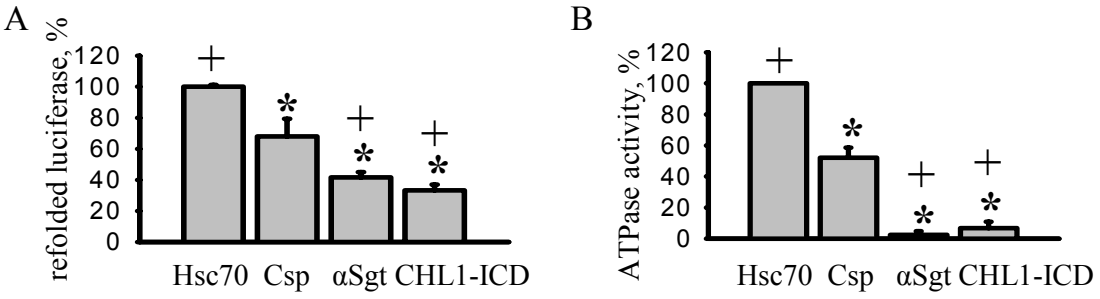

Figure 9: Hsc70 and Csp, but not αSgt and CHL1 possess intrinsic ATPase and protein refolding activities. A – Graph shows mean levels of activity ± SEM (n=6) of the luciferase, that was reactivated by refolding in the presence of recombinant Hsc70, Csp, αSgt, or CHL1-ICD. Values were normalized to the luciferase reactivation levels in the presence of Hsc70. Note, that luciferase reactivation in the presence of CHL1-ICD and αSgt was lower than in the presence of Hsc70 and Csp. Taking into account that CHL1-ICD and αSgt do not show detectible ATPase activity, luciferase reactivation in the presence of these two proteins most probably occurs via spontaneous refolding of luciferase. *,+p<0.05, paired t-test (when compared to the group incubated with Hsc70 (*), or with Csp (+)). B – Graph shows mean levels of free inorganic phosphate ± SEM (n=6) released from ATP (ATPase activity) in the presence of recombinant Hsc70, Csp, αSgt, or CHL1-ICD. Values were normalized to the ATPase activity in the presence of Hsc70. Note, that Hsc70 and Csp but not CHL1-ICD and αSgt possess detectable intrinsic ATPase activity. *,+p<0.05, paired t-test (when compared to the group incubated with Hsc70 (*), or with CSP (+)).

2. CHL1 directly interacts with Hsc70, Csp and αSgt and regulates their activity.

Csp and αSgt have been shown to functionally cooperate with Hsc70 in synapses (Tobaben et al., 2001, 2003; Fernandez-Chacon et al., 2004). Similarly to Hsc70, levels of Csp and αSgt were increased in CHL1-/- versus CHL1+/+ brains (Fig. 5B, 10).

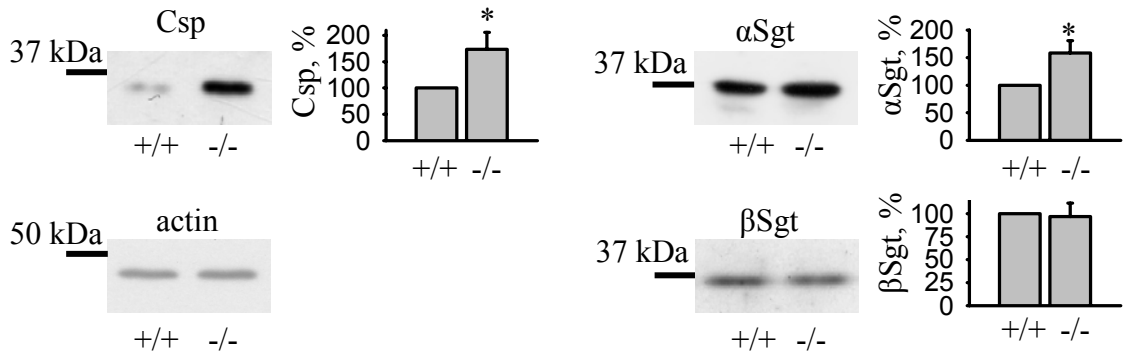

Figure 10: Levels of Csp and αSgt are increased in CHL1-/- brain homogenates. CHL1+/+ and CHL1-/- brain homogenates were probed by Western blot with antibodies against Csp, αSgt and βSgt. Representative blots are shown. Graphs show mean optical densities of the blots ± SEM (n=6) with optical density for CHL1+/+ probes set to 100%. Note that levels of Csp, αSgt, but not βSgt are increased in CHL1-/- versus CHL1+/+ brain homogenates. *p<0.05, paired t-test.

Hence, deficient functioning of Hsc70 and its co-chaperones rather than changes in expression levels are likely to result in reduced refolding activity in CHL1-/- brains. To analyze whether CHL1 interacts with the co-chaperones of Hsc70, co-immunoprecipitation experiments were carried out. Csp and αSgt, but not βSgt, co-immunoprecipitated with CHL1 from brain lysates (Fig. 11).

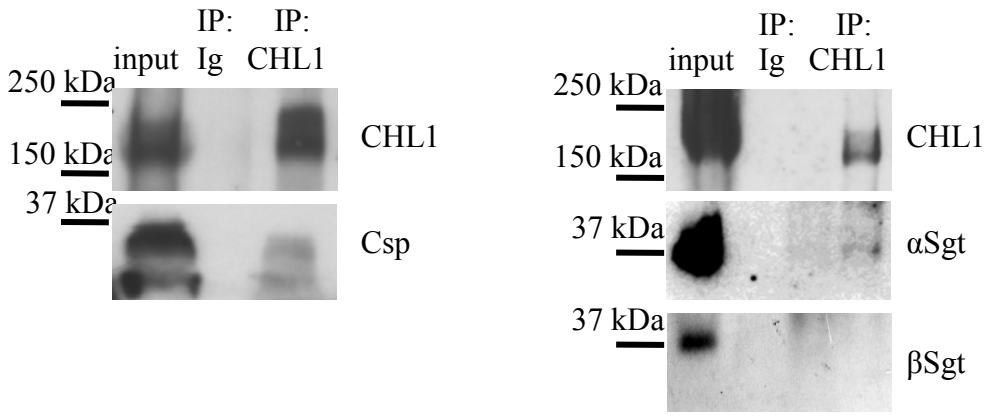

Figure 11: CHL1 interacts with Hsc70, Csp and αSgt. CHL1 immunoprecipitates (IP) from brain lysates and input material were probed with antibodies against Csp, αSgt and βSgt by Western blot. Mock IP with non-

specific immunoglobulins (Ig) was performed for control. Csp and αSgt, but not βSGT co-immunoprecipitated with CHL1. Co-immunoprecipitation was performed in cooperation with Dr. Leshchyns'ka in the group of Melitta Schachner.

To clarify whether this was due to direct binding, we tested whether CHL1-ICD could be pulled down with recombinant Csp, αSgt or βSgt, or Hsc70 used as positive control (Leshchyns'ka et al., 2006). CHL1-ICD was pulled down not only with Hsc70 (Fig. 12), but also with Csp and αSgt, but not with βSgt (Fig. 12). The interaction between Csp and CHL1-ICD was also confirmed by ELISA assay. Thus, CHL1 directly interacts with Csp and αSgt and does not require Hsc70 as a linker.

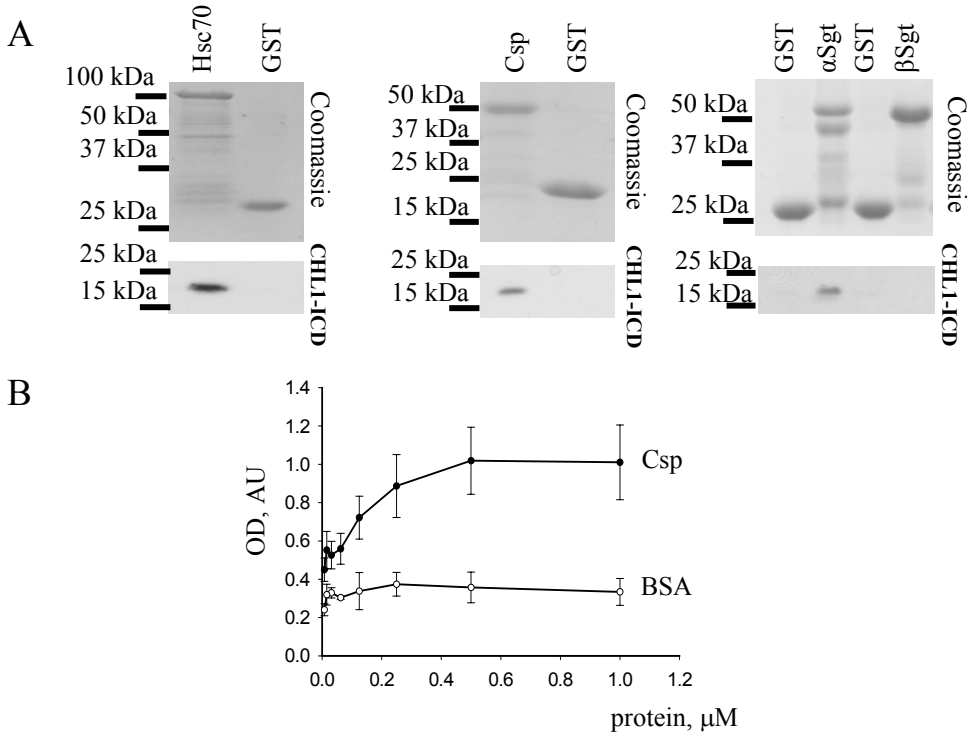

Figure 12: CHL1 directly interacts with Hsc70, Csp and αSGT. A – GST and GST-tagged Hsc70, Csp, αSgt, βSgt immobilized on beads were assayed for their ability to pull down CHL1-ICD. Coomassie blue stained gels show that levels of Hsc70, Csp, αSGT and βSGT immobilized on beads were similar or lower than levels of GST on control beads. Lower molecular weight products of the recombinant proteins derive from degradation. CHL1-ICD was pulled down with Hsc70, Csp and αSgt, but not with GST or βSGT. B – Csp was bound to plastic and assayed by ELISA for the ability to bind CHL1 intracellular domain. Binding to BSA served as a control. Mean values (OD 405) ± SEM (n = 6) are shown. Csp bound to CHL1-ICD.

To investigate whether direct binding of CHL1-ICD to Hsc70, Csp and αSgt influences their ability to refold proteins, we studied refolding of denatured luciferase by Hsc70, Csp, αSGT, and combinations thereof, in the presence or absence of CHL1-ICD. Protein refolding activity of Hsc70 was slightly inhibited by CHL1-ICD (Fig. 13). However, reactivation of luciferase

by Csp and αSgt alone, or combinations of Hsc70/Csp, Hsc70/αSgt, CSP/αSgt or Hsc70/Csp/αSgt was enhanced by approximately up to 50% when CHL1-ICD was added to the incubation buffer (Fig. 13).

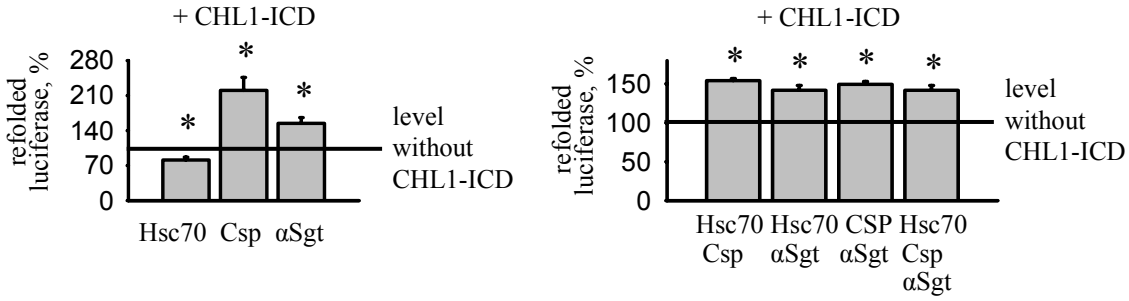

Figure 13: CHL1 regulates Hsc70, Csp and αSgt refolding activity. Graphs show mean levels of activity ± SEM (n=6) of luciferase reactivated by Hsc70, Csp, αSgt applied as indicated together with CHL1-ICD. Values were normalized to luciferase reactivation levels in the absence of CHL1-ICD set to 100%. CHL1-ICD inhibits refolding activity of Hsc70 while refolding activity of other combinations is enhanced. *p<0.05, paired t-test (compared to luciferase reactivation levels in the absence of CHL1-ICD (solid lines)).

3. CHL1 deficiency results in reduced levels of αSgt at synapses and synaptic vesicles.

CHL1 deficiency results in reduced levels of Hsc70 in synaptic vesicles (Fig. 14).

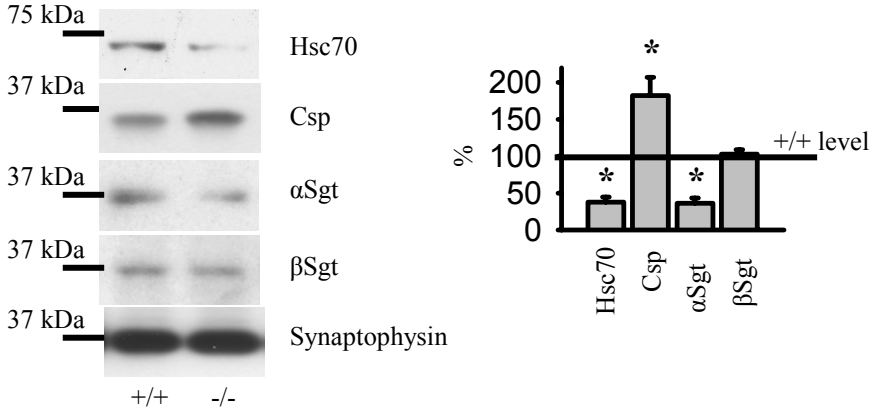

Figure 14: CHL1 recruits Hsc70 and αSgt to synaptic vesicles. CHL1+/+ and CHL1-/- synaptic vesicles were probed by Western blot with the indicated antibodies. Graphs show mean optical density of the protein bands in CHL1-/- synaptic vesicles ± SEM (n=6) normalized to the optical density in CHL1+/+ set to 100%. Levels of Hsc70 and αSgt are decreased while levels of Csp are increased in CHL1-/- synaptic vesicles. Levels of βSgt are similar in both genotypes. Synaptophysin served as a loading control. *p<0.05, paired t-test (when compared to CHL1+/+ level (solid line)).

In contrast, Csp levels were increased in CHL1-/- versus CHL1+/+ synaptic vesicles (Fig. 14), correlating with the overall enhanced expression of Csp in CHL1-/- brain homogenates (Fig. 10). Although levels of αSgt were also increased in CHL1-/- brain homogenates (Fig. 10), levels of αSgt, but not βSgt, were reduced by approximately 50% in synaptic vesicles and synaptosomes from CHL1-/- mice (Fig. 14, Fig. 15). The levels of Hsp70, an inducible counterpart of Hsc70, in CHL1-/- synaptosomes were increased by approximately 60% (Fig. 15), whereas the expression of Hsp70 in CHL1-/- brain homogenates was the same as in CHL1+/+ brain homogenates (Fig. 5). It suggests that Hsp70 is recruited to CHL1-/- synapses instead of Hsc70.

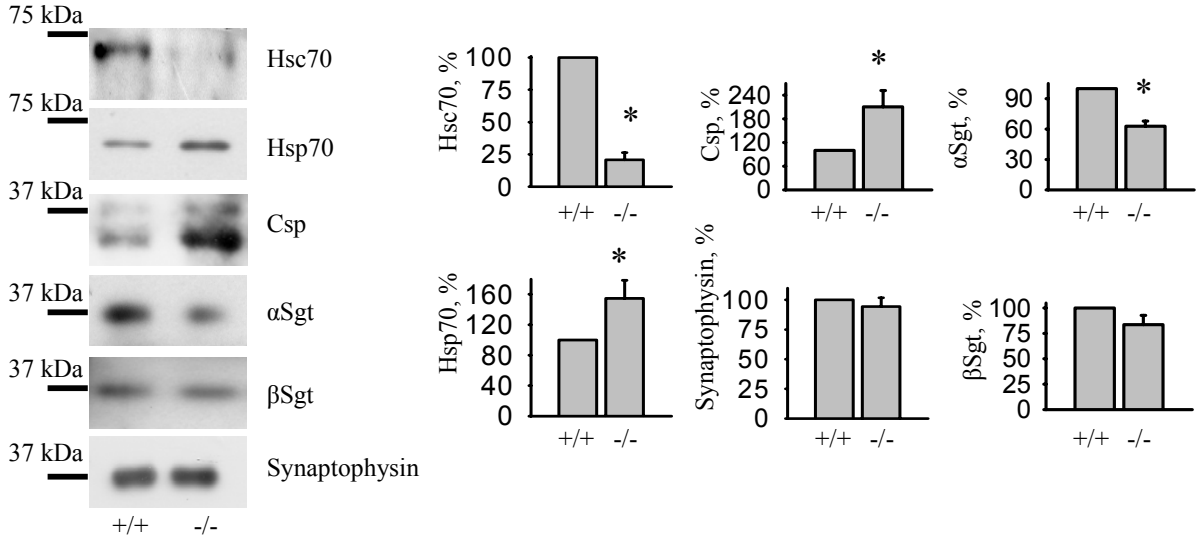

Figure 15: Levels of Hsc70, Csp and αSGT in CHL1+/+ and CHL1-/- synaptosomes. CHL1+/+ and CHL1-/- synaptosomes isolated from CHL1+/+ and CHL1-/- brains were probed by Western blot with antibodies against Hsc70, Csp, αSgt and βSgt. Representative blots are shown. Graphs show mean optical densities of the blots ± SEM (n=6) with optical density for CHL1+/+ probes set to 100%. Note that levels of αSgt, but not βSgt are decreased in CHL1-/- versus CHL1+/+ synaptosomes. Levels of Hsp70 and Csp are increased in CHL1-/- versus CHL1+/+ synaptosomes. *$p<0.05$, paired t-test.

All these observations implicate CHL1 in targeting not only Hsc70, but also αSgt to presynaptic boutons and synaptic vesicles. Csp, then, appears to be targeted to synaptic vesicles independently of CHL1, probably via palmitoylation of cysteine residues (Greaves et al., 2006).

4. CHL1 inhibits formation of the Hsc70/Csp/αSgt complex by promoting formation of the CHL1/Csp and CHL1/Hsc70/αSgt complexes.

Since CHL1-ICD associates with the individual components of the Hsc70/Csp/αSgt complex, we analyzed whether CHL1 associates with the Hsc70/Csp/αSgt complex also. Binding of Hsc70, Csp and αSgt to CHL1-ICD immobilized on beads was analyzed under conditions when Hsc70, Csp and αSgt were present together in the incubation buffer. Since nucleotides influence binding of CHL1-ICD to Hsc70 (Leshchyns'ka et al., 2006) and formation of the trimeric Hsc70/Csp/αSgt complex (Tobaben et al., 2001), interactions were analyzed in the presence of ADP or ATP. Western blot analysis of the proteins that bound to the beads showed that Hsc70, Csp and αSgt interacted with CHL1-ICD but not with L1-ICD. However, while pull down of Hsc70 and αSgt with CHL1-ICD was more efficient in the presence of ADP versus ATP, pull down of Csp with CHL1-ICD was more efficient in the presence of ATP versus ADP (Fig. 16).

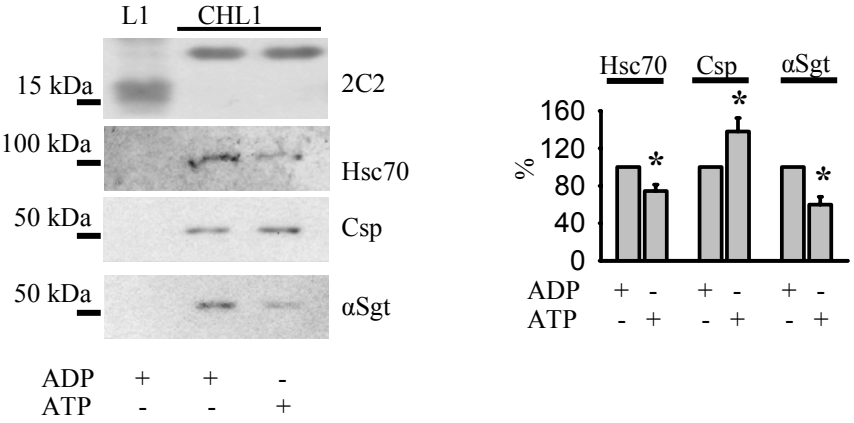

Figure 16: Association of CHL1-ICD with the components of Hsc70/Csp/αSgt complex. CHL1-ICD and L1-ICD immobilized on beads were assayed for their ability to pull down Hsc70, Csp and αSgt from a mixture of these proteins in the presence of ADP or ATP. Labeling with 2C2 antibodies recognizing CHL1-ICD and L1-ICD shows that similar levels of both proteins were immobilized on beads. Graph shows mean optical density (OD) of the blots ± SEM (n=6) with the levels of the proteins bound to beads in the presence of ADP set to 100%. Hsc70, αSgt and Csp were pulled down with CHL1-ICD but not to L1-ICD. Binding of Hsc70 and αSgt to CHL1-ICD is enhanced by ADP, while binding of Csp to CHL1-ICD is enhanced by ATP. *$p<0.05$, paired t-test (compared as indicated).

This opposite pattern of interactions between CHL1-ICD and Csp versus CHL1-ICD and Hsc70 and αSgt suggested that, rather than to form tetrameric CHL1-ICD/Hsc70/Csp/αSgt complexes, CHL1-ICD preferentially associates with Csp in dimeric CHL1-ICD/Csp complexes that are formed more efficiently in the presence of ATP, while CHL1-ICD

preferentially associates with Hsc70 and αSgt in trimeric CHL1-ICD/Hsc70/αSgt complexes that are formed more efficiently in the presence of ADP.

To analyze whether CHL1-ICD influences formation of the Hsc70/CSP/αSgt complex, binding of Hsc70 and αSgt to Csp immobilized on beads was analyzed in the presence or absence of CHL1-ICD and ADP or ATP. In the absence of CHL1-ICD, Hsc70 and αSgt bound to Csp (Fig. 17) in accordance with a previous report (Tobaben et al., 2001). Levels of Hsc70 and αSgt that were pulled down with Csp were reduced when CHL1-ICD was present in the incubation buffer in the presence of ATP (Fig. 17), that is under conditions favorable for CHL1-ICD/Csp complex formation (Fig. 16). This result suggested that CHL1-ICD binding to Csp in the presence of ATP inhibits the association of Csp with Hsc70 and αSgt. Indeed, a reduction in the binding of Csp to Hsc70 and αSgt correlated with increased binding of Csp to CHL1-ICD (Fig. 17). In the presence of ADP, that is under conditions of reduced binding of CHL1-ICD to Csp (Fig. 16), the inhibitory effect of CHL1-ICD on the interactions between Csp and αSgt and Hsc70 was less obvious.

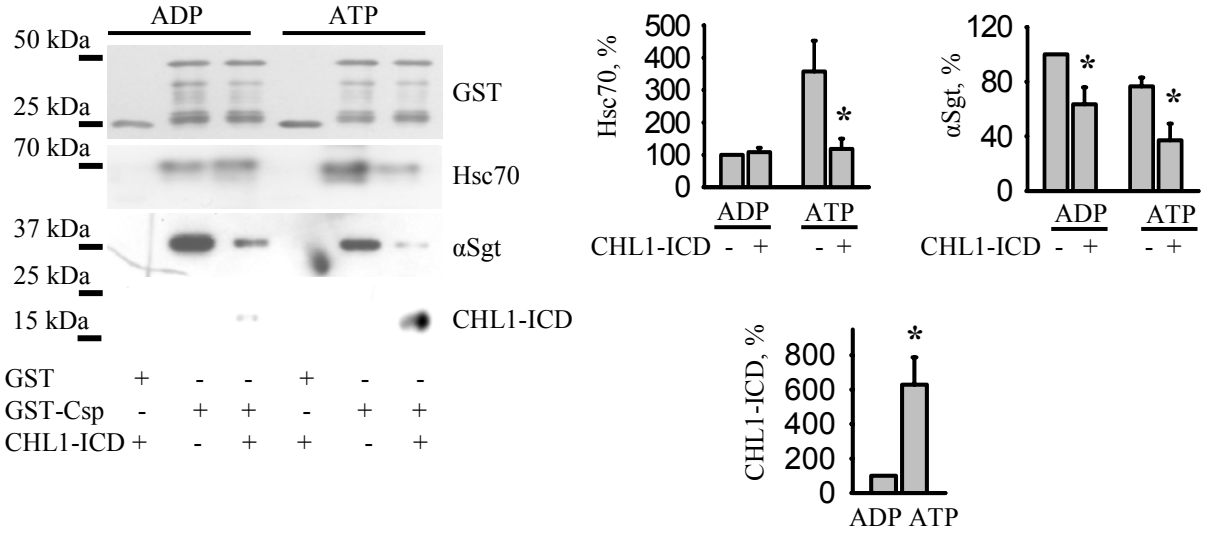

Figure 17: CHL1 inhibits association of Hsc70 and αSgt with Csp. GST and GST-tagged Csp immobilized on beads were assayed for their ability to pull down Hsc70 and αSgt from a mixture of these proteins in the presence of ADP or ATP with or without CHL1-ICD. Graphs show mean optical density of the blots ± SEM (n=6). For quantitation of the binding of Hsc70 and αSgt to Csp (left and middle graphs), levels of these proteins bound to Csp in the presence of ADP and absence of CHL1-ICD were set to 100%. For quantitation of the binding of CHL1-ICD to Csp (right graph), levels of CHL1-ICD bound to Csp in the presence of ADP were set to 100%. Note that in the presence of ATP, CHL1-ICD binds to Csp with higher efficiency than in the presence of ADP and inhibits more strongly the interaction of Csp with Hsc70 and αSgt. *$p<0.05$, paired t-test (compared as indicated).

Since CHL1-ICD and Csp bind to Hsc70 via similar HPD tripeptide based motifs (Leshchyns'ka et al., 2006; Chamberlain et al., 1997b), CHL1 may inhibit Hsc70/Csp/αSgt complex formation by competing with Csp for binding to Hsc70 (see Fig. 33 for a scheme). To further analyze the mechanism, by which CHL1 inhibits formation of the Hsc70/Csp/αSgt complex, we attempted to identify binding sites within CHL1-ICD for Hsc70, Csp, and αSgt. Fragments of CHL1-ICD that either contained the membrane adjacent portions of CHL1-ICD of different lengths ranging from 25 to 85 amino acids or the whole CHL1-ICD without the membrane proximal 25 amino acid stretch, were immobilized on beads and assayed for their ability to pull down Hsc70, Csp or αSgt. All membrane proximal fragments of CHL1-ICD bound to Hsc70 and Csp, but not to αSgt (Fig. 18), suggesting that Hsc70 and Csp bind to the same or closely located sequences within the 25 amino acid stretch containing the HPD tripeptide. In contrast, deletion of the C-terminal 19 amino acid stretch of CHL1-ICD abolished the interaction between CHL1-ICD and αSgt (Fig. 18), suggesting that this fragment contains the binding site for αSgt. Confirming this finding, the CHL1-ICD fragment without the membrane adjacent 25 amino acid stretch bound to αSgt but not Hsc70 and Csp (Fig. 18). Thus, our results suggest that not only CHL1 and Csp compete for Hsc70, but also that Csp bound to CHL1-ICD would sterically interfere with the interaction between CHL1-ICD and Hsc70 (see Fig. 33 for a scheme).

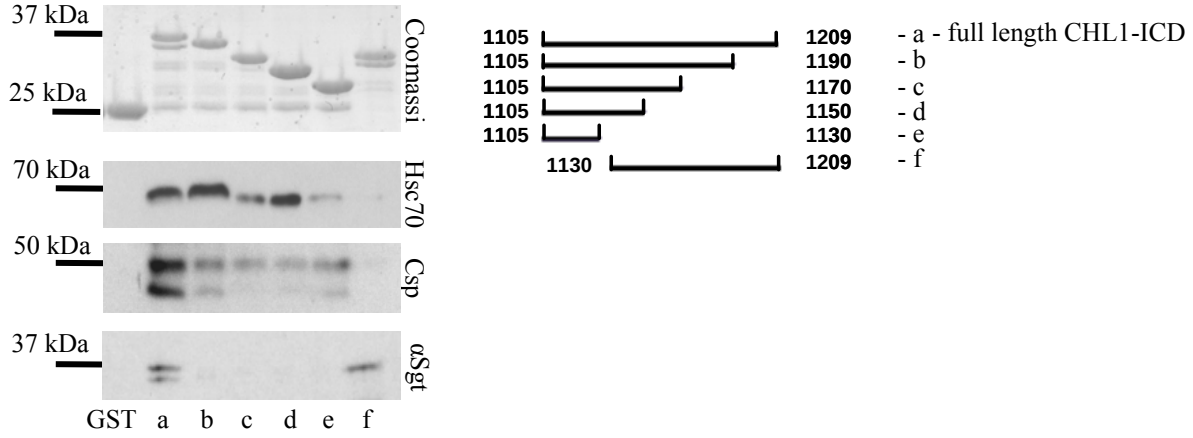

Figure 18: Binding sites within CHL1-ICD for Hsc70, Csp, and αSgt. Scheme shows CHL1-ICD fragments marked alphabetically that were immobilized on beads via the GST tag and assessed for their ability to pull down Hsc70, Csp or αSgt. Coomassie blue stained gel shows that similar levels of CHL1 fragments were immobilized on beads. Lower molecular weight degradation products of the recombinant proteins are also observed. Binding of Hsc70, Csp and αSgt to CHL1-ICD fragments was analyzed by Western blot with the corresponding antibodies. Note that amino acids 1105-1130 within CHL1-ICD are necessary to bind Hsc70 and Csp, while amino acids 1190-1209 are necessary to bind αSgt. Double bands recognized by Csp antibodies represent oligomeric forms of recombinant Csp as described previously (Swayne et al., 2003).

To support our data with purified proteins, protein complexes in synaptic vesicles and synaptic plasma membranes isolated from brain tissue were separated by PAGE under non-denaturing conditions and analyzed by Western blot. In synaptic vesicles, CHL1 was present predominantly in complexes with molecular weights above 440 kDa and at approximately 220 kDa (Fig. 19A). The CHL1 containing broad band above 440 kDa overlaped with Hsc70 and αSgt immunoreactive bands (Fig. 19A) and was negative for Csp indicating that CHL1, Hsc70 and αSgt but not Csp were present in this complex. This higher than expected molecular weight of the complex, being approximately two times higher than the sum of molecular weights of CHL1, Hsc70 and αSgt, could be due to multimerization of the complex or to the presence of other proteins in this complex. The CHL1 immunoreactive band of approximately 220 kDa overlaped with the Csp positive band and was negative for αSgt and Hsc70 (Fig. 19A), suggesting that this broad band contained the CHL1/Csp complex. Note negligible levels of Csp immunoreactivity in CHL1+/+ synaptic vesicles in the high molecular weight area that was positive for αSgt and Hsc70 (Fig. 19A) suggesting that trimeric Hsc70/Csp/αSgt complexes were not formed.

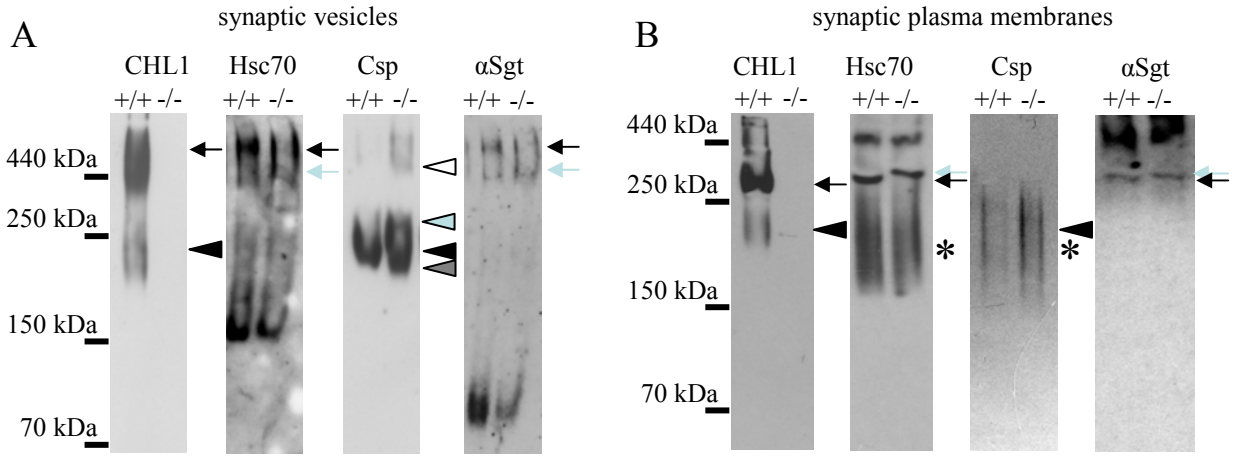

Figure 19: Molecular composition of Hsc70, Csp and αSgt containing complexes in CHL1+/+ and CHL1-/- synaptic vesicles and plasma membranes. A-B – Molecular complexes in CHL1+/+ and CHL1-/- synaptic vesicles (A) and synaptic plasma membranes (B) were separated by PAGE under non-denaturing conditions and probed by Western blot with the indicated antibodies. Note that αSgt and Hsc70 positive bands overlap with CHL1 labeled areas at around 580 kDa in synaptic vesicles and 290 kDa in synaptic plasma membranes, which contain only minor levels (in synaptic vesicles) or are negative (in synaptic plasma membranes) for Csp. Csp positive bands overlap with the CHL1 positive area at around 220 kDa that is negative for αSgt. Note that Csp, αSgt and Hsc70 bands are shifted in CHL1-/- versus CHL1+/+ probes (grey versus black arrows, respectively). High molecular weight CSP positive bands are observed in CHL1-/- but not in CHL1+/+ synaptic vesicles (arrowheads).

In synaptic plasma membranes, the major CHL1-immunoreactive band was observed at approximately 300 kDa (Fig. 19B). This band overlaped with Hsc70 and αSgt

immunoreactive bands and was negative for Csp (Fig. 19B), thus containing the CHL1/Hsc70/αSgt complex. A minor CHL1 immunoreactive band of approximately 220 kDa overlaped with the Csp positive broad band and was negative for αSgt, thus containing CHL1/Csp complexes (Fig. 19B). The Csp immunoreactive broad smear around 200 kDa was also positive for Hsc70, thus probably containing Csp/Hsc70 complexes (Fig. 19B). CHL1/Hsc70 and CHL1/Hsc70/Csp complexes that should be of a higher molecular weight of approximately 250 and 285 kDa, hence, were not present in this band.

To analyze whether CHL1 deficiency affects the composition of the chaperone complexes, CHL1-/- synaptic vesicles and synaptic plasma membranes were analyzed in parallel with CHL1+/+ probes. In CHL1-/- synaptic vesicles, Hsc70, Csp and αSgt immunoreactive bands presumably containing CHL1/Hsc70/αSgt and CHL1/Csp complexes were shifted to a lower molecular weight (Fig. 19A). Note, the Csp positive signal at 460 kDa with immunoreactivity for αSgt and Hsc70 (Fig. 19A), thus probably containing the trimeric Hsc70/Csp/αSgt complexes. An additional Csp containing high molecular weight band was also observed (Fig. 19A), suggesting that the pattern of Csp interactions with other proteins was changed in the absence of CHL1. Probably for similar reasons, CHL1 containing Hsc70 and αSgt positive bands were shifted to a higher molecular weight in CHL1-/- synaptic plasma membranes (Fig. 19B).

This analysis showed that also in brain tissue CHL1 is associated with Hsc70, Csp, and αSgt predominantly in trimeric CHL1/Hsc70/αSgt and dimeric CHL1/Csp complexes, while tetrameric CHL1/Hsc70/Csp/αSgt or trimeric Hsc70/Csp/αSgt complexes were not detectable (Fig. 19). CHL1 deficiency resulted in a shift of Hsc70, Csp and αSgt positive bands to a higher or lower molecular weight range suggesting that the composition of the molecular complexes containing these proteins is changed (Fig. 19). Interestingly, trimeric Hsc70/Csp/αSgt complexes were indeed detected in CHL1-/- synaptic vesicles (Fig. 19), confirming that CHL1 inhibits formation of this complex as observed in the binding assay (Fig. 17).

5. CHL1 associates with the SNARE complex proteins and regulates their refolding.

Hsc70 and its co-chaperones associate with the components of the synaptic vesicle recycling machinery and play a critical role in regulated neurotramsitter release (Evans et al., 2003; Bronk et al., 2001; Evans et al., 2002). To analyze whether CHL1 also associates with the synaptic vesicle exocytotic machinery, we probed CHL1 immunoprecipitates from brain

lysates by Western blot with antibodies against one of the major constituents of this machinery, the SNARE complex: the SNARE complex proteins Snap25, Syntaxin1B and Vamp2 co-immunoprecipitated with CHL1 (Fig. 20A). Another synaptic vesicle associated protein, Synapsin1, also co-immunoprecipitated with CHL1, while Synaptophysin did not (Fig. 20A).

To investigate how CHL1 and associated chaperones associate with the SNARE complex components, we first characterized the subsynaptic distribution of SNARE complex proteins in relation to CHL1 and associated chaperones. Western blot analysis of synaptic vesicle and synaptic plasma membrane fractions showed that CHL1, Hsc70, αSgt and Csp were present in synaptic vesicles and synaptic plasma membranes (Fig. 20B, 14, 19). Csp was enriched in synaptic vesicles versus synaptic plasma membrane fraction overlapping in distribution with Vamp2 and Synapsin1 (Fig. 20B).

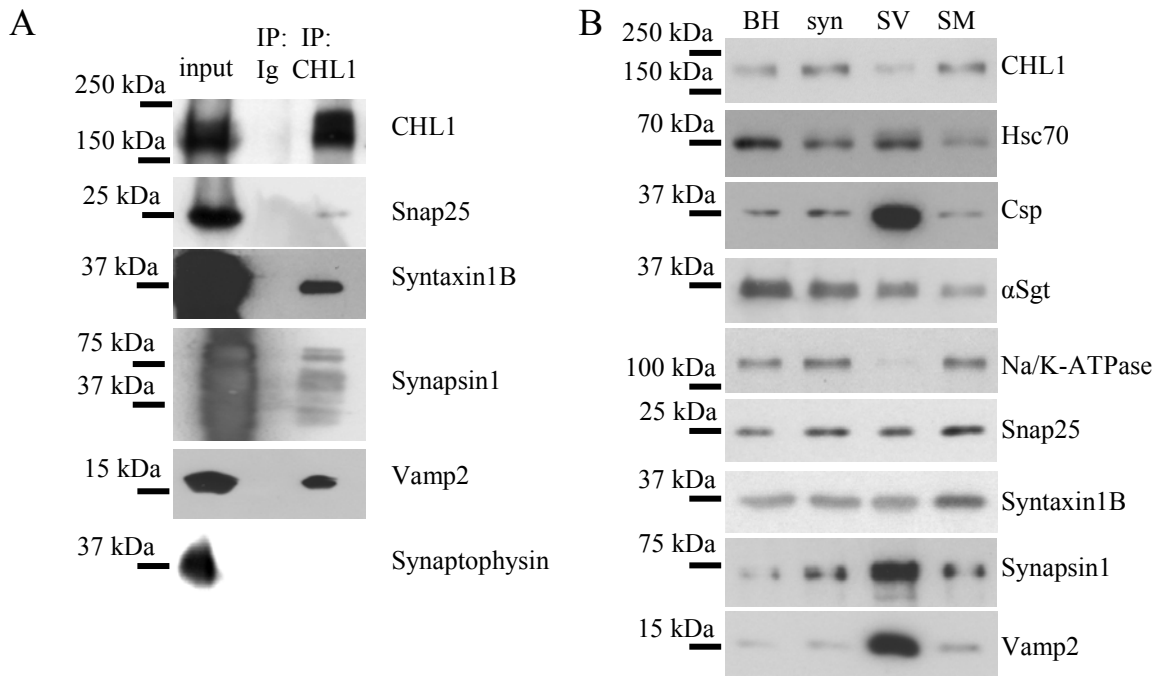

Figure 20: CHL1 interacts with SNARE complex proteins. A – CHL1 immunoprecipitates (IP) from brain lysates and input material were probed with the indicated antibodies by Western blot. Mock IP with non-specific rabbit immunoglobulins (Ig) was performed for control. Snap25, Syntaxin1B, Vamp2 and Synapsin1, but not Synaptophysin co-immunoprecipitated with CHL1. B – CHL1+/+ brain homogenates (BH), synaptosomes (syn), crude synaptic vesicle fraction (SV), and synaptic plasma membranes (SM) were probed by Western blot with the indicated antibodies. CHL1, Hsc70 and αSgt are present in synaptosomes as well as in synaptic vesicles and synaptic plasma membranes derived from synaptosomes. Subsynaptically, Csp is enriched in synaptic vesicles and reduced in synaptic plasma membranes. While Vamp2 and Synapsin1 are highly enriched in synaptic vesicles, Syntaxin1B and Snap25 are moderately enriched in the synaptic plasma membrane fraction. Na,K-ATPase served as a plasma membrane marker. Co-immunoprecipitation was performed in cooperation with Dr. Leshchyns'ka in the group of Melitta Schachner.

CHL1 showed a distribution that was similar to that of Syntaxin1B and Snap25, being present in synaptic vesicles and further enriched in the synaptic plasma membrane fraction (Fig. 20B). Hsc70 and αSgt were also present both in synaptic vesicle and synaptic plasma membrane fractions with a moderate preference for synaptic vesicles (Fig. 20B). These observations suggest that Csp-containing chaperone complexes are formed predominantly in synaptic vesicles and may take part in refolding of synaptic vesicle associated proteins, such as Vamp2. In contrast, CHL1, Hsc70 and αSgt show a lower preference for localization in synaptic vesicles and thus could also participate in refolding of synaptic plasma membrane associated proteins, such as Syntaxin1B and Snap25.

To analyze whether interactions between CHL1 and the SNARE complex depend on synaptic activity, formation of these complexes was analyzed in synaptosomes that were treated for 90 s with a buffer containing nominal 4 mM K+, or a buffer containing 47 mM K+ to depolarize synaptic plasma membranes and induce synaptic vesicle exo- and endocytosis. Western blot analysis of CHL1 immunoprecipitates from synaptosomes showed that co-immunoprecipitation of Snap25 and Syntaxin1B with CHL1 was significantly enhanced in synaptosomes activated with 47 mM K+ (Fig. 21).

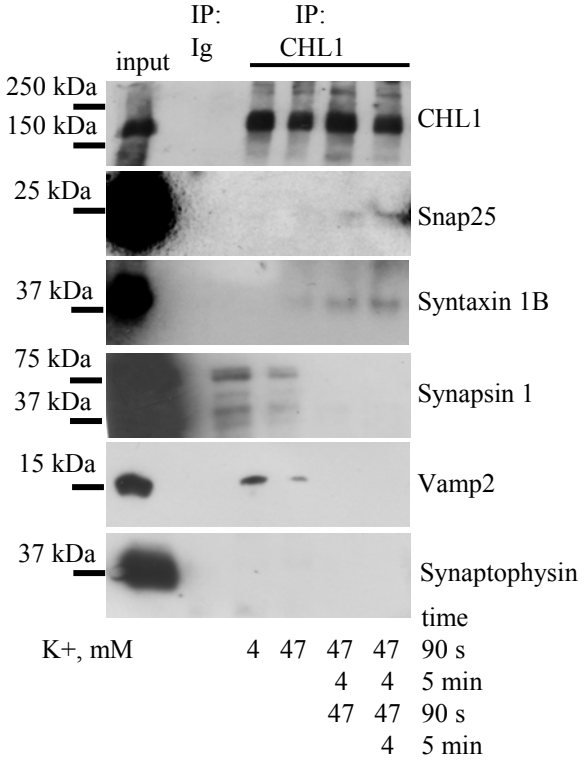

Figure 21: The interactions between CHL1 and SNARE complex components depend on synaptic activity. CHL1 was immunoprecipitated (IP) from synaptosomes that were mock-stimulated with 4 mM K+, or stimulated one or two times with 47 mM K+ for 90 s with or without 5 min recovery in 4 mM K+ after stimulations (as indicated). CHL1 immunoprecipitates and input material were then probed by Western blot with indicated antibodies. Mock IP with non-specific immunoglobulins (Ig) was performed for control. Stimulation

increases levels of co-immunoprecipitated Snap25 and Syntaxin1B, and decreases levels of co-immunoprecipitated Vamp2 and Synapsin1. Co-immunoprecipitation was performed in cooperation with Dr. Leshchyns'ka in the group of Melitta Schachner.

Interestingly, in 47 mM K+ stimulated synaptosomes that were allowed to recover for 5 min in 4 mM K+ and stimulated again for 90 s with 47 mM K+, the association between CHL1 and these SNARE complex components was further enhanced as indicated by higher levels of Snap25 and Syntaxin1B that co-immunoprecipitated with CHL1 (Fig. 21). The association of Snap25 and Syntaxin1B with CHL1 was further enhanced in synaptosomes that were incubated for 5 min in 4 mM K+ after a second stimulation with 47 mM K+ (Fig. 21). In contrast to synaptic plasma membrane enriched proteins Snap25 and Syntaxin1B, the association of CHL1 with synaptic vesicle enriched protein Vamp2 and Synapsin1 was strongest in non-stimulated synaptosomes and diminished following stimulation with 47 mM K+. Hence, interactions of CHL1 with the synaptic vesicle fusion machinery are regulated at the subsynaptic level depending on synaptic activity.

ATPase activity of chaperones is directly linked to the chaperone mediated refolding of the substrate proteins and thus can serve as a marker of the protein refolding activity. To analyze whether SNARE complex proteins with perturbed tertiary structure can specifically activate CHL1-containing chaperone complexes, we analyzed whether denatured Snap25 or Vamp2 induce ATPase activity of these chaperones by estimating levels of inorganic phosphate released from ATP by CHL1-containing chaperone complexes in the presence of denatured Snap25 and Vamp2. ATPase activity of the chaperones in the presence of denatured Snap25 and Vamp2 was always compared to ATPase activity in the presence of Snap25 and Vamp2 in the native conformation that was considered as basal ATPase activity of chaperone complexes.

An analysis of ATPase activity of CHL1-ICD, Hsc70, Csp and αSgt alone and various combinations of these proteins showed that denatured Vamp2 specifically increased ATPase activity of the CHL1-ICD/Csp complex only, with ATPse activity of this complex being approximately three times higher in the presence of denatured versus native Vamp2 (Fig. 22, Table 1). In contrast, denatured Snap25 activated only the CHL1-ICD/Hsc70/αSgt complex, with ATPase activity of this complex being approximately two times higher in the presence of denatured versus native Snap25 (Fig. 22). A slight increase in ATPase activity in the presence of denatured Snap25 was also observed for the Hsc70/αSgt combination (Fig. 22). Interestingly, denatured Snap25 inhibited the basal ATPase activity of Csp alone or in combination with CHL1-ICD (Fig. 22). A plausible explanation for this finding is that Snap25

inhibits the protein refolding activity of Csp during synaptic vesicle exocytosis, when surface plasma membrane enriched Snap25, which unfolds during fusion of synaptic vesicle with surface membranes, is in the vicinity of synaptic vesicle localized Csp. This inhibition may then be required to allow Vamp2 to change its conformation for synaptic vesicle exocytosis.

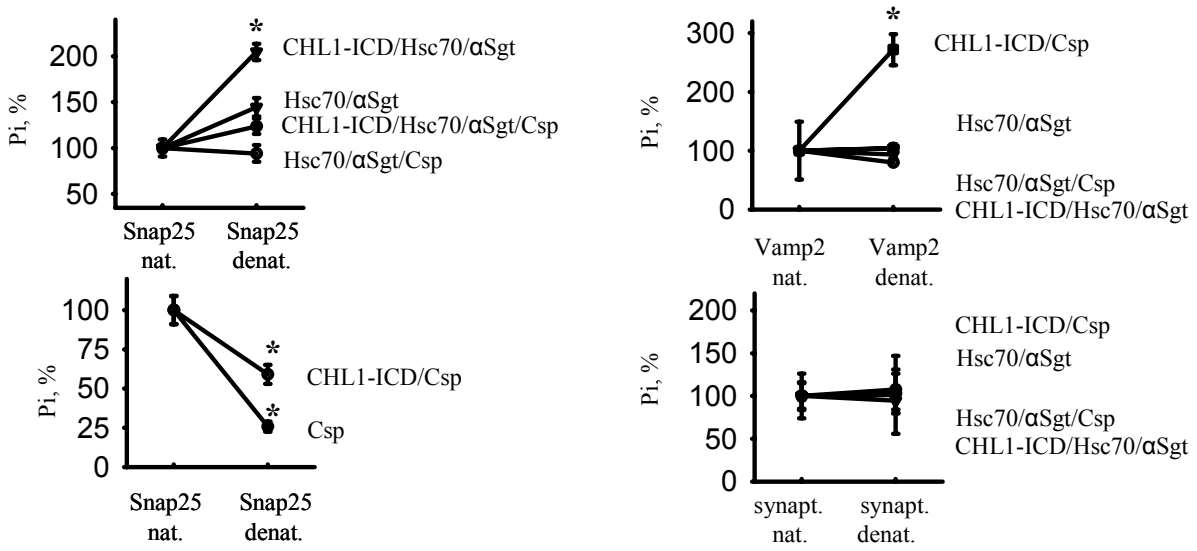

Figure 22: CHL1 regulates refolding of the SNARE complex proteins. Graphs show mean levels ± SEM of free inorganic phosphate (Pi) released from ATP (ATPase activity) by the indicated combinations of Hsc70, Csp, αSgt and CHL1-ICD in response to native or denatured Snap25, Vamp2 or synaptophysin. The complete list of all tested combinations of CHL1-ICD, Hsc70, Csp, and αSgt is shown in Table 1. Note that denatured Snap25 and Vamp2 activate ATPase activity of CHL1-ICD/Hsc70/αSgt and CHL1-ICD/Csp complexes, respectively. *p<0.05, paired t-test (compared to the ATPase activity in the presence of native proteins set to 100% (n≥6)).

Table 1: Changes in ATPase activity in different combinations of CHL1-ICD, Hsc70, Csp and αSgt in the presence of denatured versus non-denatured Snap25, Vamp2 or Synaptophysin.

combinations	Snap25	Vamp	Synaptophysin
CHL1-ICD/Hsc70/αSgt/Csp	123.713 ± 8.366	104.279 ± 6.359	107.701 ± 23.381
CHL1-ICD/Hsc70/αSgt	204.626 ± 8.930	103.94 ±6.607	94.429 ± 14.193
CHL1-ICD/Hsc70/Csp	92.983 ± 2.832	ND	ND
CHL1-ICD/Csp/αSgt	99.549 ± 4.789	ND	ND
Hsc70/αSgt/Csp	94.08 ± 9.022	79.928 ± 5.133	102.770 ± 23.334
Hsc70/Csp	93.808 ± 3.838	ND	ND
Hsc70/αSgt	144.434 ± 10.079	93.26 ± 6.146	90.989 ± 3.570
Csp/αSgt	86.977 ± 6.546	ND	ND
CHL1-ICD/Csp	59.035 ± 6.014	271.708 ± 26.493	101.344 ± 45.552
CHL1-ICD/αSgt	ND	ND	ND
CHL1-ICD/Hsc70	ND	ND	80.727 ± 7.795
CHL1-ICD	100.059 ± 0.144	100 ± 3.267	100 ± 8.820
Hsc70	89.001 ± 9.74	134.000 ± 15.183	104.649 ± 12.866
Csp	25.749 ± 3.272	114.638 ± 14.131	100 ± 4.047

αSgt	100 ± 0.900	104.878 ± 5.817	ND

Recombinant CHL1-ICD, Hsc70, Csp and αSgt in the indicated combinations were incubated with denatured and non-denatured Snap25, Vamp2 or Synaptophysin. Table shows ATPase activity in the presence of denatured proteins normalized to ATPase activity in the presence of non-denatured proteins set to 100%. ATPase activity values observed in the presence of denatured proteins that are statistically different (paired t-test, $n \geq 6$) from the values obtained for non-denatured proteins are highlighted in yellow. ND – not determined.

None of the chaperone complexes was activated in the presence of denatured Synaptophysin indicating the specificity of the chaperone – substrate protein interactions. When subsynaptic fractions were analyzed by Western blot under non-denaturing conditions, Snap25 and Vamp2 were also observed in association with CHL1/Hsc70/αSgt and CHL1/Csp complexes, respectively (Fig. 23).

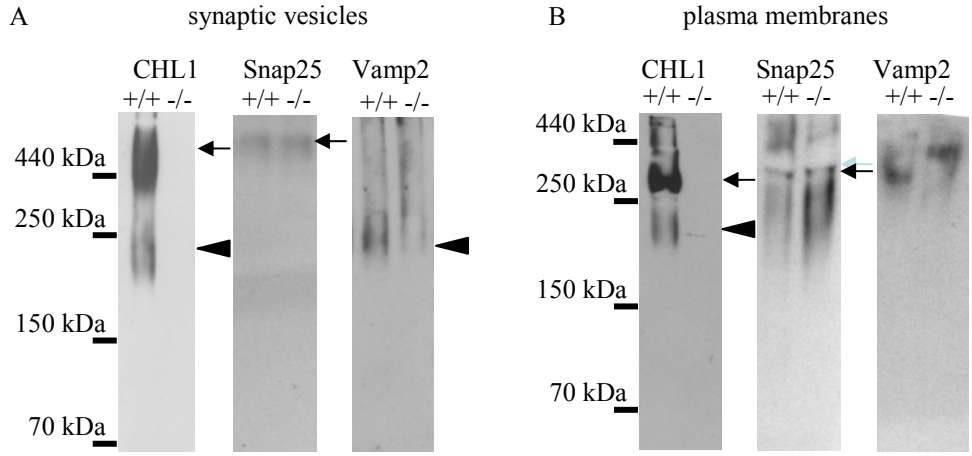

Figure 23: Snap25 and Vamp2 associate with CHL1/Hsc70/αSgt and CHL1/Csp complexes, respectively. A-B – Molecular complexes in CHL1+/+ and CHL1-/- synaptic vesicles (A) and synaptic plasma membranes (B) were separated by PAGE under non-denaturing conditions and probed by Western blot with the indicated antibodies. A – In synaptic vesicles, Snap25 and Vamp2 positive bands overlap with CHL1/Hsc70/αSgt (black arrows) and CHL1/Csp (black arrowheads) complexes, respectively. B – In synaptic plasma membranes, Snap25 positive band overlaps with the CHL1/Hsc70/αSgt complex (black arrows), while Vamp2 accumulates in a high molecular weight complex with a slightly lower molecular weight than that of CHL1/Hsc70/αSgt complex. In CHL1-/- probes, Snap25 (grey versus black arrow, respectively) and Vamp2 bands are slightly shifted to a higher molecular range, possibly due to aggregation of the proteins or abnormal composition/structure of the protein complexes containing Snap25 and Vamp2.

We investigated whether CHL1 containing chaperones contribute to the assembly of the SNARE complex: Denatured or non-denatured recombinant Snap25 and Vamp2 were assessed by pull down for their ability to bind Syntaxin1B purified by immunoprecipitation from synaptosomes. Denaturation of either Snap25 or Vamp2 inhibited SNARE complex

assembly as indicated by reduced ability of Syntaxin1B to pull down these two components (Fig. 24). However, the pull down efficiency was restored when denatured Vamp2 was preincubated with the CHL1-ICD/Csp complex, but not with the CHL1-ICD/Hsc70/αSgt complex (Fig. 24). In contrast, preincubation of denatured Snap25 with CHL1-ICD/Hsc70/αSgt complex, but not with the CHL1-ICD/Csp complex also restored the efficiency of binding of the SNARE complex components (Fig. 24).

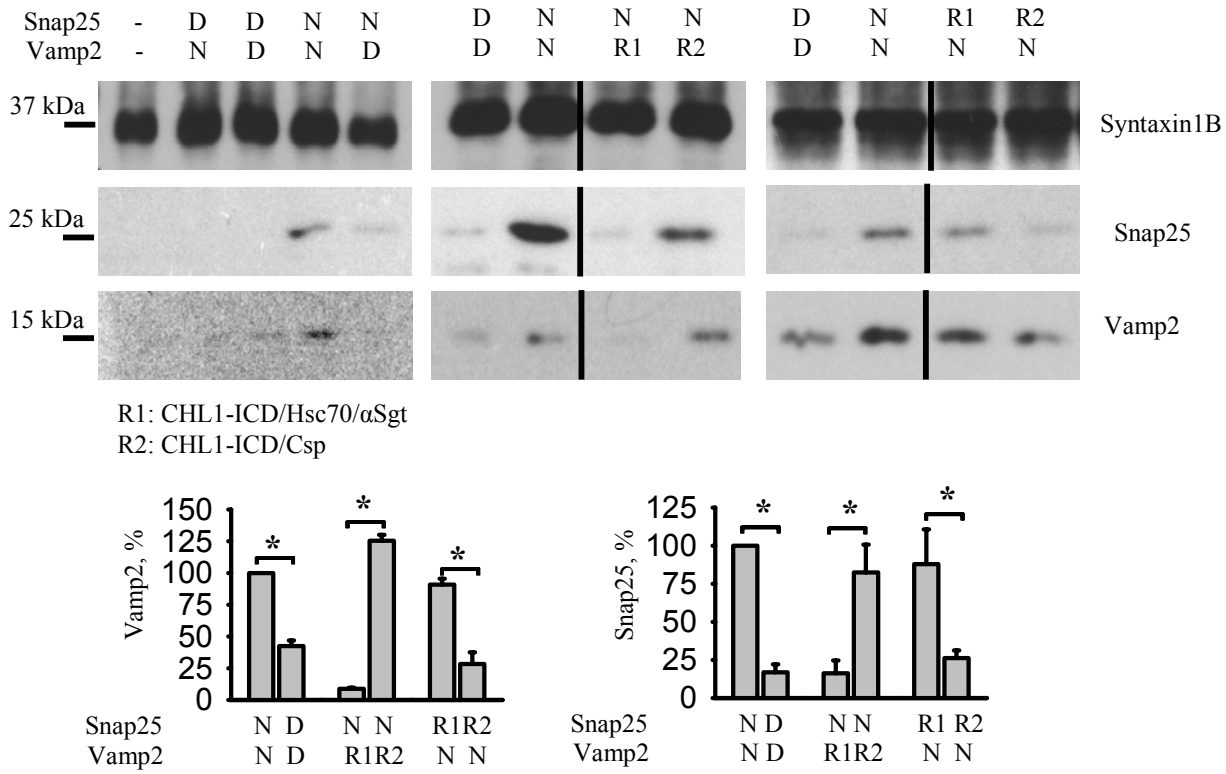

Figure 24: CHL1-containing chaperone complexes restore binding efficiency of the SNARE complex components. Syntaxin1B was immunoprecipitated from brain lysates and assayed for the ability to pull down denatured (D) or native (N) Snap25 and Vamp2. In indicated cases, denatured proteins were preincubated with CHL1-ICD/Hsc70/αSgt (R1) or CHL1-ICD/Csp (R2) complexes. Graphs show quantitation of the binding of Snap25 and Vamp2 to syntaxin 1B ± SEM (n=6) with the binding efficiency for both proteins in the native conformation set to 100%. Native Snap25 and VamP2 form a complex with Syntaxin1B, while denaturing of at least one component inhibits the pull down efficiency. Preincubation of denatured Snap25 with CHL1-ICD/Hsc70/αSgt and denatured Vamp2 with CHL1-ICD/Csp complexes increases the efficiency of the SNARE complex assembly. *$p<0.05$, paired t-test (compared as indicated).

Thus, our data indicate that two SNARE complex proteins, Vamp2 and Snap25, are specifically refolded by two distinct chaperone complexes - CHL1/Csp and CHL1/Hsc70/αSgt, respectively - and this refolding is required for their ability to assemble the SNARE complex.

6. CHL1 deficiency results in increased degradation of the SNARE complex proteins in response to stress.

Incorrectly folded proteins are rapidly degraded by cellular proteases (Parsell et al., 1993). Thus, an analysis of protein degradation rates can provide a useful estimation of the efficiency of the protein refolding machinery under varying conditions. To analyze whether CHL1 deficiency results in increased degradation of the synaptic vesicle fusion machinery in response to enhanced synaptic activity, CHL1+/+ and CHL1-/- cultured hippocampal neurons were treated for 30 min with 50 µM picrotoxin (PTX), an inhibitor of $GABA_A$ receptors that induces seizure-like activity in neurons. Western blot analysis of cell lysates of these cultures showed that levels of Snap25, Vamp2 and Synapsin1, but not synaptophysin were strongly reduced in PTX treated versus non-treated CHL1-/- neurons (Fig. 25).

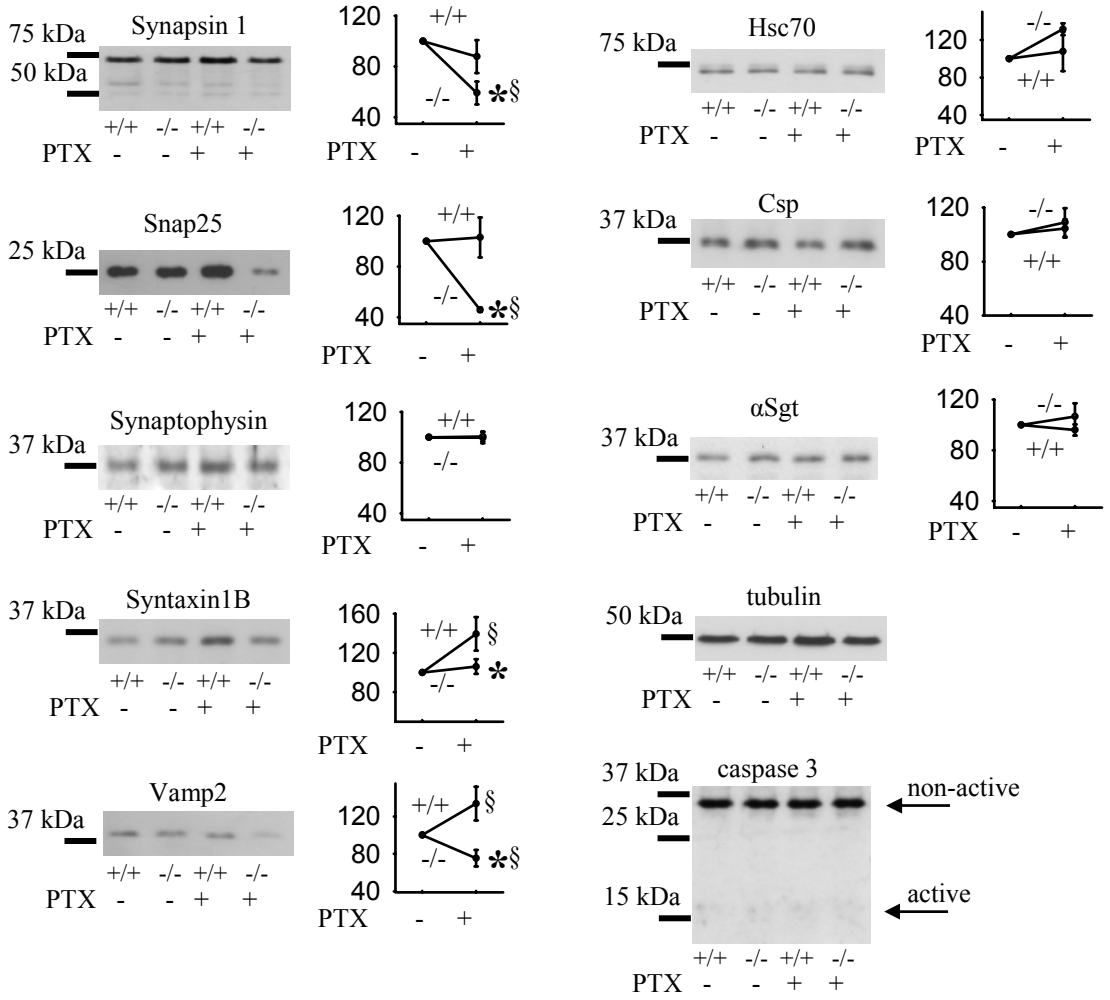

Figure 25: The synaptic vesicle fusion machinery in CHL1-/- neurons degrades in response to high levels of synaptic activity. CHL1+/+ and CHL1-/- cultured hippocampal neurons were stimulated with 50 µM PTX applied for 30 min. Lysates of non-treated and PTX treated neurons were probed by Western blot with the indicated antibodies. Graphs show mean optical density of the blots ± SEM (n=6) with signals in non-treated

neurons set to 100%. Note reduced levels of Snap25, Syntaxin1B, Vamp2 and Synapsin1 but not synaptophysin in stimulated CHL1-/- versus stimulated CHL1+/+ neurons. PTX application did not induce apoptosis as indicated by unchanged levels of non-active and active caspase 3 in both genotypes. Tubulin served as a loading control. *,§ $p<0.05$, paired t-test (PTX stimulated CHL1-/- versus CHL1+/+ neurons (*), and PTX stimulated versus non-stimulated neurons of the same genotype (§) were compared).

In contrast, PTX stimulation did not affect the SNARE complex protein levels in CHL1+/+ neurons (Fig. 25). On the contrary, levels of Vamp2 and Syntaxin1B were increased in stimulated CHL1+/+ neurons, probably due to enhanced synthesis of these proteins. Although levels of Syntaxin1B were not changed in PTX treated versus non-treated CHL1-/- neurons, they were lower than the levels of Syntaxin1B in PTX treated CHL1+/+ neurons (Fig. 25), again suggesting higher degradation of Syntaxin1B in activated CHL1-/- neurons. Enhanced degradation of the SNARE complex proteins in CHL1-/- neurons was not associated with enhanced apoptosis as indicated by unchanged levels of active caspase 3 in stimulated versus nonstimulated neurons of both genotypes (Fig. 25). Levels of Hsc70, Csp and αSgt were also not affected by PTX stimulation in both genotypes (Fig. 25). Furthermore, exposure of brain homogenates to heat, or stimulation of synaptosomes isolated from brain tissue with high K+ containing buffer induced more pronounced degradation of the SNARE complex proteins in CHL1-/- versus CHL1+/+ probes (Fig. 26). Thus, our data indicate that CHL1 deficiency results in enhanced susceptibility of the synaptic vesicle fusion machinery to degradation under stressful conditions, such as high synaptic activity.

Interestingly, levels of Syntaxin1B, Snap25, Vamp2 and Synapsin1 were slightly increased in CHL1-/- versus CHL1+/+ brain homogenates, probably reflecting a compensatory reaction to the abnormal function of these proteins (Fig. 26A). Levels of the SNARE complex proteins, however, were not upregulated in CHL1-/- synaptosomes (Fig. 26B), suggesting reduced synaptic targeting and / or re-direction of the proteins to other compartments such as accumulation of incorrectly folded proteins in the degradation pathway.

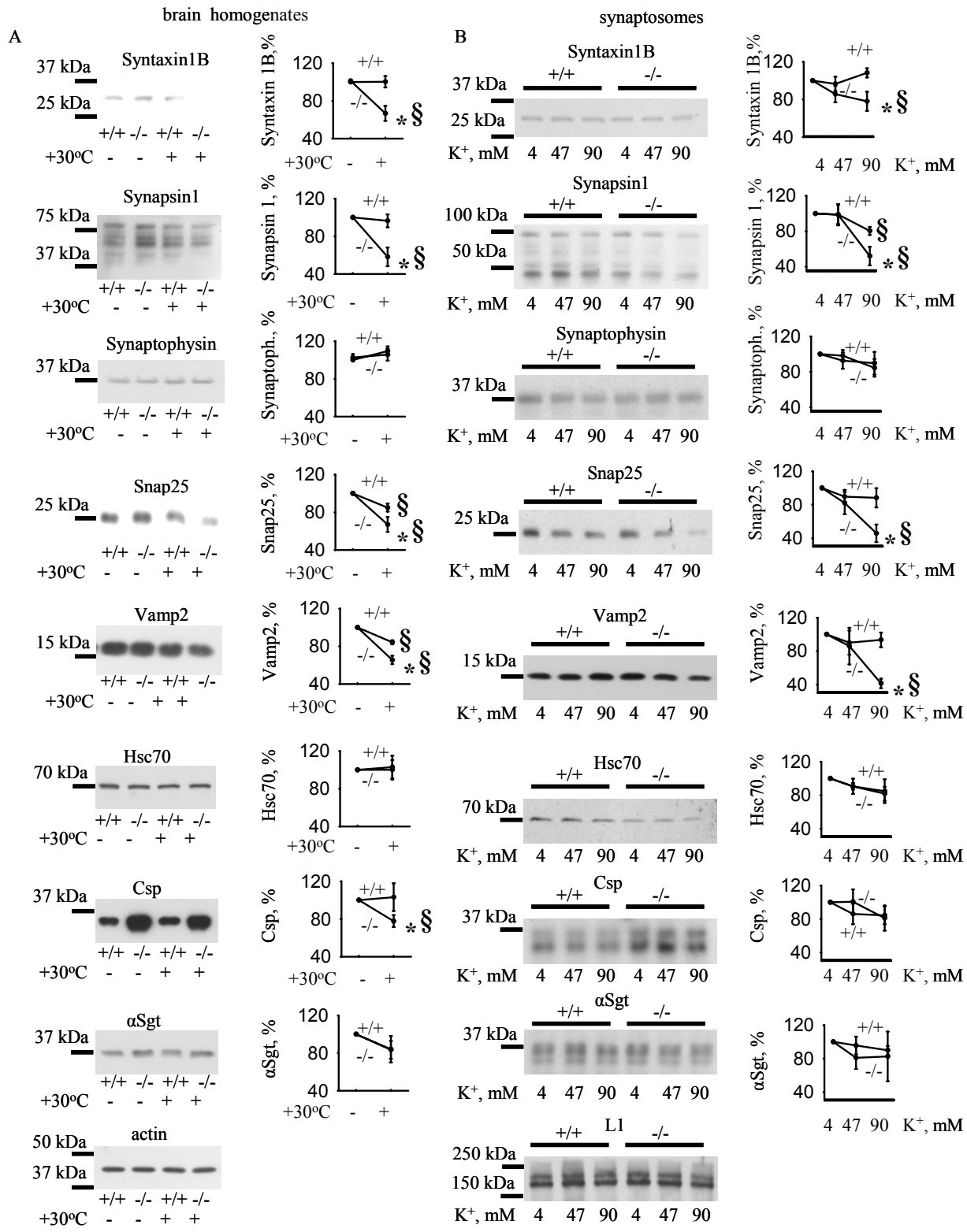

Figure 26: The synaptic vesicle fusion machinery is more susceptible to degradation in response to heat exposure and enhanced synaptic activity in CHL1-/- versus CHL1+/+ brains and synaptosomes. A – CHL1+/+ and CHL1-/- brain homogenates either freshly prepared or pre-incubated for 30 minutes at 30°C were probed by Western blot with the indicated antibodies. Note a more pronounced decline in the levels of Syntaxin1B, Snap25, Vamp2 and Synapsin1 but not synaptophysin in heat exposed CHL1-/- versus CHL1+/+ brain homogenates. Levels of Hsc70, Csp and αSgt are similar or higher in CHL1-/- versus CHL1+/+ brain

homogenates exposed to heat. Actin served as a loading control. B – CHL1+/+ and CHL1-/- synaptosomes, that were treated with the buffer containing 4, 47 or 90 mM K+, were probed by Western blot with indicated antibodies. Note that exposure to high concentrations of K+, inducing synaptic vesicle exo- and endocytosis, results in a strong decline in the levels of Syntaxin1B, Snap25, Vamp2 and Synapsin1but not synaptophysin in CHL1-/- synaptosomes. L1 served as a loading control. Graphs (A, B) show mean optical density of the blots ± SEM (n=6) with optical density in non-treated homogenates (A) or 4 mM K+ treated synaptosomes (B) set to 100%. *,§ $p<0.05$, paired t-test (CHL1-/- versus CHL1+/+ heat treated brain homogenates (*), CHL1-/- versus CHL1+/+ synaptosomes treated with 90 mM K+ (*), and non-treated versus treated groups of the same genotype (§) were compared).

In favor of the latter, levels of Snap25, Vamp2 and Syntaxin1B were increased in lysosomes isolated from CHL1-/- brains (Fig. 27) indicating higher degradation levels of the SNARE complex in CHL1-/- brains.

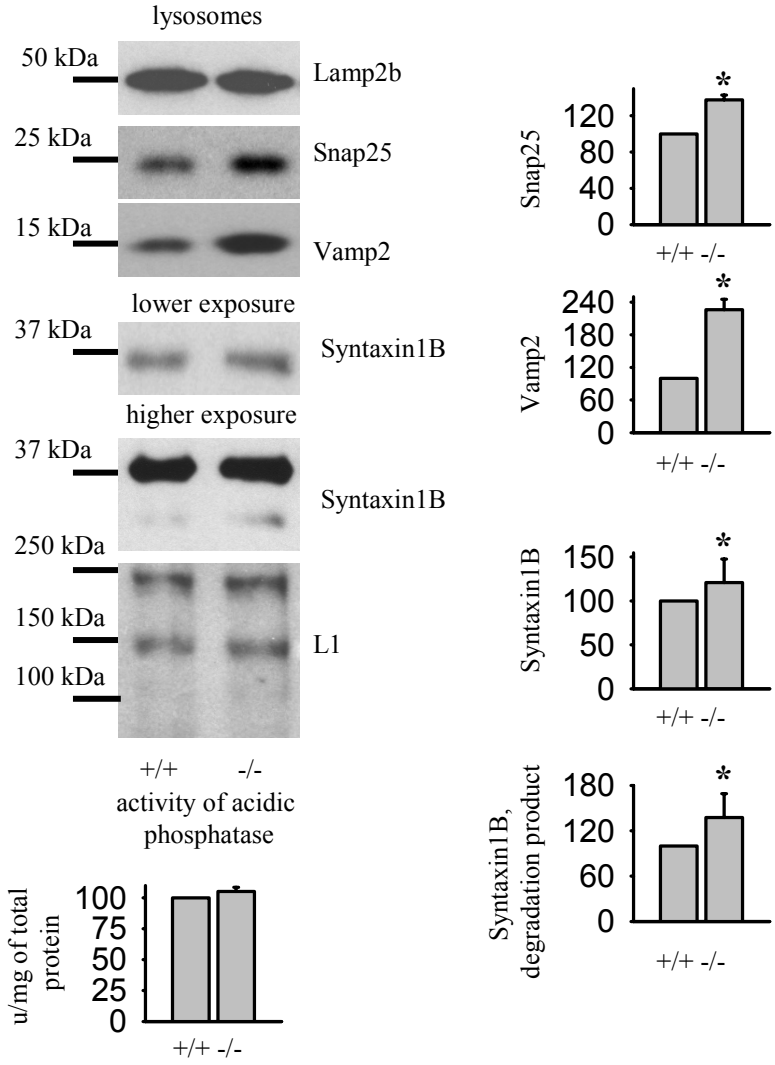

Figure 27: CHL1 deficiency results in accumulation of SNARE complex proteins in lysosomes. CHL1+/+ and CHL1-/- lysosomes were probed by Western blot with the antibodies against Snap25, Vamp2, Syntaxin1B and lysosome associated protein Lamp2b. L1 served as a loading control. Graphs on the right show mean levels ± SEM of Snap25, Vamp2 and Syntaxin1B in lysosomes with levels in CHL1+/+ lysosomes set to 100%. Note

similar levels of Lamp2b in CHL1+/+ and CHL1-/- lysosomes indicating similar total protein levels. Graph (below) shows mean levels ± SEM of acidic phosphatase activity in CHL1+/+ and CHL1-/- lysosomes that was similar in lysosomes of both genotypes again indicating that similar levels of lysosomes were isolated. Levels of Snap25, Vamp2, Syntaxin1B, but not L1 are increased in CHL1-/- lysosomes. *p<0.05, paired t-test.

7. CHL1 deficiency is associated with reduced recovery of the SNARE complex and inhibition of synaptic vesicle exocytosis following prolonged and stressful synapse activity.

To investigate whether the ability to reassemble the SNARE complex is affected by CHL1 deficiency, we analyzed co-immunoprecipitations of Snap25 and Vamp2 with Syntaxin1B from synaptosomes. Snap25 and Vamp2 co-immunoprecipitated with Syntaxin1B with a similar or slightly higher efficiency from non-stimulated CHL1-/- versus CHL1+/+ synaptosomes (Fig. 28).

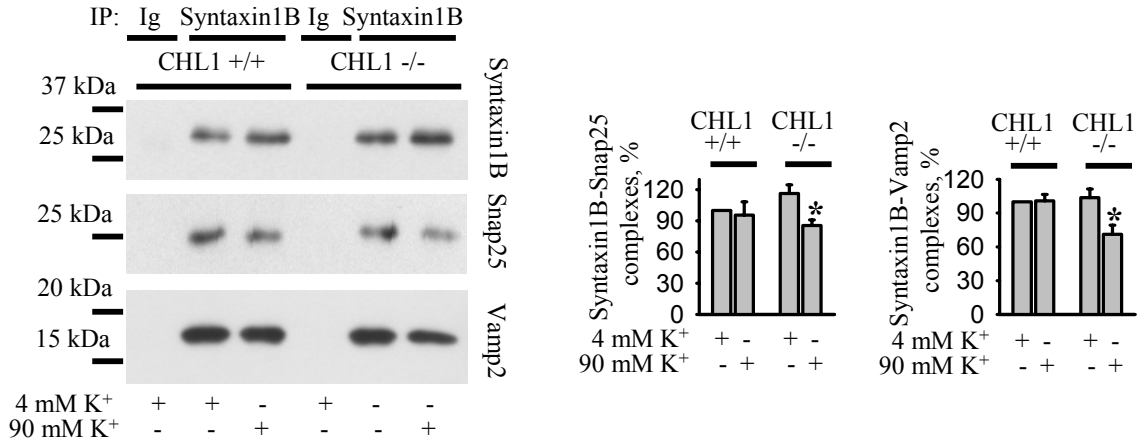

Figure 28: Sustainability of the synaptic vesicle fusion machinery is reduced in CHL1-/- neurons. Syntaxin 1B immunoprecipitates (IP) from CHL1+/+ and CHL1-/- synaptosomes, treated with 4 mM or 90 mM K+, were probed by Western blot with antibodies against Synataxin1B, Snap25 and Vamp2. Graphs show mean optical densities of the blots ± SEM (n=6) with the levels of Snap25 and Vamp2 that co-immunoprecipitate with Syntaxin1B from 4 mM K+ treated CHL1+/+ synaptosomes set to 100%. Exposure to 90 mM K+ reduces levels of Snap25 and Vamp2 that co-immunoprecipitate with syntaxin 1B from CHL1-/- synaptosomes. *p<0.05, paired t-test (compared as indicated).

However, following stimulation of synaptosomes for 90 s with 90 mM K+ to induce synaptic vesicle exo- and endocytosis, the ability of Vamp2 and Snap25 to associate with Syntaxin1B was reduced in CHL1-/- synaptosomes by approximately 25% compared to non-stimulated CHL1-/- synaptosomes (Fig. 28). These data indicate that CHL1 deficiency results not only in

enhanced degradation of the SNARE complex proteins, but also in reduced ability of these proteins to re-associate in the SNARE complex following synaptic vesicle exosytosis.

To assess the impact of prolonged synaptic activity on the synaptic vesicle recycling machinery, we analyzed activity-dependent uptake of the lipophilic fixable dye FM1-43FX to synaptic boutons, visualized by post-hoc immunofluorescence with antibodies against the synaptic vesicle protein SV2. Uptake of FM1-43FX applied in the presence of 50 µM PTX to induce synaptic vesicle exo- and endocytosis was slightly reduced in CHL1-/- versus CHL1+/+ neurons (Fig. 29). Preincubation of neurons with 50 µM PTX for 30 min before application of the dye further reduced FM1-43FX uptake in CHL1-/- but not in CHL1+/+ synaptic boutons (Fig. 29). The results suggest that the synaptic vesicle recycling machinery is impaired under prolonged excitatory synaptic activity in CHL1-/- synapses.

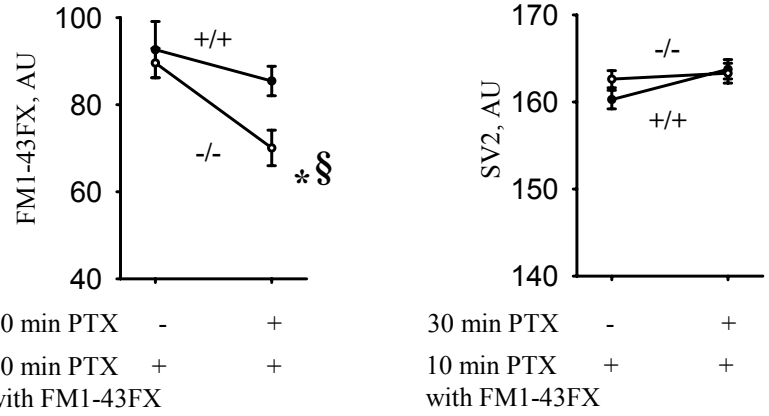

Figure 29: Activity-dependent uptake of the lipophilic fixable dye FM1-43FX to synaptic boutons. CHL1+/+ and CHL1-/- cultured hippocampal neurons that were either non-treated or pre-incubated with 50 µM PTX for 30 min were then incubated with PTX for 10 min in the presence of FM1-43FX. After fixation, neurons were co-labeled with antibodies against SV2. Graphs show mean FM1-43FX and SV2 fluorescence levels ± SEM in SV2 accumulations (N>30 images of neurons with n>200 SV2 positive synaptic boutons per image were analyzed in each group). Pre-treatment with PTX has a stronger inhibitory effect on FM1-43FX uptake in CHL1-/- versus CHL1+/+ neurons. *,§ $p<0.05$, t-test (PTX stimulated CHL1-/- versus CHL1+/+ neurons (*), and PTX stimulated versus non-stimulated neurons of the same genotype (§) were compared). Activity-dependent uptake of the lipophilic fixable dye FM1-43FX to synaptic boutons was performed in cooperation with Dr. Leshchyns'ka and Dr. Vladimir Sytnyk in the group of Melitta Schachner.

To directly analyze the impact of CHL1 deficiency on synaptic vesicle exocytosis, we transfected cultured hippocampal neurons with a pH-sensitive form of green-fluorescent protein (GFP) fused to the lumenal domain of Vamp2 (synapto-pHluorin), providing a sensitive optical probe to follow synaptic vesicle exo- and endocytosis in real time: Synaptic vesicle exocytosis exposes the pH-sensitive GFP tag to the fluorescence-permissive culture

medium, while endocytosis of the protein to recycling synaptic vesicles results in quenching of fluorescence of this tag in the acidified environment of the synaptic vesicle lumen. We thus investigated the impact of synaptic activity on the ability of synaptic vesicles to fuse with the synaptic membrane in response to consecutive stimuli: Neurons were challenged twice with 47 mM K+ for 90 s with a recovery in 4 mM K+ following each application of 47 mM K+. Time lapse recordings of axons of the transfected neurons showed that in CHL1+/+ neurons both applications of 47 mM K+ resulted in similar increases in synapto-pHluorin fluorescence in synaptic boutons (Fig. 30), indicating that comparable numbers of synaptic vesicles were exocytosed.

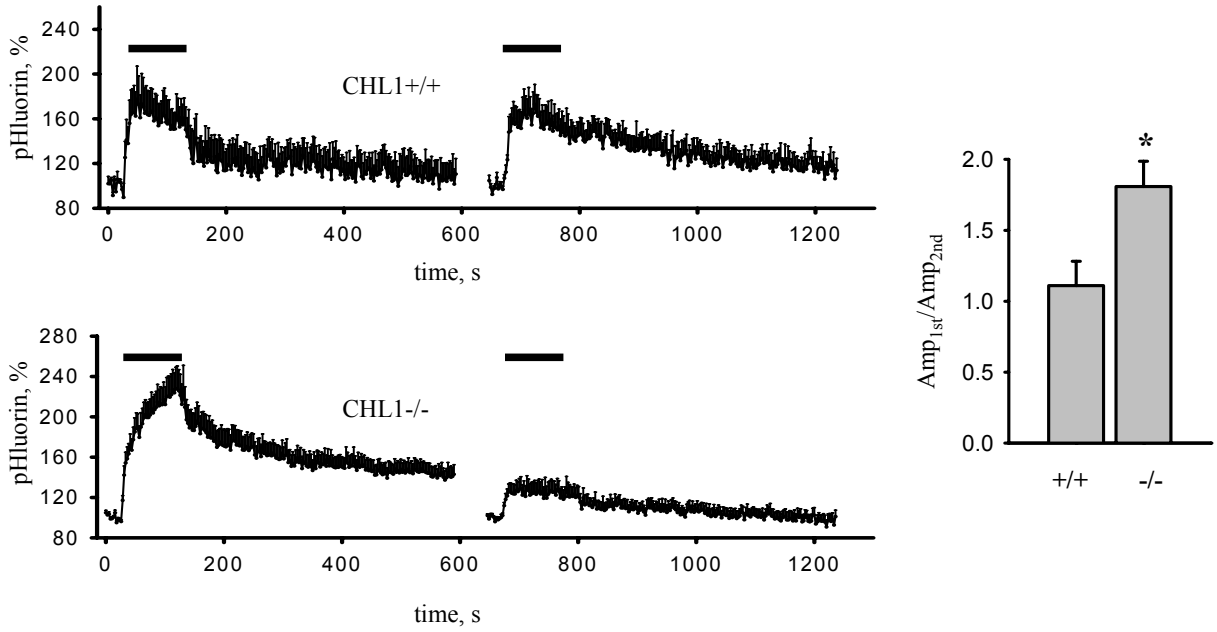

Figure 30: Impaired synaptic vesicle exocytosis in CHL1-/- synaptic boutons. CHL1+/+ and CHL1-/- cultured hippocampal neurons transfected with synapto-pHluorin were challenged twice with 47 mM K+ applied for 90 s with 8 min recovery in 4 mM K+ following each stimulation. Graphs show mean levels ± SEM of synapto-pHluorin fluorescence intensities in synaptic boutons as a function of time. The values were normalized to the synapto-pHluorin fluorescence intensity before stimulation. Black bars indicate time of 47 mM K+ application. An increase in synapto-pHluorin fluorescence intensity in response to the second application of 47 mM K+ is inhibited in CHL1-/- but not in CHL1+/+ neurons. Note a slower and incomplete decline in synapto-pHluorin fluorescence in CHL1-/- synaptic boutons following first stimulation. Graph shows mean ratio ± SEM of the amplitudes (Amp) of synapto-pHluorin fluorescence intensity increase in response to the first and second application of 47 mM K+. * $p<0.05$, t-test (n=10 synapses from five CHL1+/+ neurons and n=20 synapses from six CHL1-/- neurons were analyzed). The experiment was performed in cooperation with Dr. Leshchyns'ka and Dr. Vladimir Sytnyk in the group of Melitta Schachner.

Substitution of 47 mM K+ with 4 mM K+ resulted in a gradual decline in synapto-pHluorin fluorescence intensity, indicating synaptic vesicle endocytosis (Fig. 30). In contrast to

CHL1+/+ neurons, CHL1-/- neurons responded with a pronounced increase in synapto-pHluorin fluorescence levels in synaptic boutons only to the first application of 47 mM K+, while the second response was strongly reduced (Fig. 30), indicating impaired exocytosis of synaptic vesicles. Interestingly, the amplitude of the first response was slightly higher in CHL1-/- versus CHL1+/+ neurons (Fig. 30), possibly due to increased levels of Csp in CHL1-/- synaptic boutons (Chamberlain et al., 1998). This observation is in agreement with the previously reported enhanced basal synaptic transmission in CHL1-/- mice (Morellini et al., 2007). The endocytosis of synapto-pHluorin following the first application of 47 mM K+ was slower and more incomplete in CHL1-/- versus CHL1+/+ synaptic boutons (Fig. 30), indicating impaired synaptic vesicle endocytosis in CHL1-/- synaptic boutons as reported previously (Leshchyns'ka et al., 2006).

8. CHL1 is important for the clathrin-dependent endocytosis.

In neurons and nonneuronal cells, Hsc70 is the major ATPase mediating clathrin uncoating from clathrin-coated vesicles (Newmyer et al., 2001). In synapses, Hsc70 uncoates clathrin from synaptic vesicles recycling via a clathrin-dependent pathway (Zinsmaier et al., 2001; Morgan et al., 2001).

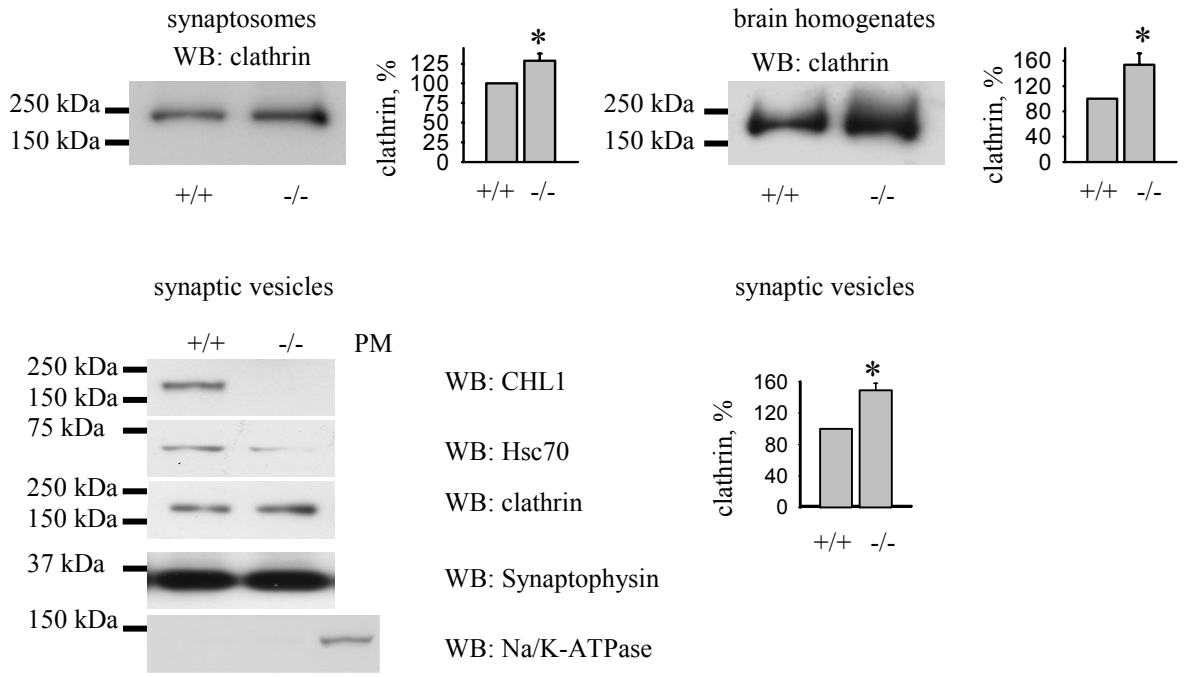

Figure 31: CHL1-/- synapses contain increased levels of clathrin. CHL1+/+ and CHL1-/- synaptosomes, brain homogenates and synaptic vesicles were probed by Western blot with the indicated antibodies. Graphs show mean optical density of the blots ± SEM (n=6) with optical density in CHL1+/+ set to 100%. *p < 0.05,

paired t test. Levels of clathrin are increased in CHL1-/- versus CHL1+/+ synaptosomes, brain homogenates, and synaptic vesicles.

We therefore investigated whether abnormalities in subcellular distribution of Hsc70 in CHL1-/- brains may affect levels of clathrin expression. Protein and mRNA levels of clathrin were higher in CHL1-/- brain homogenates (Leshchyns'ka et al., 2006; Fig. 31) and levels of clathrin protein were increased in CHL1-/- synaptosomes and synaptic vesicles (Fig. 31), suggesting that CHL1 is important for clathrin uncoating from synaptic vesicles.

VI. Discussion

In the present study we discovered a novel role for CHL1 as a co-chaperone in the presynaptic chaperone machinery consisting of Hsc70, Csp and αSgt. The physiological significance of the interactions between CHL1 containing chaperones and proteins of the synaptic vesicle fusion machinery is underscored by our observations in CHL1-/- mice: CHL1 deficiency results in enhanced susceptibility of the synaptic vesicle fusion machinery to degradation especially under stressful conditions, such as exposure to heat or prolonged synaptic activity. Syntaxin, Snap25 and Vamp not only degrade faster in CHL1-/- neurons, but also show reduced functionality under stressful conditions manifested by decreased ability to assemble the SNARE complex. As a consequence, following the first episode of strong synaptic activity, synaptic vesicles in CHL1-/- mice are not able to fuse with the presynaptic membrane in response to consecutive stimuli. In regulating the presynaptic chaperone machinery, CHL1 directly binds to Hsc70, Csp and αSgt (see Fig. 33 for a scheme). While recombinant Hsc70, Csp and αSgt readily bind to each other and form a trimeric complex (Tobaben et al., 2001; and our own observations), CHL1 inhibits the formation of this Hsc70/Csp/αSgt complex by splitting it into CHL1/Csp and CHL1/Hsc70/αSgt complexes. Binding assays with recombinant proteins suggest the following mechanism for this observation: CHL1 competes with Csp for binding to Hsc70, which binds to the similar HPD tripeptide containing sequences within CHL1-ICD and the J-domain of Csp (Leshchyns'ka et al., 2006; Smith et al., 2005). On the other hand, CHL1 binds to Csp via the HPD tripeptide containing domain within CHL1-ICD and this binding of CHL1 to Csp interferes with the binding of Csp to Hsc70 and αSgt. The latter observation suggests that CHL1 binds to the J-domain of Csp containing the binding site for Hsc70. In support of our data with recombinant proteins, in synaptic vesicles and synaptic plasma membranes from CHL1+/+ brain tissue, Hsc70 and αSgt were found together in a complex with CHL1 but not Csp, while Csp was found in a complex with CHL1 but not Hsc70 or αSGT. Furthermore, the trimeric Hsc70/Csp/αSgt complex was found in CHL1-/- synaptic vesicles, confirming that in the absence of CHL1 this complex can be formed.

Why should CHL1 disassemble the trimeric Hsc70/Csp/αSgt complex? The physiological significance of the CHL1-containing chaperone complexes is underscored by the analysis of the refolding of denatured Snap25 and Vamp2. Although all combinations of CHL1-ICD, Hsc70, Csp and αSgt showed some ability to refold denatured luciferase, denatured Snap25

and Vamp2 activated only CHL1/Hsc70/αSgt and CHL1/Csp complexes, respectively, but not others including the Hsc70/Csp/αSgt complex. Importantly, we show that not only Hsc70, but also Csp possesses ATPase activity and can function as a chaperone, in accordance with published data (Chamberlain et al., 1997b). Hence, the CHL1/Csp complex can function as a chaperone complex that is independent of Hsc70. Conformational changes induced by CHL1 binding may be required to define the specificity of the CHL1/Hsc70/αSgt and CHL1/Csp complexes towards denatured Snap25 and Vamp2. In addition, CHL1 may enhance the affinity of the chaperones to denatured Snap25 and Vamp2 since recombinant CHL1-ICD interacts directly with denatured but not native Snap25 and Vamp2 and may thus function as a sensor for the unfolded state of these proteins (Fig. 32).

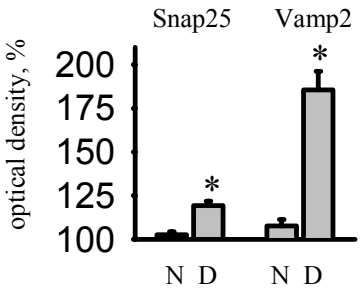

Figure 32: CHL1-ICD binds to Snap25 and Vamp2 when these proteins are denatured. CHL1-ICD (1.9 μM) was immobilized on plastic and assayed by ELISA for the ability to bind Snap25 (4 μM) and Vamp2 (6 μM) either in native form (N) or denatured (D). CHL1-ICD binds denatured Snap25 and Vamp2 but does not interact with these proteins in their native forms. *$p<0.05$, paired t-test (binding of denatured versus native protein was compared). Background optical density, i.e. binding to BSA, was set to 100%.

Interestingly, interactions between CHL1 and presynaptic proteins, including Snap25 and Vamp2, are regulated subsynaptically in an activity-dependent manner, suggesting that CHL1-containing chaperone complexes may perform different functions. Indeed, since Csp and Vamp2 are localized to synaptic vesicles, binding of CHL1 to Vamp2 and refolding of Vamp2 by the CHL1/Csp complex most probably occurs in these organelles. In favor of this idea, we observed that the association of CHL1 with Vamp2 is disrupted following induction of synaptic vesicle exocytosis which is accompanied by redistribution of Vamp2 to the synaptic surface membrane. Furthermore, binding of CHL1 to Csp is favored by ATP, which should be more abundant in non-stimulated synaptic boutons. Since in non-stimulated synaptic boutons the SNARE complexes were most likely not yet formed, refolding of Vamp2

by CHL1/Csp complex may be required to prime Vamp for binding to other SNARE complex components on the synaptic surface plasma membrane to allow rapid synaptic vesicle fusion. In contrast, Snap25, accumulating at the synaptic surface plasma membrane, most probably binds to CHL1 at the synaptic surface membrane. Our data showing that the association of CHL1 with Snap25 is enhanced following induction of synaptic vesicle exocytosis support this conclusion, since after synaptic vesicle exocytosis SNARE complex proteins further accumulate at the surface plasma membrane. Formation of the CHL1/Hsc70/αSgt complex that refolds Snap25 is favoured by ADP, which should also be present at higher levels in stimulated synapses. SNARE complexes accumulating at the surface plasma membrane following synaptic vesicle exocytosis are disassembled by NSF and must refold. Hence, the CHL1/Hsc70/αSgt complex is probably required to regenerate Snap25 following disassembly of the SNARE complex at the surface plasma membrane. Although CHL1/Hsc70/αSgt complexes are formed at the surface plasma membrane, they can redistribute to synaptic vesicles following internalization of CHL1 to these organelles (Leshchnyns'ka et al., 2006), an observation that would explain lower levels of Hsc70 and αSgt in synaptic vesicles from CHL1-/- mice.

Hsc70 is also required in the clathrin-dependent endocytosis. We found that high levels of Hsc70 cofractionate with CHL1 in the synaptic membrane fraction, indicating that Hsc70 forms a complex with CHL1 in the plasma membrane.

Increased levels of clathrin in CHL1-/- brain homogenates, synaptosomes and synaptic vesicles support the hypothesis that CHL1 is important for uncoating of clathrin-coated vesicles. Regulation of clathrin uncoating by CHL1, reduction in activity-induced formation of clathrin-coated synaptic vesicles after disruption of CHL1/Hsc70 complex, accumulation abnormally high numbers of clathrin-coated vesicles in CHL1-/- synaptic boutons also suggest a role for the cell adhesion molecule CHL1 in the regulation of uncoating of clathrin-coated vesicles (Leshchnyns'ka et al., 2006).

Altogether our data demonstrate that cell adhesion molecule CHL1 is involved in two steps of synaptic vesicle recycling: in exocytosis as a modulator of chaperons that refold SNARE proteins and in endocytosis by the regulation of uncoating of clathrin-coated synaptic vesicles. Also in the brains of CHL1-/- mice that were maintained under normal housing conditions, SNARE complex components were found to accumulate in lysosomes, suggesting that incorrectly folded proteins gradually accumulate in the brain. We would like to speculate that this phenomenon may relate to some molecular abnormalities seen in slowly developing disorders, such as schizophrenia. The etiology of schizophrenia, a disease linked to mutations

in the CHL1 gene in humans (Sakurai et al., 2002; Chen et al., 2005) not only includes a genetic predisposition but also an environmental underpinning. Changes in schizophrenic patients progress slowly over decades until they reach a critical threshold that is manifested by the disease symptoms. Our observations are in line with this hypothesis: small, genetically determined abnormalities in synaptic transmission and synaptic protein turnover can aggravate, especially following stressful conditions, and, depending on the degree of aggravation, lead to irreversible changes in the properties of information processing in the brains of humans and mice carrying mutations in CHL1, thereby contributing to the development of this disease. Independent of this hypothesis, our observations show that the adhesion molecule CHL1 is a novel regulator of the presynaptic machinery and thus a decisive player in synaptic vesicle exo- and endocytosis in central nervous system synapses.

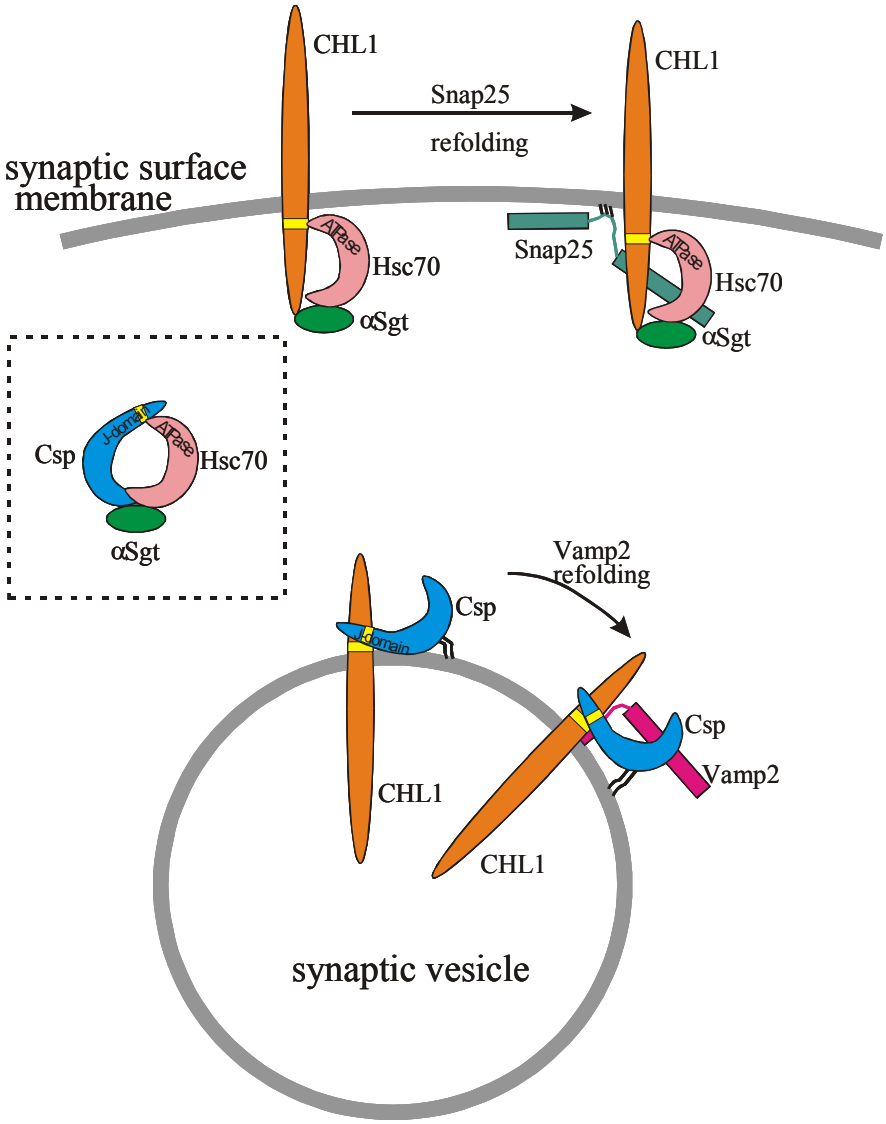

Figure 33: Schematic diagram of CHL1-containing chaperone complexes and their substrates. Two CHL1-containing chaperone complexes are shown: The CHL1/Csp complex is formed in synaptic vesicles. Csp, which

is targeted to synaptic vesicles via palmitoylation, binds to the HPD tripeptide containing region of the intracellular domain of CHL1 via its J-domain. HPD tripeptides within the intracellular domain of CHL1 and J-domain of Csp are marked in yellow. The CHL1/Csp complex refolds Vamp2. Vamp2 binds to CHL1 and is refolded by the CHL1/Csp complex in non-stimulated synaptic boutons, that is required to prime Vamp2 for binding to Syntaxin1B and Snap25 (not shown). The CHL1/Hsc70/αSgt complex is shown at the synaptic surface membrane. Hsc70 binds to the HPD tripeptide containing region of the intracellular domain of CHL1 via its ATPase domain, while αSgt binds to the C-terminals of Hsc70 and CHL1. The CHL1/Hsc70/αSgt complex refolds Snap25. Snap25 binds to CHL1 and is refolded by CHL1/Hsc70/αSgt after synapse activation that is required for Snap25 regeneration (not shown). CHL1/Hsc70/αSgt complexes may also be endocytosed to synaptic vesicles (not shown). Note, that CHL1 anchors Hsc70 and αSgt to the membranes. For comparison, the Hsc70/Csp/αSgt complex is shown (in the dashed line insert). Note, that interactions of Csp and Hsc70 with CHL1 should lead to the disassembly of the Hsc70/Csp/αSgt complex by competition for binding sites.

VII. Summary

In present study we characterize a novel role for a cell adhesion molecule: regulation of the presynaptic chaperone machinery. We show that a cell adhesion molecule of the immunoglobulin superfamily CHL1 (close homologue of L1) participates in the refolding of synaptic vesicle fusion SNARE machinery by regulation of the activity of synaptic chaperones Hsc70 (heat shock cognate 70), Csp (cysteine string protein) and αSgt (small glutamine-rich tetratricopeptide repeat-containing protein). We found that CHL1 via its intracellular domain could directly interact with Hsc70 and with two its co-chaperones: Csp and αSgt. By separating endogenous protein complexes in synaptic vesicles and synaptic plasma membranes under native conditions and by *in vitro* protein binding assay we demonstrate that CHL1 associate with these chaperones in CHL1/Hsc70/αSgt and CHL1/Csp complexes. We show that CHL1 deficient but not wild type synaptic vesicles contain the trimeric Hsc70/αSgt/Csp complex, which has been described previously in *in vitro* systems by Tobaben and colleagues (2005). The refolding activity of CHL1/Hsc70/αSgt and CHL1/Csp complexes is directed specifically towards the components of SNARE (soluble N-ethylmaleimide-sensitive factor attachment protein receptor) machinery Snap25 and Vamp2, respectively, which participate in the fusion of synaptic vesicles. Stressful conditions, such as exposure to heat or prolonged synaptic activity, result in a pronounced degradation of SNARE complex components in the brain of CHL1 deficient mice and in reduced ability of the non-degraded components to assemble the SNARE complex. The finding that in the brains of "non-stressed" CHL1 deficient mice SNARE complex components accumulated in lysosomes suggests that incorrectly folded proteins gradually accumulate in the brain. Also it is necessary to mention that protein refolding activity in CHL1 deficient synapses and recruitment of Hsc70 and αSgt to synapses are reduced as compared to wild type synapses. The defect of SNARE machinery formation following the prolonged stimulation of synaptic activity leads to the inhibition of the synaptic vesicle recycling in CHL1 deficient neurons. In other words, CHL1 deficient neurons are not able to sustain prolonged synaptic activity. Our observations demonstrate that CHL1 is a novel regulator of the presynaptic chaperone machinery and thus a decisive player in synaptic vesicle exocytosis. Also CHL1 plays an important role in the synaptic vesicles endocytosis. It regulates the uncoating of clathrin-coated synaptic vesicles. Altogether, we show that cell adhesion molecule CHL1 is involved in two steps of synaptic vesicles recycling: in exocytosis and in endocytosis.

VIII. References

Agarraberes, F.A., Dice, J.F. (2001). A molecular chaperone complex at the lysosomal membrane is required for protein translocation. J. Cell. Sci. *114* (Pt 13), 2491-2499.

Ananthan, J., Goldberg, A.L., Voellmy, R. (1986). Abnormal proteins serve as eukaryotic stress signals and trigger the activation of heat shock genes. Science *232* (4749), 522-524.

Ando, K., Kudo, Y., Takahashi, M. (2005). Negative regulation of neurotransmitter release by calpain: a possible involvement of specific SNAP-25 cleavage. J. Neurochem. *94* (3), 651-658.

Andreyeva, A., Leshchyns'ka, I., Sytnyk, V., Schachner, M. (submitted). Sustainability of synaptic vesicle exocytosis relies on CHL1 as a selective organizer of the presynaptic chaperone machinery refolding the SNARE complex.

Angeloni, D., Lindor, N.M., Pack, S., Latif, F., Wei, M.H., Lerman, M.I. (1999). CALL gene is haploinsufficient in a 3p-syndrome patient. Am. J. Med. Genet. *86* (5), 482-485.

Angeletti, P.C., Walker, D., Panganiban, A.T. (2002). Small glutamine-rich protein/viral protein U-binding protein is a novel cochaperone that affects heat shock protein 70 activity. Cell Stress Chaperones. *7* (3), 258-268.

Arion, D., Unger, T., Lewis, D.A., Levitt, P., Mirnics, K. (2007). Molecular evidence for increased expression of genes related to immune and chaperone function in the prefrontal cortex in schizophrenia. Biol. Psychiatry *62* (7), 711-721.

Arnold, O.H. (1999). Schizophrenia - A disturbance of signal interaction between the entorhinal cortex and the dentate gyrus? The contribution of experimental dibenamine psychosis to the pathogenesis of schizophrenia: A hypothesis. Neuropsychobiology *40* (1), 21-32.

Auluck, P.K., Chan, H.Y., Trojanowski, J.Q., Lee, V.M., Bonini, N.M. (2002). Chaperone suppression of alpha-synuclein toxicity in a Drosophila model for Parkinson's disease. Science *295* (5556), 865-868.

Ballinger, C.A., Connell, P., Wu, Y., Hu, Z., Thompson, L.J., Yin, L.Y., Patterson, C. (1999). Identification of CHIP, a novel tetratricopeptide repeat-containing protein that interacts with heat shock proteins and negatively regulates chaperone functions. Mol. Cell Biol. *19* (6), 4535-4545.

Bercovich, B., Stancovski, I., Mayer, A., Blumenfeld, N., Laszlo, A., Schwartz, A.L., Ciechanover, A. (1997). Ubiquitin-dependent degradation of certain protein substrates in vitro requires the molecular chaperone Hsc70. J. Biol. Chem. *272* (14), 9002-9010.

Ben-Zvi, A., De Los Rios, P., Dietler, G., Goloubinoff, P. (2004). Active solubilization and refolding of stable protein aggregates by cooperative unfolding action of individual hsp70 chaperones. J. Biol. Chem. *279* (36), 37298-37303.

Ben-Zvi, A.P., Goloubinoff, P. (2001). Review: mechanisms of disaggregation and refolding of stable protein aggregates by molecular chaperones. J. Struct. Biol. *135* (2), 84-93.

Bingol, B., Schuman, E.M. (2005). Synaptic protein degradation by the ubiquitin proteasome system. Curr. Opin. Neurobiol. *15* (5), 536-541.

Bingol, B., Schuman, E.M. (2006). Activity-dependent dynamics and sequestration of proteasomes in dendritic spines. Nature *441* (7097), 1144-1148.

Blatch, G.L., Lassle, M. (1999). The tetratricopeptide repeat: a structural motif mediating protein-protein interactions. Bioessays *21* (11), 932-939.

Braell, W.A., Schlossman, D.M., Schmid, S.L., Rothman, J.E. (1984). Dissociation of clathrin coats coupled to the hydrolysis of ATP: role of an uncoating ATPase. J. Cell Biol. *99* (2), 734-741.

Braun, J.E., Wilbanks, S.M., Scheller, R.H. (1996). The cysteine string secretory vesicle protein activates Hsc70 ATPase. J. Biol. Chem. *271* (42), 25989-25993.

Bronk, P., Nie, Z., Klose, M.K., Dawson-Scully, K., Zhang, J., Robertson, R.M., Atwood, H.L., Zinsmaier, K.E. (2005). The multiple functions of cysteine-string protein analyzed at Drosophila nerve terminals. J. Neurosci. *25* (9), 2204-2214.

Bronk, P., Wenniger, J.J., Dawson-Scully, K., Guo, X., Hong, S., Atwood, H.L., Zinsmaier, K.E. (2001). Drosophila Hsc70-4 is critical for neurotransmitter exocytosis in vivo. Neuron *30* (2), 475-488.

Brown, C.R., Hong-Brown, L.Q., Doxsey, S.J., Welch, W.J., (1996). Molecular chaperones and the centrosome. A role for HSP 73 in centrosomal repair following heat shock treatment. J. Biol. Chem. *271* (2), 833-840.

Brummendorf, T., Kenwrick, S., Rathjen, F.G. (1998). Neural cell recognition molecule L1: from cell biology to human hereditary brain malformations. Curr. Opin. Neurobiol. *8* (1), 87-97.

Buhusi, M., Midkiff, B.R., Gates, A.M., Richter, M., Schachner, M., Maness, P.F. (2003). Close homolog of L1 is an enhancer of integrin-mediated cell migration. J. Biol. Chem. *278* (27), 25024-25031.

Bukau, B., Horwich, A.L. (1998). The Hsp70 and Hsp60 chaperone machines. Cell *92* (3), 351-366.

Burgoon, M.P., Grumet, M., Mauro, V., Edelman, G.M., Cunningham, B.A. (1991). Structure of the chicken neuron-glia cell adhesion molecule, Ng-CAM: origin of the polypeptides and relation to the Ig superfamily. J. Cell Biol. *112* (5), 1017-1029.

Chaisuksunt, V., Campbell, G., Zhang, Y., Schachner, M., Lieberman, A.R., Anderson, P.N. (2000a). The cell recognition molecule CHL1 is strongly upregulated by injured and regenerating thalamic neurons. J. Comp. Neurol. *425* (3), 382-392.

Chaisuksunt, V., Campbell, G., Zhang, Y., Schachner, M., Lieberman, A.R., Anderson, P.N. (2003). Expression of regeneration-related molecules in injured and regenerating striatal and nigral neurons. J. Neurocytol. *32* (2), 161-183.

Chaisuksunt, V., Zhang, Y., Anderson, P.N., Campbell, G., Vaudano, E., Schachner, M., Lieberman, A.R. (2000b). Axonal regeneration from CNS neurons in the cerebellum and brainstem of adult rats: correlation with the patterns of expression and distribution of messenger RNAs for L1, CHL1, c-jun and growth-associated protein-43. Neuroscience *100* (1), 87-108.

Chamberlain, L.H., Burgoyne, R.D. (1997a). Activation of the ATPase activity of heat-shock proteins Hsc70/Hsp70 by cysteine-string protein. Biochem. J. *322* (Pt 3), 853-858.

Chamberlain, L.H., Burgoyne, R.D. (1997b). The molecular chaperone function of the secretory vesicle cysteine string proteins. J. Biol. Chem. *272* (50), 31420-31426.

Chamberlain, L.H., Burgoyne, R.D. (1998). The cysteine-string domain of the secretory vesicle cysteine-string protein is required for membrane targeting. Biochem. J. *335* (Pt 2), 205-209.

Chamberlain, L.H., Burgoyne, R.D. (2000). Cysteine-string protein: the chaperone at the synapse. J. Neurochem. *74* (5), 1781-1789.

Chamberlain, L.H., Graham, M.E., Kane, S., Jackson, J.L., Maier, V.H., Burgoyne, R.D., Gould, G.W. (2001). The synaptic vesicle protein, cysteine-string protein, is associated with the plasma membrane in 3T3-L1 adipocytes and interacts with syntaxin 4. J. Cell. Sci. *114* (Pt 2), 445-455.

Chan, K.M., Delfert, D., Junger, K.D. (1986). A direct colorimetric assay for Ca2+ -stimulated ATPase activity. Anal. Biochem. *157* (2), 375-380.

Chandra, S., Gallardo, G., Fernandez-Chacon, R., Schluter, O.M., Sudhof, T.C. (2005). Alpha-synuclein cooperates with CSPalpha in preventing neurodegeneration. Cell *123* (3), 383-396.

Chang, H.C., Newmyer, S.L., Hull, M.J., Ebersold, M., Schmid, S.L., Mellman, I. (2002). Hsc70 is required for endocytosis and clathrin function in Drosophila. J. Cell. Biol. *159* (3), 477-487.

Chappell, T.G., Konforti, B.B., Schmid, S.L., Rothman, J.E. (1987). The ATPase core of a clathrin uncoating protein. J. Biol. Chem. *262* (2), 746-751.

Chappell, T.G., Welch, W.J., Schlossman, D.M., Palter, K.B., Schlesinger, M.J., Rothman, J.E. (1986). Uncoating ATPase is a member of the 70 kilodalton family of stress proteins. Cell *45* (1), 3-13.

Cheetham, M.E., Jackson, A.P., Anderton, B.H. (1994). Regulation of 70-kDa heat-shock-protein ATPase activity and substrate binding by human DnaJ-like proteins, HSJ1a and HSJ1b. Eur. J. Biochem. *226* (1), 99-107.

Chen, Q.Y., Chen, Q., Feng, G.Y., Lindpaintner, K., Chen, Y., Sun, X., Chen, Z., Gao, Z., Tang, J., He, L. (2005). Case-control association study of the close homologue of L1 (CHL1) gene and schizophrenia in the Chinese population. Schizophr. Res. *73* (2-3), 269-274.

Chen, S., Mantei, N., Dong, L., Schachner, M. (1999). Prevention of neuronal cell death by neural adhesion molecules L1 and CHL1. J. Neurobiol. *38* (3), 428-439.

Chen, Y.A., Scheller, R.H. (2001). SNARE-mediated membrane fusion. Nat. Rev. Mol. Cell. Biol. *2* (2), 98-106.

Chin, L.S., Vavalle, J.P., Li, L. (2002). Staring, a novel E3 ubiquitin-protein ligase that targets syntaxin 1 for degradation. J. Biol. Chem. *277* (38), 35071-35079.

Chirico, W.J., Waters, M.G., Blobel, G. (1988). 70K heat shock related proteins stimulate protein translocation into microsomes. Nature *332* (6167), 805-810.

Crossin, K.L., Krushel, L.A. (2000). Cellular signaling by neural cell adhesion molecules of the immunoglobulin superfamily. Dev. Dyn. *218* (2), 260-279.

Cuervo, A.M., Dice, J.F. (1996). A receptor for the selective uptake and degradation of proteins by lysosomes. Science *273* (5274), 501-503.

Cuervo, A.M., Dice, J.F., Knecht, E. (1997). A population of rat liver lysosomes responsible for the selective uptake and degradation of cytosolic proteins. J. Biol. Chem. *272* (9), 5606-5615.

Cummings, C.J., Sun, Y., Opal, P., Antalffy, B., Mestril, R., Orr, H.T., Dillmann, W.H., Zoghbi, H.Y. (2001). Over-expression of inducible HSP70 chaperone suppresses neuropathology and improves motor function in SCA1 mice. Hum. Mol. Genet. *10* (14), 1511-1518.

Cziepluch, C., Lampel, S., Grewenig, A., Grund, C., Lichter, P., Rommelaere, J. (2000). H-1 parvovirus-associated replication bodies: a distinct virus-induced nuclear structure. J. Virol. *74* (10), 4807-4815.

D'Andrea, L.D., Regan, L. (2003). TPR proteins: the versatile helix. Trends Biochem. Sci. *28* (12), 655-662.

DeLuca-Flaherty, C., McKay, D.B., Parham, P., Hill, B.L. (1990). Uncoating protein (hsc70) binds a conformationally labile domain of clathrin light chain LCa to stimulate ATP hydrolysis. Cell *62* (5), 875-887.

De Maio, A. (1999). Heat shock proteins: facts, thoughts, and dreams. Shock *11* (1), 1-12.

Deshaies, R.J., Koch, B.D., Werner-Washburne, M., Craig, E.A., Schekman, R. (1988). A subfamily of stress proteins facilitates translocation of secretory and mitochondrial precursor polypeptides. Nature *332* (6167), 800-805.

Demyanenko, G.P., Schachner, M., Anton, E., Schmid, R., Feng, G., Sanes, J., Maness, P.F. (2004). Close homolog of L1 modulates area-specific neuronal positioning and dendrite orientation in the cerebral cortex. Neuron *44* (3), 423-437.

Dice, J.F., Terlecky, S.R., Chiang, H.L., Olson, T.S., Isenman, L.D., Short-Russell, S.R., Freundlieb, S., Terlecky, L.J. (1990). A selective pathway for degradation of cytosolic proteins by lysosomes. Semin. Cell. Biol. *1* (6), 449-455.

Dong, L., Chen, S., Richter, M., Schachner, M. (2002). Single-chain variable fragment antibodies against the neural adhesion molecule CHL1 (close homolog of L1) enhance neurite outgrowth. J. Neurosci. Res. *69* (4), 437-447.

D'Souza, S.M., Brown, I.R. (1998). Constitutive expression of heat shock proteins Hsp90, Hsc70, Hsp70 and Hsp60 in neural and non-neural tissues of the rat during postnatal development. Cell Stress Chaperones *3* (3), 188-199.

D'Souza, S.E., Ginsberg, M.H., Plow, E.F. (1991). Arginyl-glycyl-aspartic acid (RGD): a cell adhesion motif. Trends Biochem. Sci. *16* (7), 246-250.

Evans, G.J., Morgan, A. (2002). Phosphorylation-dependent interaction of the synaptic vesicle proteins cysteine string protein and synaptotagmin I. Biochem. J. *364* (Pt 2), 343-347.

Evans, G.J., Morgan, A., Burgoyne, R.D. (2003). Tying everything together: the multiple roles of cysteine string protein (CSP) in regulated exocytosis. Traffic *4* (10), 653-659.

Evans, G.J., Wilkinson, M.C., Graham, M.E., Turner, K.M., Chamberlain, L.H., Burgoyne, R.D., Morgan, A. (2001). Phosphorylation of cysteine string protein by protein kinase A. Implications for the modulation of exocytosis. J. Biol. Chem. *276* (51), 47877-47885.

Fasshauer, D., Eliason, W.K., Brünger, A.T., Jahn, R. (1998). Identification of a minimal core of the synaptic SNARE complex sufficient for reversible assembly and disassembly. Biochemistry *37* (29), 10354-10362.

Fasshauer, D., Otto, H., Eliason, W.K., Jahn. R., Brünger, A.T. (1997). Structural changes are associated with soluble N-ethylmaleimide-sensitive fusion protein attachment protein receptor complex formation. J. Biol. Chem. *272* (44), 28036-28041.

Fatemi, S.H., Earle, J.A., Stary, J.M., Lee, S., Sedgewick, J. (2001). Altered levels of the synaptosomal associated protein SNAP-25 in hippocampus of subjects with mood disorders and schizophrenia. Neuroreport *12* (15), 3257-3262.

Fergestad, T., Wu, M.N., Schulze, K.L., Lloyd, T.E., Bellen, H.J., Broadie, K. (2001). Targeted mutations in the syntaxin H3 domain specifically disrupt SNARE complex function in synaptic transmission. J. Neurosci. *21* (23), 9142-9150.

Fernandez-Chacon, R., Wolfel, M., Nishimune, H., Tabares, L., Schmitz, F., Castellano-Munoz, M., Rosenmund, C., Montesinos, M.L., Sanes, J.R., Schneggenburger, R., Sudhof, T.C. (2004). The synaptic vesicle protein CSP alpha prevents presynaptic degeneration. Neuron *42* (2), 237-251.

Frints, S.G., Marynen, P., Hartmann, D., Fryns, J.P., Steyaert, J., Schachner, M., Rolf, B., Craessaerts, K., Snellinx, A., Hollanders, K., D'Hooge, R., De Deyn, P.P., Froyen, G. (2003). CALL interrupted in a patient with non-specific mental retardation: gene dosage-dependent alteration of murine brain development and behavior. Hum. Mol. Genet. *12* (13), 1463-1474.

Flaherty, K.M., DeLuca-Flaherty, C., McKay, D.B. (1990). Three-dimensional structure of the ATPase fragment of a 70K heat-shock cognate protein. Nature *346* (6285), 623-628.

Flynn, G.C., Chappell, T.G., Rothman, J.E. (1989). Peptide binding and release by proteins implicated as catalysts of protein assembly. Science *245* (4916), 385-390.

Foster, J.A., Rush, S.J., Brown, I.R. (1995). Localization of constitutive and hyperthermia-inducible heat shock mRNAs (hsc70 and hsp70) in the rabbit cerebellum and brainstem by non-radioactive in situ hybridization. J. Neurosci. Res. *41* (5), 603-612.

Fouchaq, B., Benaroudj, N., Ebel, C., Ladjimi, M.M. (1999). Oligomerization of the 17-kDa peptide-binding domain of the molecular chaperone HSC70. Eur. J. Biochem. *259* (1-2), 379-384.

Gebauer, M., Zeiner, M., Gehring, U. (1997). Proteins interacting with the molecular chaperone hsp70/hsc70: physical associations and effects on refolding activity. FEBS Lett. *417* (1), 109-113.

Gething, M.J., Sambrook J. (1992). Protein folding in the cell. Nature *355* (6355), 33-45.

Glickman, M.H., Raveh, D. (2005). Proteasome plasticity. FEBS Lett. *579* (15), 3214-3223.

Goff, S.A., Goldberg, A.L. (1985). Production of abnormal proteins in E. coli stimulates transcription of lon and other heat shock genes. Cell *41* (2), 587-595.

Graham, J., Ford, T., Rickwood, D. (1994). The preparation of subcellular organelles from mouse liver in self-generated gradients of iodixanol. Anal. Biochem. *220* (2), 367-373.

Greaves, J., Chamberlain, L.H. (2006). Dual Role of the Cysteine-String Domain in Membrane Binding and Palmitoylation-dependent Sorting of the Molecular Chaperone Cysteine-String Protein. Mol. Biol. Cell. *17* (11), 4748-4759.

Green, L.A., Liem, R.K. (1989). Beta-internexin is a microtubule-associated protein identical to the 70-kDa heat-shock cognate protein and the clathrin uncoating ATPase. J. Biol. Chem. *264* (26), 15210-15215.

Gundersen, C.B., Mastrogiacomo, A., Faull, K., Umbach, J.A. (1994). Extensive lipidation of a Torpedo cysteine string protein. J. Biol. Chem. *269* (30), 19197-19199.

Gundersen, C.B., Umbach, J.A. (1992). Suppression cloning of the cDNA for a candidate subunit of a presynaptic calcium channel. Neuron *9* (3), 527-537.

Ha, J.H., McKay, D.B. (1994). ATPase kinetics of recombinant bovine 70 kDa heat shock cognate protein and its amino-terminal ATPase domain. Biochemistry *33* (48), 14625-14635.

Ha, J.H., McKay, D.B. (1995). Kinetics of nucleotide-induced changes in the tryptophan fluorescence of the molecular chaperone Hsc70 and its subfragments suggest the ATP-induced conformational change follows initial ATP binding. Biochemistry *34* (36), 11635-11644.

Hamos, J.E., Oblas, B., Pulaski-Salo, D., Welch, W.J., Bole, D.G., Drachman, D.A. (1991). Expression of heat shock proteins in Alzheimer's disease. Neurology *41* (3), 345-350.

Hartl, F.U. (1996). Molecular chaperones in cellular protein folding. Nature *381* (6583), 571-579.

Hartl, F.U., Hayer-Hartl, M. (2002). Molecular chaperones in the cytosol: from nascent chain to folded protein. Science *295* (5561), 1852-1858.

Hillenbrand, R., Molthagen, M., Montag, D., Schachner, M. (1999). The close homologue of the neural adhesion molecule L1 (CHL1): patterns of expression and promotion of neurite outgrowth by heterophilic interactions. Eur. J. Neurosci. *11* (3), 813-826.

Hoffman, K.B. (1998). The relationship between adhesion molecules and neuronal plasticity. Cell. Mol. Neurobiol. *18* (5), 461-475.

Hohfeld, J., Cyr, D.M., Patterson, C. (2001). From the cradle to the grave: molecular chaperones that may choose between folding and degradation. EMBO Rep. *2* (10), 885-890.

Hohfeld, J., Jentsch, S. (1997). GrpE-like regulation of the hsc70 chaperone by the anti-apoptotic protein BAG-1. EMBO J. *16* (20), 6209-6216.

Hohfeld, J., Minami, Y., Hartl, F.U. (1995). Hip, a novel cochaperone involved in the eukaryotic Hsc70/Hsp40 reaction cycle. Cell *83* (4), 589-598.

Holm, J., Hillenbrand, R., Steuber, V., Bartsch, U., Moos, M., Lubbert, H., Montag, D., Schachner, M. (1996). Structural features of a close homologue of L1 (CHL1) in the mouse: a new member of the L1 family of neural recognition molecules. Eur. J. Neurosci. *8* (8), 1613-1629.

Honer, W.G., Falkai, P., Bayer, T.A., Xie, J., Hu, L., Li, H.Y., Arango, V., Mann, J.J., Dwork, A.J., Trimble, W.S. (2002). Abnormalities of SNARE mechanism proteins in anterior frontal cortex in severe mental illness. Cereb. Cortex. *12* (4), 349-356.

Horigome, T., Sugano, H. (1983). A rapid method for removal of detergents from protein solution. Anal. Biochem. *130* (2), 393-396.

Hortsch, M. (2000). Structural and functional evolution of the L1 family: are four adhesion molecules better than one? Mol. Cell. Neurosci. *15* (1), 1-10.

Hsu, C.C., Davis, K.M., Jin, H., Foos, T., Floor, E., Chen, W., Tyburski, J.B., Yang, C.Y., Schloss, J.V., Wu, J.Y. (2000). Association of L-glutamic acid decarboxylase to the 70-kDa heat shock protein as a potential anchoring mechanism to synaptic vesicles. J. Biol. Chem. *275* (27), 20822-20828.

Hu, S.M., Wang, C. (1996). Involvement of the 10-kDa C-terminal fragment of hsc70 in complexing with unfolded protein. Arch. Biochem. Biophys. *332* (1), 163-169.

Huang, S.P., Tsai, M.Y., Tzou, Y.M., Wu, W.G., Wang, C. (1993). Aspartyl residue 10 is essential for ATPase activity of rat hsc70. J. Biol. Chem. *268* (3), 2063-2068.

Huttner, W.B., Schiebler, W., Greengard, P., De Camilli, P. (1983). Synapsin I (protein I), a nerve terminal-specific phosphoprotein. III. Its association with synaptic vesicles studied in a highly purified synaptic vesicle preparation. J. Cell Biol. *96* (5), 1374-1388.

Imamoto, N., Matsuoka, Y., Kurihara, T., Kohno, K., Miyagi, M., Sakiyama, F., Okada, Y., Tsunasawa, S., Yoneda, Y. (1992). Antibodies against 70-kD heat shock cognate protein inhibit mediated nuclear import of karyophilic proteins. J. Cell Biol. *119* (5), 1047-1061.

Ingolia, T.D., Craig, E.A. (1982). Drosophila gene related to the major heat shock-induced gene is transcribed at normal temperatures and not induced by heat shock. Proc. Natl. Acad. Sci. U S A. *79* (2), 525-529.

Inoue, H., Nojima, H., Okayama, H. (1990). High efficiency transformation of Escherichia coli with plasmids. Gene *96* (1), 23-28.

Irintchev, A., Koch, M., Needham, L.K., Maness, P., Schachner, M. (2004). Impairment of sensorimotor gating in mice deficient in the cell adhesion molecule L1 or its close homologue, CHL1. Brain Res. *1029* (1), 131-134.

Jahn, R., Niemann, H. (1994). Molecular mechanisms of clostridial neurotoxins. Ann. N. Y. Acad. Sci. *733*, 245-255.

Jiang, J., Ballinger, C.A., Wu, Y., Dai, Q., Cyr, D.M., Höhfeld, J., Patterson, C. (2001). CHIP is a U-box-dependent E3 ubiquitin ligase: identification of Hsc70 as a target for ubiquitylation. J. Biol. Chem. *276* (46), 42938-42944.

Jiang, R., Gao, B., Prasad, K., Greene, L.E., Eisenberg, E. (2000). Hsc70 chaperones clathrin and primes it to interact with vesicle membranes. J. Biol. Chem. *275* (12), 8439-8447.

Jin, H., Wu, H., Osterhaus, G., Wei, J., Davis, K., Sha, D., Floor, E., Hsu, C.C., Kopke, R.D., Wu, J.Y. (2003). Demonstration of functional coupling between gamma -aminobutyric acid (GABA) synthesis and vesicular GABA transport into synaptic vesicles. Proc. Natl. Acad. Sci. U S A. *100* (7), 4293-4298.

Joglekar, A.P., Hay, J.C. (2005). Evidence for regulation of ER/Golgi SNARE complex formation by hsc70 chaperones. Eur. J. Cell. Biol. *84* (5), 529-542.

Kabani, M., McLellan, C., Raynes, D.A., Guerriero, V., Brodsky, J.L. (2002). HspBP1, a homologue of the yeast Fes1 and Sls1 proteins, is an Hsc70 nucleotide exchange factor. FEBS Lett. *531* (2), 339-342.

Kamiguchi, H., Long, K.E., Pendergast, M., Schaefer, A.W., Rapoport, I., Kirchhausen, T., Lemmon, V. (1998). The neural cell adhesion molecule L1 interacts with the AP-2 adaptor and is endocytosed via the clathrin-mediated pathway. J. Neurosci. *18* (14), 5311-5321.

Kelley, W.L. (1998). The J-domain family and the recruitment of chaperone power. Trends Biochem. Sci. *23* (6), 222-227.

Kiryushko, D., Berezin, V., Bock, E. (2004). Regulators of neurite outgrowth: role of cell adhesion molecules. Ann. N. Y. Acad. Sci. *1014*, 140-154.

Kleene, R., Yang, H., Kutsche, M., Schachner, M. (2001). The neural recognition molecule L1 is a sialic acid-binding lectin for CD24, which induces promotion and inhibition of neurite outgrowth. J. Biol. Chem. *276* (24), 21656-21663.

Koticha, D., Babiarz, J., Kane-Goldsmith, N., Jacob, J., Raju, K., Grumet, M. (2005). Cell adhesion and neurite outgrowth are promoted by neurofascin NF155 and inhibited by NF186. Mol. Cell. Neurosci. *30* (1), 137-148.

Lamb, J.R., Tugendreich, S., Hieter, P. (1995). Tetratrico peptide repeat interactions: to TPR or not to TPR? Trends. Biochem. Sci. *20* (7), 257-259.

Leshchyns'ka, I., Sytnyk, V., Richter, M., Andreyeva, A., Puchkov, D., Schachner, M. (2006). The adhesion molecule CHL1 regulates uncoating of clathrin-coated synaptic vesicles. Neuron. *52* (6), 1011-1025.

Leveque, C., Pupier, S., Marqueze, B., Geslin, L., Kataoka, M., Takahashi, M., De Waard, M., Seagar, M. (1998). Interaction of cysteine string proteins with the alpha1A subunit of the P/Q-type calcium channel. J. Biol. Chem. *273* (22), 13488-13492.

Li, L., Chin, L.S., Shupliakov, O., Brodin, L., Sihra, T.S., Hvalby, O., Jensen, V., Zheng, D., McNamara, J.O., Greengard, P., Andersen, P. (1995). Impairment of synaptic vesicle clustering and of synaptic transmission, and increased seizure propensity, in synapsin I-deficient mice. Proc. Natl. Acad. Sci. U S A. *92* (20), 9235-9239.

Lin, R.C., Scheller, R.H. (1997). Structural organization of the synaptic exocytosis core complex. Neuron *19* (5), 1087-1094.

Liou, S.T., Wang, C. (2005). Small glutamine-rich tetratricopeptide repeat-containing protein is composed of three structural units with distinct functions. Arch. Biochem. Biophys. *435* (2), 253-263.

Liu, Q., Dwyer, N.D., O'Leary, D.D. (2000). Differential expression of COUP-TFI, CHL1, and two novel genes in developing neocortex identified by differential display PCR. J. Neurosci. *20* (20), 7682-7690.

Liu, F.H., Wu, S.J., Hu, S.M., Hsiao, C.D., Wang, C. (1999). Specific interaction of the 70-kDa heat shock cognate protein with the tetratricopeptide repeats. J. Biol. Chem. *274* (48), 34425-34432.

Loones, M.T., Rallu, M., Mezger, V., Morange, M. (1997). HSP gene expression and HSF2 in mouse development. Cell. Mol. Life. Sci. *53* (2), 179-190.

Ma, Z., Portwood, N., Foss, A., Grill, V., Björklund, A. (2005). Evidence that insulin secretion influences SNAP-25 through proteasomal activation. Biochem. Biophys. Res. Commun. *329* (3), 1118-1126.

Mason, M.R., Lieberman, A.R., Anderson, P.N. (2003). Corticospinal neurons up-regulate a range of growth-associated genes following intracortical, but not spinal, axotomy. Eur. J. Neurosci. *18* (4), 789-802.

Massey, A., Kiffin, R., Cuervo, A.M. (2004). Pathophysiology of chaperone-mediated autophagy. Int. J. Biochem. Cell. Biol. *36* (12), 2420-2434.

Mastrogiacomo, A., Parsons, S.M., Zampighi, G.A., Jenden, D.J., Umbach. J.A., Gundersen C.B. (1994). Cysteine string proteins: a potential link between synaptic vesicles and presynaptic Ca2+ channels. Science *263* (5149), 981-982.

Majeski AE, Dice JF. (2004). Mechanisms of chaperone-mediated autophagy. Int. J. Biochem. Cell. Biol. *36* (12), 2435-2444.

McDonough, H., Patterson, C. (2003). CHIP: a link between the chaperone and proteasome systems. Cell Stress Chaperones *8* (4), 303-308.

McNaught, K.S., Belizaire, R., Isacson, O., Jenner, P., Olanow, C.W. (2003). Altered proteasomal function in sporadic Parkinson's disease. Exp. Neurol. *179* (1), 38-46.

Miesenböck, G., De Angelis, D.A., Rothman, J.E. (1998). Visualizing secretion and synaptic transmission with pH-sensitive green fluorescent proteins. Nature *394* (6689), 192-5.

Miller, L.C., Swayne, L.A., Chen, L., Feng, Z.P., Wacker, J.L., Muchowski, P.J., Zamponi, G.W., Braun, J.E. (2003). Cysteine string protein (CSP) inhibition of N-type calcium channels is blocked by mutant huntingtin. J. Biol. Chem. *278* (52), 53072-53081.

Minami, Y., Hohfeld, J., Ohtsuka, K., Hartl, F.U. (1996). Regulation of the heat-shock protein 70 reaction cycle by the mammalian DnaJ homolog, Hsp40. J. Biol. Chem. *271* (32), 19617-19624.

Montag-Sallaz, M., Baarke, A., Montag, D. (2003). Aberrant neuronal connectivity in CHL1-deficient mice is associated with altered information processing-related immediate early gene expression. J. Neurobiol. *57* (1), 67-80.

Montag-Sallaz, M., Schachner, M., Montag, D. (2002). Misguided axonal projections, neural cell adhesion molecule 180 mRNA upregulation, and altered behavior in mice deficient for the close homolog of L1. Mol. Cell. Biol. *22* (22), 7967-7981.

Morellini, F., Lepsveridze, E., Kähler, B., Dityatev, A., Schachner, M. (2007). Reduced reactivity to novelty, impaired social behavior, and enhanced basal synaptic excitatory activity in perforant path projections to the dentate gyrus in young adult mice deficient in the neural cell adhesion molecule CHL1. Mol. Cell. Neurosci. *34*, 121-136.

Morgan, J.R., Prasad, K., Jin, S., Augustine, G.J., Lafer, E.M. (2001). Uncoating of clathrin-coated vesicles in presynaptic terminals: roles for Hsc70 and auxilin. Neuron *32* (2), 289-300.

Morishima, N. (2005) Control of cell fate by Hsp70: more than an evanescent meeting. J. Biochem. (Tokyo) *137* (4), 449-453.

Morshauser, R.C., Hu, W., Wang, H., Pang, Y., Flynn, G.C., Zuiderweg, E.R. (1999). High-resolution solution structure of the 18 kDa substrate-binding domain of the mammalian chaperone protein Hsc70. J. Mol. Biol. *289* (5), 1387-1403.

Muchowski, P.J., Wacker, J.L. (2005). Modulation of neurodegeneration by molecular chaperones. Nat. Rev. Neurosci. *6* (1), 11-22.

Mukaetova-Ladinska, E.B., Hurt, J., Honer, W.G., Harrington, C.R., Wischik, C.M. (2002). Loss of synaptic but not cytoskeletal proteins in the cerebellum of chronic schizophrenics. Neurosci. Lett. *317* (3), 161-165.

Murata, S., Chiba, T., Tanaka, K. (2003). CHIP: a quality-control E3 ligase collaborating with molecular chaperones. Int. J. Biochem. Cell. Biol. *35* (5), 572-578.

Natochin, M., Campbell, T.N., Barren, B., Miller, L.C., Hameed, S., Artemyev, N.O., Braun, J.E. (2005). Characterization of the G alpha(s) regulator cysteine string protein. J. Biol. Chem. *280* (34), 30236-30241.

Newmyer, S.L., Christensen, A., Sever, S. (2003). Auxilin-dynamin interactions link the uncoating ATPase chaperone machinery with vesicle formation. Dev. Cell. *4* (6), 929-940.

Newmyer, S.L., Schmid, S.L. (2001). Dominant-interfering Hsc70 mutants disrupt multiple stages of the clathrin-coated vesicle cycle in vivo. J. Cell. Biol. *152* (3), 607-620.

Nie, Z., Ranjan, R., Wenniger, J.J., Hong, S.N., Bronk, P., Zinsmaier, K.E. (1999). Overexpression of cysteine-string proteins in Drosophila reveals interactions with syntaxin. J. Neurosci. *19* (23), 10270-10279.

Nishimune, H., Bernreuther, C., Carroll, P., Chen, S., Schachner, M., Henderson, C.E. (2005). Neural adhesion molecules L1 and CHL1 are survival factors for motoneurons. J. Neurosci. Res. *80* (5), 593-599.

Ohtsuka, K., Suzuki, T. (2000). Roles of molecular chaperones in the nervous system. Brain Res. Bull. *53* (2), 141-146.

Parsell, D.A., Lindquist, S. (1993). The function of heat-shock proteins in stress tolerance: degradation and reactivation of damaged proteins. Annu. Rev. Genet. *27*, 437-496.

Parsell, D.A., Sauer, R.T. (1989). Induction of a heat shock-like response by unfolded protein in Escherichia coli: dependence on protein level not protein degradation. Genes Dev. *3* (8), 1226-1232.

Pilon, M., Schekman, R. (1999). Protein translocation: how Hsp70 pulls it off. Cell *97* (6), 679-682.

Pratte, M., Rougon, G., Schachner, M., Jamon, M. (2003). Mice deficient for the close homologue of the neural adhesion cell L1 (CHL1) display alterations in emotional reactivity and motor coordination. Behav. Brain Res. *147* (1-2), 31-39.

Ranjan, R., Bronk, P., Zinsmaier, K.E. (1998). Cysteine string protein is required for calcium secretion coupling of evoked neurotransmission in drosophila but not for vesicle recycling. J. Neurosci. *18* (3), 956-964.

Richter, M. (2002). Identification and characterization of intracellular binding partners of the CHL1 (close homologue of L1) neural cell recognition molecule. PhD thesis.

Rothman, J.E., Schmid, S.L. (1986). Enzymatic recycling of clathrin from coated vesicles. Cell *46* (1), 5-9.

Rubinsztein, D.C. (2006). The roles of intracellular protein-degradation pathways in neurodegeneration. Nature *443* (7113), 780-786.

Sadis, S., Hightower, L.E. (1992). Unfolded proteins stimulate molecular chaperone Hsc70 ATPase by accelerating ADP/ATP exchange. Biochemistry *31* (39), 9406-9412.

Sakisaka, T., Meerlo, T., Matteson, J., Plutner, H., Balch, W.E. (2002). Rab-alphaGDI activity is regulated by a Hsp90 chaperone complex. EMBO J. *21* (22), 6125-6135.

Sakurai, K., Migita, O., Toru, M., Arinami, T. (2002). An association between a missense polymorphism in the close homologue of L1 (CHL1, CALL) gene and schizophrenia. Mol. Psychiatry *7* (4), 412-415.

Salvador, N., Aguado, C., Horst, M., Knecht, E. (2000). Import of a cytosolic protein into lysosomes by chaperone-mediated autophagy depends on its folding state. J. Biol. Chem. *275* (35), 27447-27456.

Sambrook, J., Fritsch, E. F., Maniatis, T. (1989). Molecular cloning: A Laboratory Manual. (Cold Spring Habor, NY: Cold Spring Habor Laboratory Press).

Sarter, M., Bruno, J.P., Parikh, V. (2007). Abnormal neurotransmitter release underlying behavioral and cognitive disorders: toward concepts of dynamic and function-specific dysregulation. Neuropsychopharmacology *32* (7), 1452-1461.

Shao, J., Diamond, M.I. (2007). Polyglutamine diseases: emerging concepts in pathogenesis and therapy. Hum. Mol. Genet. *16* (2), R115- R123.

Schlossman, D.M., Schmid, S.L., Braell, W.A., Rothman, J.E. (1984). An enzyme that removes clathrin coats: purification of an uncoating ATPase. J. Cell. Biol. *99* (2), 723-733.

Schmid, S.L., Braell, W.A., Schlossman, D.M., Rothman, J.E. (1984). A role for clathrin light chains in the recognition of clathrin cages by 'uncoating ATPase'. Nature *311* (5983), 228-231.

Schmitz, F., Tabares, L., Khimich, D., Strenzke, N., de la Villa-Polo, P., Castellano-Munoz, M., Bulankina, A., Moser, T., Fernandez-Chacon, R., Sudhof, T.C. (2006). CSP{alpha}-deficiency causes massive and rapid photoreceptor degeneration. Proc. Natl. Acad. Sci. U S A *103* (8), 2926-2931.

Seo, H., Sonntag, K.C., Isacson, O. (2004). Generalized brain and skin proteasome inhibition in Huntington's disease. Ann. Neurol. *56* (3), 319-328.

Shimura, H., Hattori, N., Kubo, S., Mizuno, Y., Asakawa, S., Minoshima, S., Shimizu, N., Iwai, K., Chiba, T., Tanaka, K., Suzuki, T. (2000). Familial Parkinson disease gene product, parkin, is a ubiquitin-protein ligase. Nat. Genet. *25* (3), 302-305.

Smith, G.B., Umbach, J.A., Hirano, A., Gundersen, C.B. (2005). Interaction between constitutively expressed heat shock protein, Hsc 70, and cysteine string protein is important for cortical granule exocytosis in Xenopus oocytes. J. Biol. Chem. *280*, 32669-32675.

Speese, S.D., Trotta, N., Rodesch, C.K., Aravamudan, B., Broadie, K. (2003). The ubiquitin proteasome system acutely regulates presynaptic protein turnover and synaptic efficacy. Curr. Biol. *13* (11), 899-910.

Spillantini, M.G., Crowther, R.A., Jakes, R., Hasegawa, M., Goedert, M. (1998). Alpha-Synuclein in filamentous inclusions of Lewy bodies from Parkinson's disease and dementia with lewy bodies. Proc. Natl. Acad. Sci. U S A *95* (11), 6469-6473.

Stahl, B., Tobaben, S., Sudhof, T.C. (1999). Two distinct domains in hsc70 are essential for the interaction with the synaptic vesicle cysteine string protein. Eur. J. Cell. Biol. *78* (6), 375-381.

Sutton, R.B., Fasshauer, D., Jahn, R., Brunger, A.T. (1998). Crystal structure of a SNARE complex involved in synaptic exocytosis at 2.4 A resolution. Nature *395* (6700), 347-353.

Swayne, L.A., Beck, K.E., Braun, J.E. (2006). The cysteine string protein multimeric complex. Biochem. Biophys. Res. Commun. *348* (1), 83-91.

Swayne, L.A., Blattler, C., Kay, J.G., Braun, J.E. (2003). Oligomerization characteristics of cysteine string protein. Biochem. Biophys. Res. Commun. *300* (4), 921-926.

Sytnyk, V., Leshchyns'ka, I., Delling, M., Dityateva, G., Dityatev, A., Schachner, M. (2002). Neural cell adhesion molecule promotes accumulation of TGN organelles at sites of neuron-to-neuron contacts. J. Cell. Biol. *159* (4), 649-661.

Szabo, A., Langer, T., Schröder, H., Flanagan, J., Bukau, B., Hartl, F.U. (1994). The ATP hydrolysis-dependent reaction cycle of the Escherichia coli Hsp70 system DnaK, DnaJ, and GrpE. Proc. Natl. Acad. Sci. USA *91* (22), 10345-10349.

Takeuchi, H., Kobayashi, Y., Yoshihara, T., Niwa, J., Doyu, M., Ohtsuka, K., Sobue, G. (2002). Hsp70 and Hsp40 improve neurite outgrowth and suppress intracytoplasmic aggregate formation in cultured neuronal cells expressing mutant SOD1. Brain Res. *949* (1-2), 11-22.

Terada, K., Mori, M. (2000). Human DnaJ homologs dj2 and dj3, and bag-1 are positive cochaperones of hsc70. J. Biol. Chem. *275* (32), 24728-24734.

Terlecky, S.R., Chiang, H.L., Olson, T.S., Dice, J.F. (1992). Protein and peptide binding and stimulation of in vitro lysosomal proteolysis by the 73-kDa heat shock cognate protein. J. Biol. Chem. *267* (13), 9202-9209.

Thoidis, G., Chen, P., Pushkin, A.V., Vallega, G., Leeman, S.E., Fine, R.E., Kandror, K.V. (1998). Two distinct populations of synaptic-like vesicles from rat brain. Proc. Natl. Acad. Sci. USA *95* (1), 183-188.

Tobaben, S., Thakur, P., Fernandez-Chacon, R., Sudhof, T.C., Rettig, J., Stahl, B. (2001). A trimeric protein complex functions as a synaptic chaperone machine. Neuron *31* (6), 987-999.

Tobaben, S., Varoqueaux, F., Brose, N., Stahl, B., Meyer, G. (2003). A brain-specific isoform of small glutamine-rich tetratricopeptide repeat-containing protein binds to Hsc70 and the cysteine string protein. J. Biol. Chem. *278* (40), 38376-38383.

Thelen, K., Kedar, V., Panicker, A.K., Schmid, R.S., Midkiff, B.R., Maness, P.F. (2002). The neural cell adhesion molecule L1 potentiates integrin-dependent cell migration to extracellular matrix proteins. J. Neurosci. *22* (12), 4918-4931.

Ungewickell, E. (1985). The 70-kd mammalian heat shock proteins are structurally and functionally related to the uncoating protein that releases clathrin triskelia from coated vesicles. EMBO J. *4* (13A), 3385-3391.

Ungewickell, E., Ungewickell, H., Holstein, S.E., Lindner, R., Prasad, K., Barouch, W., Martin, B., Greene, L.E., Eisenberg, E. (1995). Role of auxilin in uncoating clathrin-coated vesicles. Nature *378* (6557), 632-635.

Valtorta, F., Benfenati, F., Greengard, P. (1992). Structure and function of the synapsins. J. Biol. Chem. *267* (11), 7195-7198.

Virmani, T., Han, W., Liu, X., Sudhof, T.C., Kavalali, E.T. (2003). Synaptotagmin 7 splice variants differentially regulate synaptic vesicle recycling. EMBO J. *22* (20), 5347-5357.

Walsh, P., Bursac, D., Law, Y.C., Cyr, D., Lithgow, T. (2004). The J-protein family: modulating protein assembly, disassembly and translocation. EMBO Rep. *5* (6), 567-571.

Walsh, F.S., Doherty, P. (1997). Neural cell adhesion molecules of the immunoglobulin superfamily: role in axon growth and guidance. Annu. Rev. Cell. Dev. Biol. *13*, 425-456.

Wang, T.F., Chang, J.H., Wang, C. (1993). Identification of the peptide binding domain of hsc70. 18-Kilodalton fragment located immediately after ATPase domain is sufficient for high affinity binding. J. Biol. Chem. *268* (35), 26049-26051.

Washbourne, P., Thompson, P.M., Carta, M., Costa, E.T., Mathews, J.R., Lopez-Bendito, G., Molnar, Z., Becher, M.W., Valenzuela, C.F., Partridge, L.D., Wilson, M.C. (2002). Genetic ablation of the t-SNARE SNAP-25 distinguishes mechanisms of neuroexocytosis. Nat. Neurosci. *5* (1), 19-26.

Watanabe, M., Dykes-Hoberg, M., Culotta, V.C., Price, D.L., Wong, P.C., Rothstein, J.D. (2001). Histological evidence of protein aggregation in mutant SOD1 transgenic mice and in amyotrophic lateral sclerosis neural tissues. Neurobiol. Dis. *8* (6), 933-941.

Wheeler, T.C., Chin, L.S., Li, Y., Roudabush, F.L., Li, L. (2002). Regulation of synaptophysin degradation by mammalian homologues of seven in absentia. J. Biol. Chem. *277* (12), 10273-10282.

Wei, M.H., Karavanova, I., Ivanov, S.V., Popescu, N.C., Keck, C.L., Pack, S., Eisen, J.A., Lerman, M.I. (1998). In silico-initiated cloning and molecular characterization of a novel human member of the L1 gene family of neural cell adhesion molecules. Hum. Genet. *103* (3), 355-364.

Willeumier, K., Pulst, S.M., Schweizer, F.E. (2006). Proteasome inhibition triggers activity-dependent increase in the size of the recycling vesicle pool in cultured hippocampal neurons. J. Neurosci. *26* (44), 11333-11341.

Winnefeld, M., Rommelaere, J., Cziepluch, C. (2004). The human small glutamine-rich TPR-containing protein is required for progress through cell division. Exp. Cell. Res. *293* (1), 43-57.

Wu, S.J., Liu, F.H., Hu, S.M., Wang, C. (2001). Different combinations of the heat-shock cognate protein 70 (hsc70) C-terminal functional groups are utilized to interact with distinct tetratricopeptide repeat-containing proteins. Biochem. J. *359* (Pt 2), 419-426.

Wu, S.J., Wang, C. (1999). Binding of heptapeptides or unfolded proteins to the chimeric C-terminal domains of 70-kDa heat shock cognate protein. Eur. J. Biochem. *259* (1-2), 449-455.

Zhang, H., Kelley, W.L., Chamberlain, L.H., Burgoyne, R.D., Lang, J. (1999). Mutational analysis of cysteine-string protein function in insulin exocytosis. J. Cell. Sci. *112* (Pt 9), 1345-1351.

Zhang, Y., Roslan, R., Lang, D., Schachner, M., Lieberman, A.R., Anderson, P.N. (2000). Expression of CHL1 and L1 by neurons and glia following sciati nerve and dorsal root injury. Mol. Cell. Neurosci. *16* (1), 71-86.

Zinsmaier, K.E., Bronk, P. (2001). Molecular chaperones and the regulation of neurotransmitter exocytosis. Biochem. Pharmacol. *62* (1), 1-11.

Zinsmaier, K.E., Eberle, K.K., Buchner, E., Walter, N., Benzer, S. (1994). Paralysis and early death in cysteine string protein mutants of Drosophila. Science *263* (5149), 977-980.

Publications

1. Leshchyns'ka, I., Sytnyk, V., Richter, M., Andreyeva, A., Puchkov, D., Schachner, M. (2006). The adhesion molecule CHL1 regulates uncoating of clathrin-coated synaptic vesicles. Neuron. 52 (6), 1011-1025.

2. Andreyeva, A., Leshchyns'ka, I., Sytnyk, V., Schachner, M. (submitted). Sustainability of synaptic vesicle exocytosis relies on CHL1 as a selective organizer of the presynaptic chaperone machinery refolding the SNARE complex.

Acknowledgments

The present study was performed in the Institute for Biosynthesis of Neuronal Structures of the Centre for Molecular Neurobiology (ZMNH) at the University of Hamburg. I would like to thank my supervisors Prof. Melitta Schachner, Dr. Vladimir Sytnyk and Dr. Iryna Leshchyns'ka. I thank Prof. Melitta Schachner, the director of this institute, for the opportunity to work on this project, for providing the facilities for this research, constructive discussions and guidance.

I am extremely grateful to Dr. Vladimir Sytnyk and Dr. Iryna Leshchyns'ka for supervising me, for providing me with the bright ideas, constant help with all experiments, helpful discussions, proofreading of this manuscript and patience.

I also would like to thank all the colleagues of our lab for everyday help, cordiality and useful remarks during the seminars. Yana Chernyshova, Aparna Shetty, Vasudharani Devanathan, Vsevolod Bodrikov, Dmytro Puchkov, Nan Tian, Babett Baraniec, Doreen Westphal and Shen Li, thank you very much for your interesting presentations and attention to my own during our group seminars, new ideas, friendship and support in science, as well as in life. I am also grateful to Ute Eicke-Kohlmorgen, Achim Dahlmann, Joseph Thorairajoo, Peggy Putthoff, Fritz Kutschera, Torsten Renz and Eva Kronberg for technical assistance, genotyping and animal care. I would like to thank the EDV group for solving computer-related problems. Dr. Carol Stocking (Heinrich-Pette-Institut, Hamburg, Germany), thank you very much for helping me to improve the language of this manuscript.

I wish to thank Dr. Melanie Richter (Burnham Institute, La Jolla, CA, USA) for CHL1-ICD-pQE30 and L1-ICD-pET-28a constructs, for the production of antibody against the extracellular domain of CHL1 and for the help at the first stage of this project, Dr. Guido Meyer and Prof. Nils Bröse (Max-Planck-Institute for Experimental Medicine, Göttingen, Germany) for antibodies against Csp, αSgt, βSgt and Csp-pGEX-KG, Hsc70-pGEX-KG, αSgt-pGEX-KG, αSgt-pET-28a, βSgt-pGEX-KG constructs, Dr. Dirk Fasshauer (Max-Planck-Institute for Biophysical Chemistry, Göttingen, Germany) for Snap25- pET-28b and Vamp2-pET-28b constructs, Dr. Marty Grumet (Rutgers University, NJ, USA) for 2C2 antibody, Prof. Reinhard Jahn (Max-Planck-Institute for Biophysics, Göttingen, Germany) for antibodies against Synaptophysin, Dr. Christine Knuehl (Charité, Berlin, Germany) for Hsc70-pQE30 construct and Dr. Suzhen Chen for pEE14-CHL1-Fc construct, Dr. Gero Miesenboeck (Yale University School of Medicine, New Haven, CT, USA) for synapto-pHluorin construct.

I want to thank Dr. Anton Liopo and Dr. Olga Chumakova (University of Texas Medical Branch, Galveston, USA) for the help at the beginning of my scientific career, for their trust in me and for the helpful advice in science and in life. I would like to thank also the co-workers of the Laboratory of Neurochemistry, Institute of Biochemistry, National Academy of Sciences of Belarus, particularly Dr. Valentina Tayurskaya, Anna Shevalye, Oleg Zakharov, Sjargey Kirko and Ludmila Gerashchenko for the help and friendship. Dr. Oleg Stukalov (University of Guelph, Canada), Dr. Igor Zverinski (Institute of Biochemistry, National Academy of Sciences of Belarus) and Prof. Ilja Zavodnik (Grodno State University, Belarus) thank you very much.

I am grateful to my parents, my sister Svetlana, my parents-in-law and my family for the support and understanding.

I want to thank, especially, my husband Dr. Oleg Zaitsev for the help in improving my language, proofreading of this manuscript, for the patience, support, understanding and love.